P-REX2 PH Domain Inhibition of PTEN Regulates Transformation, Insulin Signaling, and Glucose Homeostasis

Cindy Hodakoski

Submitted in partial fulfillment of the
requirements for the degree of
Doctor of Philosophy
under the Executive Committee
of the Graduate School of Arts and Sciences

COLUMBIA UNIVERSITY

2012

ABSTRACT

P-REX2 PH Domain Inhibition of PTEN Regulates Transformation, Insulin Signaling, and Glucose Homeostasis

Cindy Hodakoski

PTEN, a tumor suppressor lost in multiple cancers, antagonizes PI3-kinase signaling by dephosphorylating the second messenger phosphatidylinositol (3,4,5) trisphosphate. PTEN expression and enzymatic activity is regulated through various mechanisms, including oxidation, phosphorylation, and protein-protein interactions. Our lab has recently identified a PTEN interacting protein, the Rac GEF P-REX2, which inhibits PTEN phosphatase activity in a non-competitive manner. This thesis focuses on understanding the physiological relevance of this interaction in the regulation of PI3K signaling, as well as determining the mechanism of P-REX2 mediated PTEN inhibition. The first chapter focuses on the role of P-REX2 overexpression in PI3K signaling, proliferation, and transformation. We first find that P-REX2 Rac GEF activity is dispensable for PTEN inhibition by utilizing a P-REX2 GEF dead mutant N212A. Next, we determined the effect of P-REX2 overexpression on PI3K signaling in normal mammary epithelial cells. Expression of P-REX2 or the DHPH inhibitory domain increased AKT phosphorylation, promoted cellular proliferation, and disrupted acini morphogenesis. Furthermore, P-REX2 cooperated with other oncogenes, including the PI3K E545K oncogenic mutant, c-MYC, and HER2 to promote proliferation, colony formation in soft agar, and tumor formation in mice. We also analyzed the effects of expression of P-REX2 cancer mutants, and discovered two transforming mutants, V432M and R498I that cooperated with PI3K E545K to increase anchorage independent growth and cellular proliferation.

The next chapter examines the role of P-rex2 in PI3K signaling regulation *in vivo*. We generated *Prex2* knockout mice using a gene trap method, and found that baseline signaling and proliferation in fibroblasts was not affected by P-rex2 deletion. However, insulin and IGF-1, but not PDGF or EGF stimulated PI3K signaling was reduced in *Prex2*$^{-/-}$ fibroblasts. The activity of PTEN from *Prex2*$^{+/+}$ fibroblasts was reduced following insulin stimulation, but remained elevated in *Prex2*$^{-/-}$ cells, suggesting that insulin stimulated PTEN inhibition is dependent on P-rex2. Furthermore, P-REX2 interacted with phosphorylated insulin receptor and recruited PTEN to the membrane following insulin stimulation. *Prex2*$^{-/-}$ mice are intolerant to insulin and glucose, and have reduced PI3K signaling in the fat and liver following insulin stimulation. Furthermore, the activity of PTEN from *Prex2*$^{-/-}$ liver samples is elevated, and correlated with a decrease in cellular PIP3 levels.

After uncovering an essential role for P-REX2 in PI3K signal transduction, we next examined the mechanism and regulation of P-REX2 mediated PTEN inhibition. We found that P-REX2 interacts with two different sites on PTEN. The PH domain of P-REX2 bound to the phosphatase and C2 domains of PTEN, while the inositol polyphosphate-4 phosphatase domain interacted with the PDZ-binding domain on the PTEN C-terminal tail. We discovered that the PH domain was the minimal domain that constitutively inhibited PTEN. However, the DHPH domain and full length P-REX2 required phosphorylation of the PTEN C-terminal tail for inhibition, suggesting the DH domain of P-REX2 restricts PH domain inhibition of PTEN when the C-terminal tail of PTEN is unphosphorylated. Furthermore, the PH domain of P-REX1 was not able to inhibit PTEN, and full length P-REX1 did not interact with PTEN, suggesting that there is a level of specificity involved in P-REX2 PH domain mediated phosphatase inhibition

and binding. Overall, this thesis identifies P-REX2 as a dynamic inhibitor of PTEN phosphatase activity that regulates PI3K mediated cellular transformation, insulin signaling, and glucose metabolism.

TABLE OF CONTENTS

LIST OF FIGURES

CHAPTER I

CHAPTER II

CHAPTER III

CHAPTER IV

ABBREVIATIONS

Arp2/3	actin-related protein 2 and 3
BAD	Bcl-2-associated death promoter
Cdc	cell division cycle
Clp1	Cdc14 like protein 1
Dbl	Diffuse B-cell lymphomas cells
DEP	Disheveled, EGL-10, and pleckstrin homology
DH	Dbl homology
EGFR	epidermal growth factor receptor
ER	Estrogen receptor
FOXO	forkhead box transcription factors
FAK	focal adhesion kinase
GAP	GTPase activating protein
GDI	guanine nucleotide dissociation inhibitor
GEF	guanine nucleotide exchange factor
GSK3- β	glycogen synthase kinase 3-β
GLUT4	glucose transporter type 4
H_2O_2	hydrogen peroxide
HER2	Human epidermal growth factor receptor 2
IGF-1R	insulin-like growth factor-1 receptor
IP4P	inositol polyphosphate 4-phosphatase
IR	insulin receptor
LOH	loss of heterozygosity
MEF	mouse embryonic fibroblast
MTM	myotubularins
mTOR	mammalian target of rapamycin
PAK	p21 activated kinase
PB	phosphatase buffer
PDGFR	platelet derived growth factor receptor
PDK1	3-phosphoinositide-dependent kinase-1

PDZ-BD	PDZ- binding domain
PDZ	PSD-95, Discs-large, ZO-1
PH	pleckstrin homology
PI3K	phosphoinositide-3 kinase
PI(3)P	Phosphotidylinositol 3-phosphatase
PI(3,4)P2	Phosphatidylinositol 4,5-bisphosphatase
PI(4,5)P2	Phosphatidylinositol 4,5-bisphosphatase
PI(3,4,5)P3	Phosphotidylinositol 3,4,5-trisphosphatase
PKC	protein kinase C
PIP3	PI(3,4,5)P3
PP	protein phosphatase
P-REX1/2	PI(3,4,5)P3-dependent Rac exchanger 1/2
PtdIns	Phosphoinositides
PTEN	phosphatase and tensin homolog deleted on chromosome 10
PTP	protein tyrosine phosphatase
ROS	reactive oxygen species
RTKs	receptor tyrosine kinases
SHIP	Src homology-2 domain-containing inositol 5-phosphatase
TSC2	Tuberous sclerosis protein 2
WASP	Wiskott-Aldrich syndrome protein

ACKNOWLEDGEMENTS

I owe the completion of this thesis to many people who supported me in various different ways. First and foremost, I would like to thank my mentor, Ramon Parsons. I wouldn't have gotten here if it wasn't for his guidance, support, and contagious passion for science and learning. Just as importantly, he made the lab feel like a family, and it will be very hard to find another lab environment like this.

To past and current lab members, I am fortunate to consider you all my friends. I am grateful for their help and advice, and I would especially like to thank Barry Fine for handing me over his project and getting me started my first year, and Benjamin Hopkins, whose help with my project and friendship has been invaluable. I would also like to thank Sarah Mense and Doug Barrow for letting me borrow their reagents, even though I might not have always replaced them. To all the new lab members, I wish you all the best in the next few years.

I would also like to thank my thesis committee members Stephen Goff, Lawrence Shapiro, and Carol Prives for arranging their busy lives around my thesis committee meetings and for giving feedback and asking interesting questions on my project, and to Rodney Rothstein, for agreeing to be my outside reader. Thanks to Rodney Rothstein, Brent Stockwell, and their labs for allowing me to rotate with them. Also, I must acknowledge Professor Liem and Zaia Sivo for guiding all of us in the Integrated Program.

To Christopher Tan, Shahrnaz Kemal, Punita Bhansali, and Jennifer Tung, who all started this journey with me, and the many other friends I have gained other these past years, thank you for all the years of fun, I hope that they will continue in the future. A special thanks to Joseph Ulichny, David Grizzanti, and Tom Umile for a decade of support and fun.

Finally, I cannot express how thankful I am for my family. I would like to thank my brother Brandon for being my friend, keeping me entertained, and always supporting me even though our interests couldn't be more different. Most importantly, to my parents, there are not enough 'thank you's' to express how grateful I am for your constant love and support. Thank you for always believing in me and telling me there was nothing I couldn't do.

For my parents

CHAPTER I

INTRODUCTION

The regulation of cellular activities occurs through a complex network of signaling events that allows cells to respond to changes in their microenvironment and communicate with other cells. Disruption of a cell's ability to respond to signaling events is often the root of many diseases including cancer, diabetes, and neurodegenerative disorders. Second messengers regulate intracellular responses to extracellular stimuli by relaying signals received on the cell surface to target molecules inside of the cell. Phosphoinositides are a family of phospholipids whose role as second messengers in signaling transduction has been well characterized and also highly implicated in disease. The phosphoinositide phosphatidylinositol (3,4,5) trisphosphate is a critical second messenger, and is dephosphorylated by the tumor suppressor PTEN. In this thesis, we focus on understanding how PTEN inhibition by the Rac GEF P-REX2 impacts phosphatidylinositol (3,4,5) trisphosphate mediated signaling and disease.

PHOSPHOINOSITIDE SIGNALING

Phosphoinositides (PtdIns) are membrane lipids that are phosphorylated at the 3, 4, and 5 positions of the inositol ring. Seven different phosphorylated PtdIns exist, and although they only make a minor component of membrane phospho-lipids in the cell, they play critical roles in many different cellular processes (Cantley, 2002). PtdIns are made up of two acyl groups, a glycerol backbone and a phospho-inositol ring. Various kinases and phosphatases are involved in the conversion of phosphoinositides from one form to another. PtdIns are generated in the endoplasmic reticulum, and then compartmentalized

to different membrane surfaces where they perform regulatory roles in cellular processes by targeting many different proteins to the membrane surface.

Substrate recognition

Phosphatidylinositol 4,5-bisphosphate (PI(4,5)P2) is the most abundant phophoinositide in the cell, comprising 95% of phosphorylated PtdIns, and less selective in its targeted domains. PI(4,5)P2 is found at the plasma membrane and at membranes of trafficking vesicles, and many of its target proteins control endocytosis, exocytosis, and cytoskeletal rearrangements (Holtz and Axelrod, 2002; Jones et al., 2000; Watt et al., 2002). PI(4,5)P2 binds with weak affinity and low specificity to pleckstrin homology (PH) domains, with the exception of the phospholipase-C (PLC)-δ1 PH domain, which has strong affinity and high specificity for PI(4,5)P2 (Lemmon et al., 1995). Many PI(4,5)P2 target proteins are involved in clathirin-mediated endocytosis. Several examples of target proteins involved in the initial steps of endocytosis include associated protein (AP)-2, which interacts through an N-terminal lysine rich domain, AP180, which binds through an N-terminal domain termed AP180 N-terminal homology (ANTH), and epsin, which also binds through a similar Epsin N-terminal homology (ENTH) domain (Ford et al., 2001; Gaidarov and Keen, 1999; Itoh et al., 2001). Membrane invagination and fission of vesicles is also regulated by PI(4,5)P2 by recruiting and activating proteins such as dynamin to the membrane through its PH domain (Barylko et al., 1998; Cremona et al., 2001; Zheng et al., 1996). PI(4,5)P2 targets are also involved in cytoskeletal rearrangement. For example, a lysine rich region of the Wiskott-Aldrich syndrome

protein (WASP) binds to PI(4,5)P2 and cooperates with cell division cycle (Cdc) 24 to activate actin-related protein 2 and 3 (Arp2/3) and actin assembly at the membrane (Rohatgi et al., 1999).

Phosphotidylinositol 3-phosphate (PI(3)P) is produced by the kinase vacuolar protein sorting 34 (Vps34) as well as by dephosphorylation of PI(3,4,5)P3 by 4- and 5-phosphatases. PI(3)P is a specific marker of endosomes, and thusly plays a role in regulating early endocytic trafficking and lysosome/vacuole sorting in the Golgi (Corvera et al., 2001; Gillooly et al., 2000). PI(3)P has the most known specific binding partners, and is recognized by most FYVE domain proteins (found in Fab1p, YOTB, Vac1p, and EEA1) (Bravo et al., 2001; Misra et al., 2001) and phox homology (PX) domain proteins (Cheever et al., 2001; Kanai et al., 2001; Song et al., 2001). Interaction of these domains with PI(3)P is complex and not only involves the phosphorylated inositol head group, but other interactions with the membrane as well (Kutateladze et al., 2001).

Phosphotidylinositol 3,4,5-trisphosphate (PI(3,4,5)P3), whose regulation is a major theme in this thesis, is found at the plasma membrane at very low concentrations in unstimulated cells, however its abundance increases significantly following stimulation and phosphorylation by phosphoinositide-3 kinase (PI3K) (Rameh and Cantley, 1999; Stephens et al., 1993; Vanhaesebroeck and Waterfield, 1999). The only domain known to bind PI(3,4,5)P3 is the PH domain, and this interaction occurs with a high degree of specificity (Kavran et al., 1998). Although many proteins contain PH domains, only a small fraction are able to recognize and bind PI(3,4,5)P3. The few existing PI(3,4,5)P3

targets control many cellular processes including growth, apoptosis, migration, and metabolism. The most thoroughly described PIP3 effector is the threonine (Thr)/serine (Ser) kinase AKT (Frech et al., 1997, Klippel et al., 1997), but it is also known to target 3-phosphoinositide-dependent kinase-1 (PDK1), a kinase for AKT (Anderson et al., 1997; McManus et al., 2004), Grp1 (general receptor for phosphoinositides, isoform 1), which regulates the actin cytoskeleton (Kavran et al., 1998; Venkateswarlu et al., 1998), and Btk1 (Bruton's tyrosine kinase), which regulates B-cell development, differentiation, and signaling (Fukuda et al., 1996; Salim et al., 1996). PI(3,4,5)P3 is hydrolyzed at the 3 position by phosphatase and tensin homolog deleted on chromosome 10 (PTEN) (Maehama and Dixon, 1998) and the 5- phosphatases Src homology-2 domain-containing inositol 5-phosphatase 1 and 2 (SHIP1 and SHIP2) (Damen et al., 1996; Kavanaugh et al., 1996; Lioubin et al., 1996;). Formation of PI(4,5)P2 by PTEN dephosphorylation results in termination of PI(3,4,5)P3 signaling. Conversely, PI(3,4)P2 targets and activates many of the same PH domain proteins as PI(3,4,5)P3, including AKT (Franke et al., 1997). Therefore, PI(3,4)P2 also serves as a second messenger involved cellular growth and proliferation.

Phosphoinositide regulation and disease

Because specific PtdIns play such critical roles in diverse cellular functions, it is not surprising that the dysregulation of enzymes involved in maintaining proper PtdIns levels are implicated in many syndromes and diseases. Mutations in gene encoding inositol-5-phosphatase, which dephosphorylates PI(4,5)P and PI(3,4,5)P3 at the 5 position , are the cause of Lowe Syndrome, an X-linked disorder with symptoms including mental

retardation neonatal hypotonia, and blindness. Dent disease is also caused by inositol-5 phosphatase mutations. Although still unclear, it is thought that mutations in this phosphatase result in defective endocytosis and membrane recycling (Attree et al., 1992; Erdmann et al., 2007; Hoopes et al., 2005; Hyvola et al., 2006). Myotubular myopathy and Charcot-Marie-Tooth disease result in part from mutations in myotubularins (MTM) or myotubularin-related (MTMR) proteins, inositol-3-phosphatases that specifically dephosphorylate PI3P and PI(3,5)P2 (Blondeau et al., 2000; Taylor et al., 2000). Mytobularin myopathy, an X-linked disease, is caused by mutations in MTM1, and is characterized by severe muscle weakness in newborns (Herman et al., 1999). Charcot-Marie-Tooth disease type 4B1 and 4B2 are neurodegenerative diseases caused by mutations in MTMR2 and MTMR13 (Azzedine et al., 2003; Senderek et al., 2003). Due to PI3P and PI(3,5)P2 compartmentalization at endosome membranes, it is believed that these syndromes are a result of defective endosomal function. Early onset Alzheimer's disease associated with Down Syndrome may involve synaptojanin-1, an inositide 5-phosphatase in neurons that dephosphorylates most of the PI(4,5)P2 in the brain. It is believed that increased Aβ42 in Alzheimer's patients stimulates PI(4,5)P2 cleavage, inhibiting hippocampal long-term potentiation. Increased synaptojanin-1 may cooperate with high levels of Aβ42 to further deplete PI(4,5)P2 levels in Alzheimer's patients. (Voronov et al., 2008).

PI(3,4,5)P3, termed PIP3 from this point on, regulates survival, apoptosis, growth, and metabolism in the cell. Therefore, alterations in the kinases and phosphatases that regulate PIP3 levels, including PI3K, PTEN, and SHIP1/2 are highly implicated in cancer

and diabetes. The catalytic subunit of PI3K phosphorylates PI(4,5)P2 at the 3 position to generate PIP3. Mutations in the gene encoding the catalytic subunit of PI3K have been identified in many cancer types including brain, breast, colon, ovary, and lung (Campbell et al., 2004; Samuels et al., 2004). The inositol-3-phosphatase PTEN converts PIP3 back to PI(4,5)P2, and therefore inhibits cell growth and survival. Loss of PTEN occurs in many tumor types, and germline mutations in PTEN are associated with cancer predisposition syndromes such as Cowden's disease (Ali et al., 1999; Liaw et al., 1997). Furthermore, PIP3 is converted to PI(3,4)P2 by the inositol-5-phosphatase SHIP1, whose expression is limited to the hematopoietic system. Mutations in the SHIP1 gene have been found in patients with acute myeloid leukemia and acute lymphoblastic leukemia. Finally, PTEN and SHIP2 play major roles in glucose metabolism due to the response of PIP3 to insulin stimulation. A 16 base pair deletion of the 3' untranslated region of SHIP2, important in promoting messenger RNA (mRNA) stability and translation, was found in patients with Type 2 diabetes (Marion et al., 2002). Also, a germline polymorphism in the 5 untranslated region of the PTEN promoter was a ssociated with Type 2 diabetes in a Japanese cohort (Ishihara et al., 2003).

PHOSPHOINOSITIDE-3 KINASE

Classes of Phosphoinsotide- 3 kinases

PI3K phosphorylate PtdIns at the 3- position, generating the second messengers PI(3)P, PI(3,4)P2 and PI(3,4,5)P3 (Downward, 1998; Toker and Cantley, 1997; Vanhaesebroeck et al., 1997). These kinases are composed of catalytic and regulatory subunits, and

various isoforms exist which are divided into several different classes, including Class I, II, and III PI3Ks (Wymann et al., 2003). Class I PI3Ks generate PI(3,4)P2 and PI(3,4,5)P3 at the plasma membrane, and are subdivided into two groups: Class IA and Class IB PI3Ks. Class 1A includes the catalytic subunit isoforms p110α, p110β, and p110δ which are activated by receptor tyrosine kinases (RTKs) (Hiles et al., 1992; Hu et ah, 1993; Vanhaesebroeck et al., 1997). They are composed of several different domains including a catalytic lipid kinase domain, a helical domain, a Ca^{2+} binding (C2) domain, and a Ras (rat sarcoma) binding domain. Class IA PI3Ks have an N-terminal region that interacts with regulatory subunits p85α, p85β or p55γ, to form a heterodimeric complex (Djordjevic and Driscoll, 2002; Walker et al., 1999; Zvelebil et al., 1996). All of the Class IA regulatory subunits contain two Src-homology 2 (SH2) domains, and protects the catalytic subunit from degredation and inhibits kinase activity (Dhand et al., 1994; Yu et al., 1998). Class IB has one member, p110γ, which is expressed primarily in leukocytes and is activated by direct association with G protein Gβγ subunits, dissociated by heterotrimeric GTP-binding protein–coupled receptor (GPCRs) activation, and Ras, and is regulated by the adaptor subunit p101 (Stoyanov et al., 1995; Stephens et al., 1997). Class II has three catalytic subunit isoforms, PI3KC2α, β, and γ, and are identified by their C-terminal C2 domain necessary for lipid interaction. As of yet, no regulatory subunits for this class of kinases have been identified. Class II kinases mainly target unphosphorylated PtdIns and PI(4)P, and are activated by integrins and RTKs including insulin, epidermal growth factor receptor (EGFR), and platelet derived growth factor receptor (PDGFR) (Arcaro et al., 2000; Brown et al., 1999; Domin et al., 1997; Zhang et al., 1998). The Class III kinases are homologous to the yeast PI3K Vps34p, and

form a complex with the regulatory myristoylated kinase p150. It produces a majority of PtdIns(3)P in the cell, and therefore regulates protein and vesicular trafficking (Herman and Erm, 1990; Panaretou et al., 1997; Schu et al., 1993; Volinia et al., 1995).

Activation of Class IA PI3K

Class IA PI3Ks are primarily activated by growth factor stimulation of RTKs, including insulin receptor (IR), insulin-like growth factor-1 receptor (IGF-1R), and EGFR. Ligand binding leads to receptor activation and autophosphorylation at tyrosine pYxxM motifs. The SH2 domain of the regulatory subunits is then recruited directly to pYxxM motifs or indirectly through adaptors such and insulin receptor substrate-1 and 2 (IRS-1/2) (Backer et al., 1992; Rordorf-Nikolic et al., 1995; Songyang et al., 1993; White, 1998). Binding to phosphorylated receptors releases the PI3K catalytic subunit from inhibition by the regulatory subunit, resulting in PIP3 generation. Furthermore, Ras can activate PI3K activity beyond the level achieved by receptor binding alone, and occurs through a direct interaction with the catalytic domain of PI3K (Rodriguez-Viciana et al., 1994).

AKT

As mentioned earlier, PI3K activation and consequent phosphorylation of PI(4,5)P2 to PIP3 leads to recruitment of PH domain containing proteins to the plasma membrane. The most studied PIP3 target is the cellular homolog of the retroviral oncogene v-Akt, AKT, also termed protein kinase B (PKB) (Bellacosa et al., 1991). AKT is a serine/threonine kinase that regulates many downstream effectors. There are three

isoforms of AKT that are encoded by different genes, and include AKT1, AKT2, and AKT3. AKT1 and AKT2 are ubiquitously expressed, while AKT3 appears to be more limited to the brain, heart, and kidney (Brodbeck et al., 1999; Cheng et al., 1992; Coffer and Woodgett, 1991; Jones et al., 1991). While all three isoforms have identical substrate specificity, specific roles for each isoform are emerging. *Akt1* deficient mice are smaller than wild-type littermates and exhibit aberrant apoptosis (Chen et al., 2001; Cho et al., 2001), while *Akt2* appears critical for maintaining glucose homeostasis. Specifically, mice deficient for *Akt2* have elevated blood glucose and serum insulin levels as well as reduced glucose tolerance and increased insulin resistance in skeletal muscle (Cho et al, 2001; Garofalo et al, 2003). Futhermore, knockdown of AKT2 specifically results in decreased insulin stimulated translocation of glucose transporter type 4 (GLUT4) and reduced glucose uptake in cultured adipocytes (Katome et al., 2003; Jiang et al., 2003). Despite these differences, mice lacking individual *Akt* isoforms are viable and only display subtle phenotypes, suggesting that the isoforms have compensatory function (Chen et al., 2001; Cho et al., 2001; Easton et al., 2005; Yang et al., 2003). The lethality *Akt1* and *Akt2* or *Akt3* double knockout mice provides further evidence for functional overlap of AKT isoforms (Dummler et al., 2006; Peng et al., 2003; Yang et al., 2005).

Structure

AKT is a member of the AGC (related to *A*MP/*G*MP kinase and protein kinase *C)* serine/threonine kinase family, and is comprised of an N-terminal pleckstrin homology domain, a catalytic kinase domain, and a C-terminal extension region (Peterson and Schreiber, 1999). Among the three isoforms, the PH domains are 80% identical, the

catalytic domains are 90% identical, and the C-terminal extension regions are 70% identical. The PH domain binds PIP3 and is therefore critical for AKT membrane recruitment and activation. The central kinase domain of AKT is closely related to protein kinase C (PKC), protein kinase A (PKA), and serum-and glucocorticoid-induced protein kinase (SGK) and phosphorylation of a critical residue within the catalytic domain is necessary for kinase activation. The C-terminal extension of AKT is similar to PKC and contains a regulatory hydrophobic motif. Full activation of AKT requires phosphorylation at a second site located within this hydrophobic motif (Alessi et al., 1996; Kumar et al., 2001; Liao and Hung, 2010).

Activation

AKT activation is a multiple step process that requires phosphorylation at several sites. PI3K activation and phosphorylation of PI(4,5)P2 to PIP3 leads to recruitment of AKT to the plasma membrane where it binds to PIP3 through its lipid binding PH domain. At the membrane, AKT is then phosphorylated by PDK1, which is also recruited to the membrane through its PH domain. This phosphorylation event occurs at Thr-308, located in the activation loop of the kinase domain (Alessi et al., 1997; Stephens et al., 1998). Full activation of AKT requires phosphorylation of a second site at Ser-473, located in the hydrophobic motif of the C-terminal tail (Alessi et al., 1996). The rictor- mammalian target of rapamycin (mTOR) complex, or mTORC2, has been shown to regulate phosphorylation at this site (Guertin et al., 2006; Sarbassov et al., 2005). Interestingly, mTOR is a target of AKT, suggesting that partial AKT activation by phosphorylation at Thr-308 can stimulate its own phosphorylation at Ser-473. AKT is further regulated by

dephosphorylation of these residues, which deactivates AKT kinase activity. Specifically, protein phosphatase-2A (PP-2A) dephosphorylates AKT mainly at Thr-308 with minimal activity toward Ser-473, whereas PH domain and leucine rich repeat protein phosphatases (PHLPP) dephosphorylate AKT specifically at Ser-473 (Brognard et al., 2007; Gao et al., 2005; Kuo et al., 2007).

Biological effects of AKT activation

Targets of the activated AKT kinase regulate various cellular functions, including proteins involved in cell survival. Studies have shown that expression of constitutively active AKT blocks PTEN induced apoptosis, whereas expression of a dominant negative form of AKT blocks survival signaling through IGF-1 (Kandasamy et al., 2001; Kulik and Weber, 1998). AKT targets many components of the cell death machinery including Bcl-2-associated death promoter (BAD), the forkhead box transcription factors (FOXO), and nuclear factor-κB (NF-κB). BAD induces apoptosis by binding to and inhibiting the survival factor B-cell lymphoma 2 and extra large (Bcl-2 and Bcl-xL) in the mitochondria. However, phosphorylation of BAD by AKT results in its cytoplasmic localization, disrupting its interaction with Bcl-2 and Bcl-xL and restoring survival (Datta et al., 1997; Datta et al., 2000; delPeso et al., 1997). AKT can also promote cell survival by initiating the transcription pro-survival genes through the indirect activation of the transcription factor NF-κB. NF-κB is sequestered to the cytoplasm and inhibited through its interaction with inhibitor of κB (IκB). Activated AKT phosphorylates and activates IκB kinase (IκK), which phosphorylates IκB, targeting it for degradation. This releases NF-κB from IκB inhibition, allowing it to enter the nucleus and activate transcription of

anti-apoptotic genes (Tanaka et al., 2005). AKT also phosphorylates the pro-apoptotic FOXO transcription factors, resulting in their inactivation and accumulation in the cytoplasm (Arden, 2007; Biggs et al., 1999; Brunet et al., 1999). The E3 ubiquitin ligase mouse double minute 2 (MDM2) is also phosphorylated by AKT, leading to its stabilization and subsequent degradation of the tumor suppressor p53 (Mayo and Donner, 2001; Zhou et al., 2001).

AKT also targets many proteins involved in cell growth, including Tuberous sclerosis protein 2 (TSC2). Phosphorylation of TSC2 by AKT blocks the formation of the TSC1/2 complex. The TSC1/2 complex is a Rheb GTPase activating protein (GAP) and deactivates Rheb GTPase activity. It is known that Rheb activates mTOR, although the mechanism is not fully understood. Therefore, AKT indirectly inactivates mTOR by phosphoryating TSC2 (Inoki et al., 2002; Manning et al., 2002; Zhang et al., 2003). mTOR is a serine/threonine kinase that interacts with raptor and rictor to form the complexes mTORC1 and mTORC2, respectively (Hara et al., 2002; Kim et al., 2002; Loewith et al., 2002, Sarbassov et al., 2004). The mTORC1 complex stimulates protein translation by phosphorylating and activating p70 S6 kinase, which then phosphorylates ribosomal protein S6 and eIF4B (Burnett et al., 1998; Raught et al., 2004; Wang et al., 2001). mTORC1 also activates translation by phosphorylating and inhibiting the translational repressor 4E-BP1 (Burnett et al., 1998). As mentioned above, the mTORC2 complex has been shown to phosphorylate AKT on Ser-473, and can therefore further promote its own phosphorylation and activation.

Many AKT targets induce cell cycle progression and proliferation. The G1 cyclins cyclin D and cyclin E activate Gap 1 and stationary phase (G1/S) cell cycle progression, as well as mitosis. Phosphorylation of cyclins by glycogen synthase kinase 3-β (GSK3-β) targets them for proteasomal degradation. However, AKT phosphorylates and inhibits GSK3-β, therefore activating cyclins and inducing cell-cycle progression (Alt et al., 2000; Diehl et al., 1998). AKT also promotes cell cycle progression and proliferation by phosphorylating the cell cycle inhibitors p21 and p27 (Liang et al., 2002; Shin et al., 2002; Zhou et al., 2001b). Phosphorylation of these proteins prevents their nuclear localization, therefore blocking the formation of inhibitory complexes with cyclins and cyclin dependent kinases.

AKT also phosphorylates proteins involved in regulating cellular metabolism. It is well established that insulin signaling is a key regulator of glucose homeostasis in the cell. Insulin regulates glucose uptake in adipose and muscle tissue by activating the membrane translocation of glucose transporter 4 (GLUT4). Studies have shown that AKT mediates insulin stimulated glucose uptake, as expression of WT or constitutively active AKT increases glucose transport and GLUT4 translocation in 3T3-L1 adipocytes, rat adipocytes, and L6 muscle cells (Cong et al., 1997; Kohn et al., 1996; Wang et al., 1999). AKT substrate 160 (AS160) has been identified as the AKT target that is responsible for GLUT4 translocation. AS160 is a Rab-GTPase activating protein, and it is thought that phosphorylation by AKT results in inhibition of AS160 GAP activity, therefore activating Rab and increasing GLUT4 transport (Sano et al, 2003; Welsh et al., 2005). AKT also regulates metabolism by phosphorylating and inactivating the kinase GSK3-β, therefore

activating glycogen synthase and stimulating the conversion of stored glucose to glycogen (Cross et al., 1995).

PTEN

PI3K activation and downstream AKT phosphorylation is negatively regulated by the phosphatase PTEN. PTEN (phosphatase and tensin homologue deleted on chromosome 10), also known as MMAC1 (mutated in multiple advanced cancers) and TEP1 (transforming growth factor [TGF]-b-regulated and epithelial cell-enriched phosphatase) is a tumor suppressor located on chromosome 10q23, a region that frequently undergoes loss of heterozygosity (LOH) in many different cancer types. It was identified by three independent groups using different techniques. Li et. al identified PTEN by representational difference analysis of brain tumor samples and cell lines followed by precise mapping with yeast artificial chromosomes to identify the specific region deleted in breast tumor samples (Li et al., 1997). A second group performed a high-density scan of chromosome 10q in glioma cell lines to isolate the PTEN gene, which they termed MMAC1 (Steck et al., 1997). PTEN was later identified by a third group, and named TEP1, by screening human cDNA clones for novel protein tyrosine phosphatases that were regulated by transforming growth factor-β (TGF-β) stimulation (Li and Sun, 1997).

Mouse models of PTEN loss reveal the importance of PTEN in normal development and confirm its tumor suppressive function. Homozygous loss of *Pten* results in embryonic lethality at embryonic day E9.5. Mice heterozygous for *Pten* develop tumors in a variety

of tissues and organs systems including the uterus, prostate, thyroid, endometrium, liver, adrenal medulla, and breast, among others (Di Cristofano et al., 1998; Podsypanina et al., 1999; Suzuki et al., 1998; Trotman et al., 2003). Tissue specific *Pten* knockout mice have been generated to study PTEN function in more detail. Complete loss of *Pten* in mammary tissue results in disrupted mammary development and high-frequency tumor development. Specific loss of *Pten* in the prostate results in high-grade prostatic intraepithelial neoplasia (HGPIN) which often progresses to become invasive cancer. Additionally, *Pten* loss in hepatocytes results in the onset of fatty liver disease and the formation hepatocellular carcinomas. These examples, as well as many others not mentioned, verify the function of PTEN as a tumor suppressor (Backman et al., 2004; Horie et al., 2004; Li et al., 2002; Wang et al., 2003).

Genetic alterations of PTEN in cancer

PTEN is frequently altered at both the message and protein levels in many different sporadic cancers. In breast cancer, somatic mutations in a PTEN are a relatively rare event, occuring at a frequency of less than 5%, however LOH and loss of protein expression occur more frequently at 40% (Bose et al., 1998; Perez-Tenorio et al., 2007; Singh et al., 1998). Biallelic inactivation of *PTEN* occurs in about 40% of glioblastomas, and is rarely seen in lower-grade glioma tumors. LOH occurs in more than 70% of glioblastoma (Choe et al, 2003; Rasheed et al., 1997; Wang et al., 1997). PTEN is the most commonly mutated gene in endometrial cancer, occurring at a frequency of 50%, with mutations in the endometrioid sub-type found in 80% to 90% of patients (Kong et al., 1997; Risinger et al., 1997; Tashiro et al., 1997; Terakawa et al., 2003). In

melanoma, LOH occurs at 30–60%, whereas somatic mutations are found at a rate of 10–20% in metastatic melanoma (Guldberg et al., 1997; Robertson et al., 1998; Tsao et al., 1998). Mutations in PTEN are also found in colon, bladder, liver, thyroid and prostate cancer (Ali et al., 1999).

In addition to the somatic mutations identified, PTEN mutation have also been found in patients with various hereditary cancer susceptibility syndromes, identified as PTEN hamaratoma tumor syndromes. PTEN mutations are found in 80% of Cowden's syndrome patients, which present with hamaratomas of the breast, skin, and mucous membranes and often develop carcinomas of the breast, uterus, and thyroid (Carlson et al., 1986; Liaw et al., 1997; Marsh et al., 1998). Mutations in PTEN are also found in 60% of patients with Bannayan-Riley-Ruvalcaba Syndrome, characterized by macrocephaly, lipomatosis, and hemangiomatosis (Gorlin et al., 1992; Marsh et al.,1999). Furthermore, PTEN mutations are found in 20% and 50% of patients with Proteus syndrome and Proteus-like syndrome, respectively, which present similar symptoms to Cowdens disease and Bannayan-Riley-Ruvalcaba syndrome (Zhou et al., 2000; Zhou et al., 2001c).

PTEN structure

PTEN encodes a 403-amino acid cytoplasmic peptide. The amino acid sequence contains the signature motif of the protein-tyrosine and dual specificity phosphatase catalytic domain, HCXXGXXRS/T. However, the amino terminal 190 amino acids resemble the sequences of tensin and auxilin rather than the sequence of other protein tyrosine

phosphatases (Li et al., 1997). Analysis of the PTEN crystal structure revealed amino acids 1-179 make up the phosphatase domain, which contains a deeper and wider catalytic pocket to accommodates lipid substrates. The N-terminus also contains a basic motif that binds PI(4,5)P2 and is important for lipid recruitment and phosphatase activity. Amino acids 186-351 form a C2 domain which lacks the canonical Ca^{2+} chelating residues which binds to phospholipid-membranes independent of calcium. The phosphatase and C2 domains together make up the minimal catalytic region of PTEN (Lee et al., 1999). C-terminal amino acids 353-403 were not included in the crystal structure, but are important for PTEN regulation and stability. The C-terminus contains a PDZ (PSD-95, Discs-large, ZO-1) binding domain involved in various protein interactions (Vazquez and Devreotes, 2006).

PTEN function

Based on the presence of the dual specificity phosphatase consensus sequence, it was believed that PTEN dephosphorylated protein substrates. It has been demonstrated that PTEN has dual-specificity phosphatase activity, dephosphorylating phosphotyrosine, phosphoserine, and phosphothreonine peptides of highly acidic substrates, although the level of activity is poor (Li and Sun, 1997; Myers et al., 1997). *In vitro*, PTEN can dephosphorylate focal adhesion kinase (FAK), but evidence for protein dephosphorylation *in vivo* is poor, suggesting that PTEN has other targets (Tamura et al., 1999). A search for non-protein targets revealed that PTEN has high phosphatase activity for PIP3 at the 3' position and reduced activity for PIP(3)P, PI(3,4)P2, PI(1,3,4,5)P4, and Ins(1,3,4,5)P4 (Maehama and Dixon, 1998). Due to its high specificity toward PIP3, it

was proposed that the PTEN tumor suppressor activity occurs through inhibition of AKT activation and PI3K signaling by dephosphorylation of PtdIn(3,4,5) to PtdIn(4,5)P2. This hypothesis was supported through various studies. One study showed $PTEN^{-/-}$ mouse embryonic fibroblasts displayed decreased sensitivity to apoptosis which correlated with elevated levels of AKT activation. Re-introduction of PTEN restored sensitivity to apoptotic stimuli and led to reduced levels of activated AKT. Consistent with this data, fibroblasts were rescued from PTEN-induced apoptosis by expression of constitutively active AKT, placing PTEN action upstream of AKT (Stambolic et al., 1998). Furthermore, transfection of PTEN in HEK293 cells and stable expression of PTEN in rat1-fibroblats both resulted in increased AKT activity that was dependent on PTEN phosphatase activity. In addition, tumors from PTEN null prostate cancer cell line xenografts had higher levels of AKT phosphorylation compared to tumors from xenograft PTEN positive cell lines (Wu et a., 1998). Genetic evidence also supports that the tumor suppressive role of PTEN occurs through decreased AKT activation. For instance, Akt deficiency inhibits tumor formation in $PTEN^{+/-}$ mice. Also, in Drosophila, expression of an Akt mutant that has reduced affinity for PIP3 rescues flies from lethality induced by PTEN loss (Chen et al., 2006; Stocker et al, 2002).

Studies using glioblastoma cell lines identified a role for PTEN in cell cycle regulation. In one study, re-introduction of WT and mutant PTEN into U87-MG cells results in growth suppression, but not induction of apoptosis. Furthermore, cell cycle analysis under reduced serum conditions revealed that PTEN expression causes a G1 cell cycle block that is dependent lipid phosphatase activity, but not protein phosphatase activity.

Another study found that transient expression of PTEN in glioblastoma cells by adenoviral infection leads to decreased proliferation, reduced growth in soft agar and reduced tumorigenicity in nude mice (Cheney et al., 1998; Furnari et al., 1997). In another report, PTEN expression induced G1 cell cycle arrest, decreased anchorage independent growth and growth in nude mice that was linked to increased expression of the cell cycle kinase inhibitor $p27^{kip1}$ and decreased activity of G1 cyclin-dependent kinases (Li and Sun, 1998). In addition to cell cycle arrest, PTEN also induces apoptosis specifically in breast cancer cell lines. Expression of PTEN in various epithelial cell lines inhibits cell growth and is associated with an induction of apoptosis and decreased PI3K signaling (Li et al., 1998). However, it has been suggested that cell-cycle arrest and apoptosis induced by PTEN expression may not mutually exclusive. For instance, in the breast cancer cell line MCF-7, inducible expression of PTEN results in decreased proliferation and G1 cell cycle arrest 72 hours after PTEN induction. However, cells undergo apoptosis after prolonged induction of PTEN for 120 hours, suggesting that PTEN expression initially blocks cell cycle progression that is followed by induction of cell death (Weng et al., 1999). In addition, transient PTEN expression in the glioma cell line U251 results in both cell cycle arrest and anoikis (Davies et al., 1998).

Various studies have shown that PTEN is localized to both the cytoplasm and nucleus, and specific roles of nuclear PTEN have been identified. The subcellular localization of PTEN appears to be cell cycle dependent, with increased levels of nuclear PTEN found during G0 and G1 (Ginn-Pease and Eng, 2003). Furthermore, PTEN appears to be differentially localized between normal tissue and tumor samples. In normal tissues

where cells are predominantly at G0-G1, PTEN is mainly nuclear; however in actively proliferating tumor cells, PTEN is more cytoplasmic (Brenner et al., 2002; Depowski et al., 2001; Perren et al., 2000; Whiteman et al., 2002). There are many proposed mechanisms for PTEN nuclear import and include simple diffusion (Liu et al., 2005), Ras-related nuclear protein (RAN)-mediated or major vault protein (MVP)-mediated nuclear import (Gil et al., 2006; Yu et al., 2002) and by monoubiquitination by neural precursor cell expressed developmentally down-regulated protein 4-1 (NEDD4-1) (Trotman et al., 2007; Wang et al., 2007). Additionally, phosphorylation of the C-terminal tail of PTEN has been shown to affect nuclear localization. Various functions of nuclear PTEN have been identified. While cytoplasmic PTEN decreases AKT activation, nuclear PTEN specifically decreases mitogen-activated protein kinase (MAPK) phosphorylation and cyclin D1 levels, resulting in cell cycle arrest (Weng et al., 2002; Weng et al., 2001). Nuclear PTEN also plays a role in the maintenance of chromosome stability. In the nucleus, PTEN associates with centromere protein C (CENP-C), and this interaction is required for centromere stability. Furthermore, PTEN null cells exhibit more double strand breaks (Shen et al., 2007). PTEN also induces radiation sensitive 51 (RAD51) expression, which is involved to double-stranded break repair (Shen et al., 2007).

By opposing insulin stimulated PI3K signaling, PTEN also regulates glucose metabolism. In *C.elegans*, loss of the PTEN homolog daf-18 partially bypasses the need for signaling via ageing alteration family member-1 (AGE-1) and abnormal dauer formation-2 (DAF-2), homologs of p110 and insulin/insulin like growth factor receptor respectively, to

regulate metabolism and energy storage, as well as development, and life span (Ogg and Ruvkun, 1998). Mice haploinsufficient for *Pten* are protected from diabetes induced by loss of *Irs2* (Kushner et al., 2005), and loss of *Pten* by antisense oligonucleotide delivery results in increased PI3K signaling in cultured liver cells, and increased insulin sensitivity in *db/db* and *ob/ob* mice (Butler et al., 2002). Specific loss of *Pten* in adipose tissue results in increased insulin sensitivity and glucose tolerance, as well as protection from streptozotocin-induced diabetes. Conversely, overexpression of PTEN in cultured adipocytes decreases insulin induced AKT phosphorylation, glucose uptake, and GLUT4 translocation (Nakashima et al., 2000; Ono et al., 2001; Tang et al., 2005). *Pten* loss also affects insulin signaling in muscle, as mice deficient for *Pten* in skeletal muscle are protected from diabetes and insulin resistance induced by a high fat diet (Wijesekara et al., 2005; Kurlawalla-Martinez et al., 2005).

PI3K independent functions of PTEN

There is increasing evidence that PTEN has functions in the cell that are independent of PIP3 dephosphorylation. For example, it has been reported that PTEN expression inhibits cellular migration in multiple glioblastoma cell lines. Furthermore, blocked migration occurs through the C2 and C-terminal tail domain and does not require lipid phosphatase activity, suggesting that PIP3 dephosphorylation is not involved in PTEN inhibited migration (Tamura et al., 1998; Raftopoulou et al., 2004). It has also been reported that nuclear PTEN mediated inhibition of tumor growth cell cycle arrest occurs through p70S6 dephosphorylation by activation of AMP-activated protein kinase and not AKT (Liu et al., 2005). Additionally, it has been reported that PTEN, through a direct

interaction, can inhibit the oncogenic potential of microspherule protein-1 (MSP58), and does not require PTEN lipid phosphatase activity, providing a PIP3 independent function for PTEN in the regulation of cellular transformation (Okumura et al., 2005).

PTEN Regulation

PTEN expression is critical for normal cellular activity and is regulated through multiple mechanisms. Protein tyrosine phosphatase inactivation by reversible oxidation of the catalytic cystein (Cys) has been well documented. Crystal structure analysis of PTEN revealed that Cys71 and Cys124 lie in close proximity to each other, and could therefore form disulfide bonds, which was later confirmed by gel shift analysis. PTEN is oxidized and inactivated following treatment with hydrogen peroxide (H_2O_2) in Swiss 3T3 cells. Furthermore, primary T-cell acute lymphoblastic leukemia cells have high intracellular ROS levels that correlate with detectable levels of oxidized PTEN, which is upregulated by addition of H_2O_2. Also, (reactive oxygen species) ROS scavengers restore PTEN activity and decrease PI3K/Akt signaling in T-ALL cells (Cho et al., 2004; Lee et al., 2002; Silva et al., 2008). Oxidation of PTEN seems to be further regulated through its interaction with thioredoxin-interacting protein, an inhibitor of the ROS scavenger thioredoxin (Hui et al., 2008, Meuillet et al, 2004).

Ubiquitination of PTEN at lysine (Lys) 13 and Lys 289 promotes PTEN protein degradation as well as nuclear localization. NEDD4-1 was the first identified E3 ubiquitin ligase for PTEN. NEDD4-1 protein levels inversely correlate with PTEN protein levels in bladder cancer, and NEDD4-1 cooperated with Ras to transform cells in

PTEN dependent manner (Wang et al., 2007). Although polyubiquitination at these sites of PTEN result in protein degradation, monoubiquitination by NEDD4-1 appears to be important in nuclear transport. Interestingly, K13E and K289E, two mutations found in Cowden's syndrome patients, are defective in nuclear translocation, but retain enzymatic activity, further linking PTEN localization and regulation of protein function. However, there is no evidence of increased PTEN protein levels or changes in localization in cells from NEDD4-1 knockout mice, suggesting that other E3 ligases are involved in PTEN ubiquitination. X-linked inhibitor of apoptosis (XIAP), a ring domain E3 ligase has also been implicated in PTEN poly- and mono ubiquitination. Knockdown of XIAP reduces PTEN ubiquitination, increases PTEN activity and reduces nuclear localization of PTEN. Furthermore, XIAP-/- MEFs have decreased levels of ubiquitinated and nuclear PTEN compared to XIAP+/+ MEFs. Another E3 ligase, WW domain-containing protein 2 (WWP2), has been shown to ubiquitinate PTEN and regulate PTEN dependent apoptosis and tumorigenicity (Van Themsche et al., 2009; Maddika et al., 2011).

Acetylation has also been implicated in PTEN regulation. For example, PTEN seems to be acetylated at Lys125–Lys128, located in the catalytic cleft of PTEN, by p300/CREB-binding protein (CBP)-associated factor (PCAF) and at Lys402 by CBP and SIRT-1. Acetylation of PTEN by PCAF results in decreases catalytic activity, increased AKT phosphorylation, and decreased PTEN dependent G1 cell cycle arrest (Okumura et al., 2006). It has also been reported that PTEN is acetylated on Lys402, located in the PDZ binding domain by CBP. Furthermore, in-vitro experiments showed that the PDZ domain containing proteins human discs large protein (hDLG), and membrane-associated

guanylate kinase inverted-2 (MAGI-2) bound with higher affinity to acetylated PTEN, suggesting that CBP may regulate interactions with the PDZ-binding domain of PTEN (Ikenoue et al., 2008).

PTEN is also regulated at the transcriptional level. Hypermethylation of the CpG islands in the PTEN promoter has been observed in many cancers, including those of the ovary, breast, lung, and endometrium, among others (Garcia et al., 2004; Ho et al., 2009; Salvesen et al., 2001; Soria et al., 2002). However, promoter hypermethylation and decreased PTEN protein level are not always correlative; therefore the role of PTEN transcriptional silencing by promoter hypermethylation in cancer is still unclear. PTEN transcription is also regulated by several transcription factors inluding sal-like protein 4 (SALL4), which represses PTEN transcription by recruiting a chromotin-remodelling ATPase and a histone decetylase to the PTEN promoter (Lu et al., 2009). The transcription factors SNAIL and inhibitor of DNA binding 1 (ID1) also repress PTEN transcription by binding to the PTEN promoter and blocking binding of the PTEN transcriptional activator p53 (Escriva et al., 2008; Lee et al., 2009). PTEN transcription is positively regulated by early growth response factor 1 (EGR-1) in response to ultra violet (UV) radiation and IGF-2 stimulation (Moorehead et al., 2003; Virolle et al., 2001). Coordinated upregulation of PTEN and EGR-1 protein is associated with poor prognosis in non-small cell lung cancer (Ferraro et al., 2005). Proliferator-activated receptor γ (PPARγ) also regulates *PTEN* transcription. Binding of PPARγ to the *PTEN* promoter in cancer and epithelial cells results in upregulated PTEN expression, reduced AKT phosphorylation and decreased cellular proliferation (Chen et al., 2005; Lee et al.,

2007; Patel et al., 2001). However, PPARγ decreases PTEN expression in muscle and adipocytes cells, suggesting that its effect on PTEN expression is cell-type specific (Kim et al., 2007). Notch1 signaling has also been implicated in PTEN transcriptional regulation. It has been reported that during T-cell development, Notch induces the expression of the transcription factor Hes1, which in turn decreases the expression of PTEN and activates c-MYC to drive proliferation (Wong el a., 2012). The PTEN promoter also contains a binding element for p53, and induction of p53 results in increased PTEN mRNA and protein levels (Stambolic et al., 2001). Interestingly, PTEN is also required for p53 induced apoptosis, suggesting the two tumor suppressors can regulate each other.

The C-terminal tail of PTEN, although absent from the crystal structure known to date, is critical for PTEN regulation. Deletion of the PTEN C-terminal tail results in a substantial decrease in protein half-life, as well as an increase in enzymatic activity. Furthermore, phosphorylation of the PTEN tail is important in maintaining protein stability and reducing enzymatic activity (Vazquez et al, 2000). The PTEN tail contains many serine and threonine residues, and mutation analysis has shown that the majority of phosphorylation events occur on Ser-370, as well as at a cluster consisting of Ser-380, Thr-382, Thr-383 and Ser-385. Substitution of alanine at these phosphorylation sites results in a reduction of PTEN half-life, as well as a significant increase in enzymatic activity. Casein kinase 2 (CK2) has been implicated in phosphorylation at Ser-370 and Ser-385, and although not considered major phosphorylation targets, Ser-362 and Thr-366 are phosphorylated by CK2 and GSK3 (Al-Khouri et al., 2005; Torres and Pulido,

2001). Mutational analysis of Ser-380, Thr-382, and Thr-383 revealed a role for phosphorylation in membrane localization. Specifically, alanine substitution at these three sites did not affect the affinity of PTEN for lipid membranes; however glutamine substitutions, which mimic phosphorylation, resulted in an 83 fold reduction in membrane localization by interfering with its electrostatic membrane binding (Das et al., 2002). Further studies have revealed that tail phosphorylation regulates an intramolecular interaction that occurs between the tail and the catalytic region of PTEN. Phosphorylation of the tail results in a closed PTEN conformation that restricts PTEN recruitment to the plasma membrane and PIP3 access (Odriozola et al., 2007; Rahdar et al., 2009).

In addition to sites of phosphorylation, the C-terminus of PTEN contains a PDZ-binding domain (PDZ-BD), which mediates interactions with proteins containing PDZ domains. One such family of proteins is the MAGI proteins, which act as membrane-associated scaffold proteins and guanylate kinases. Identified in a two-hybrid screen for PTEN interacting proteins, MAGI-2, MAGI-3, and MAGI-1b contain PDZ domains that interact with the PDZ binding domain of PTEN. There is evidence that MAGI proteins increase PTEN suppression of Akt activation by aiding its recruitment to the plasma membrane and increasing its stability. Interestingly, phosphorylation of the C-terminal tail at Thr-382 and Thr-383 reduces the affinity for MAGI-2 (Kotelevets et al.,2005; Tolkacheva et al., 2001; Wu et al, 2000; Wu et al. 2000b). PTEN also interacts with microtubule-associated serine/threonine kinases (MAST) 205 and MAST3, which phosphorylates and stabilizes PTEN protein. The human homologue of hDlg also interacts with the PTEN

PDZ-binding domain, although the implications of this interaction have not been thoroughly investigated (Adey et al.,2000; Valiente et al., 2005). A two-hybrid screen identified the interaction between PTEN and Na^+/H^+ Exchanger Regulatory Factor 1 and 2 (NHERF1 and NHERF2). NHERF1 and NHERF2 interact through the PDZ binding domain of PTEN, and regulate PDGF stimulated PI3K activity by forming a ternary complex with PTEN and PDGFR (Pan et al., 2004; Takahashi et al., 2006). As mentioned previously, PTEN interacts with the oncogene MSP58 through its C-terminal tail and inhibits cellular transformation independently of its lipid phosphatase activity. Furthermore, phosphorylation at Thr-366 is required for binding of MSP58 (Okumura et al., 2005). .

P-REX2 and RHO GTPASES

Recently, we identified a novel PTEN interacting protein, PI(3,4,5)P3-dependent Rac exchanger 2 (P-REX2) (Fine et al., 2009). P-REX2 is a Dbl family guanine-nucleotide exchange factor (GEF) for the Rho GTPase Rac (Donald et al., 2004 Rosenfeldt et al., 2004). The Dbl family of Rho guanine nucleotide exchange factors consists of approximately 70 different proteins which create a highly specific network of Rho-family GTPase activation. GEFs exhibit varying degrees of GTPase selectivity, but a large number only activate a single GTPase. Regulation of GEF activity occurs through various mechanisms, including activation by second messengers such as PIP3 and Gβγ, intramolecular inhibition, and subcellular localization (Das et al., 2002; Schmidt et al., 2002; Rossman et al., 2005; Welch et al., 2002).

Rac GTPase function

Members of the family of Rho-GTPases, including Rac, Rho, Cdc24, RhoBTB, and RhoT, are highly involved in cytoskeletal reorganization and therefore regulate many biological functions including cellular migration, adhesion, and proliferation (Chimini and Chavrier, 2000; Evers et al., 2000). Rho GTPases cycle between an inactive guanosine biphosphate (GDP) bound state and an active guanosine triphosphate (GTP) bound state. The balance between these two states is regulated by several classes of proteins including GEFs, which catalyze the exchange of GDP to GTP, GTPase activating proteins (GAPs), which increase the rate GTP hydrolysis and turn off GTPase signaling, and guanine nucleotide dissociation inhibitors (GDIs), which inhibit GDP dissociation as well as GTPase membrane association (Nassar et al., 1998; Olofsson et al., 1999; Rittinger et al., 1997). The Dbl family of GEFs is named for the Rho-GEF Dbl (from diffuse B-cells lymphoma cells), the first mammalian Rho GEF identified (Eva et al., 1988; Hart el al., 1991). Rac activation occurs through binding of Dbl homology (DH) domains of GEFs to switch regions 1 and 2 of Rac, which alters the nucleotide and magnesium binding pocket resulting in GDP dissociation and binding of GTP to the empty nucleotide binding pocket (Rossman et al., 2002). Activated Rac interacts with specific effectors to promote cytoskeletal reorganization, ROS formation, trafficking, and transcriptional activation. Rac1 regulates actin polymerization through interaction with proteins such as insulin receptor tyrosine kinase substrate p53 (IRSp53), which forms a trimeric complex with WAVE/Scar and leads to Arp2/3 activation (Miki et al., 2000). Rac1 also interacts with to Nap125 and PIR121 and disrupts an inactive WAVE/Scar complex (Eden et al., 2002; Suetsugu et al., 2006). Binding of Rac to the effector the

p21-activated kinase (PAK) promotes cytoskeleton reorganization, motility, transcription, survival, and cell-cycle progression through PAK-mediated phosphorylation of downstream targets including, LIM kinase and mysonin light chain kinase (Bokoch et al., 2003; Edwards et al., 1999; Manser et al., 1994; Sanders et al., 1999). Activated Rac is also part of the NADPH oxidase complex involved in ROS production and actives actin remondeling necessary for GLUT4 translocation (Khayat et al., 2000; Diekmann et al.,1994; Koga et al., 1999).

P-REX2 function

The Rac GEF P-REX2 was identified by two different groups through a database search for proteins homologous to P-REX1 (Donald et. al., 2004; Rosenfeldt et al., 2004). P-REX1, also a Rac-GEF, was purified through a biochemical screen targeting enzymes that increase Rac-GEF activited ROS formation from neutrophil cytosolic fractions (Welch et al., 2003). P-REX2 shares 59% homology with P-REX1 and is broadly expressed in many different tissue types, while P-REX1 expression is limited to neutrophils and cells of the brain and spinal chord. P-REX2 was shown to activate Rac and to a lesser degree, Cdc24 in-vitro (Rosenfeldt et al., 2004). Furthermore, in-vivo experiments using Sf9 and HEK293 cells showed that P-REX2, like P-REX1, activates Rac in response to both phosphatidylinositol (3,4,5)-triphosphate and the beta-gamma subunits of G-proteins (Rosenfeldt et al., 2004). P-REX2 plays an important role in endothelial cell Rac1 activation and migration. Studies have shown depletion of P-REX2 by siRNA results in decreased Rac activation as well as reduced migration in response to sphingosine-1-phosphate (Li et al., 2005). P-REX2 has also been implicated in purkinje

cell dendrite morphology. Dendrites of purkinje cells from the cerebellum of *Prex2* null mice are decreased diameter and length. *Prex2* null mice also display motor coordination defects that become more pronounced with co-deletion of *Prex1* (Donald et al., 2008).

P-REX2 structure

P-REX2 shares the same structural domains as P-REX1, which includes the catalytic DH/PH domain tandem, two DEP (Disheveled, EGL-10, and pleckstrin homology) domains thought to be involved in membrane targeting, two PDZ domains, important for protein-protein interactions, and a C-terminal tail that is homologous to an inositol polyphosphate-4 phosphatase (IP4P) domain. However, the phosphatase domain of P-REX1 shows no activity towards proteins or lipids (Donald et al., 2004 Rosenfeldt et al., 2004). A splice variant of P-REX2, named P-REX2b exists which lacks this C-terminal phosphatase domain. The DH/PH domain of P-REX2 is important for its Rac GEF activity. The DH domain catalyzes the exchange of GDP to GTP, while the adjacent PH domain has many proposed functions including localizing P-REX2 to the plasma membrane by binding to phosphoinositides, and well as providing substrate specificity and direct binding to Rac (Joseph and Norris, 2005). Intramolecular interactions between domains of P-REX1 have also been implicated in regulation of P-REX1 GEF activity, and therefore may also be important for P-REX2 regulation. For instance, the IP4P domain of P-REX1 forms intramolecular interactions between the IP4P domain and the second DEP and first PDZ domain of P–REX1 are important for Gβγ mediated activation of GEF activity (Urano et al., 2008)

.

Rac activation in disease

There is evidence of Rac1 overexpression and hyperactivity in breast, lung, and colon cancer, and activated Rac1 can also cooperate with p53 loss of function to transform normal primary fibroblasts (Boettner et al., 2002; Guo and Zheng, 2004; Jordan et al., 1999; Schnelzer et al., 2000). Dysregulation of Rac2 expression has been found in cancers of the breast, brain, head and neck, colon, and blood, and somatic mutations in Rac2 have been identified in brain tumors (Boettner et al., 2002; Guo and Zheng, 2004; Hwang et al., 2005; Jordan et al., 1999; Schnelzer et al., 2000). Rac target proteins have also been implicated in tumorigenesis, including Pak1, which is overexpressed or hyperactive in 50% of breast tumors (Balasenthil et al., 2004; Dummler at al., 2009). Furthermore, there has been mounting evidence of GEF involvement in cancer. Vav3 and Trio are both overexpressed in human breast tumors, and Tiam1 expression correlates with high grade breast tumors (Lane et al., 2008; Lee et al., 2008). P-REX1 is overexpressed in breast cancers and derived cell lines, especially in those with elevated ErbB2 and estrogen recetor (ER) expression, and also regulates ErbB2 activated cell migration and growth (Montero et al., 2011; Sosa et al., 2010). Furthermore, upregulation of P-REX1 in prostate cancer tumors and cell lines has positively correlates with metastasis, while overexpression of P-REX1 in normal prostate cells results in increased metastasis in mouse xenograft models (Qin et al., 2009). P-REX1 also promotes melanoma metastasis in a manner that requires Rac activation (Lindsay et al., 2011).

Alterations in *PREX2* have also been identified in human cancer. *PREX2* is located on chromosome 8q13, an area that has increased copy number in breast cancer, and is amplified in colorectal and prostate cancers. Analysis of available genetic expression data sets revealed that *PREX2* mRNA is significantly elevated in breast, prostate, pancreatic, brain and ovarian tumors compared to normal tissues. By surveying publically available cancer mutation data sets, we also found non-synonymous mutations in *PREX2* in many cancers including those of the pancreas, lung, colon, and kidney (Fine et al, 2009). Furthermore, a recent report found that *PREX2* is mutated frequently in metastatic melanoma. Specifically, 44% of metastatic melanoma biopsies had mutations in *PREX2*, and an independent cohort of melanoma samples were mutant for *PREX2* at a rate of 14%. Several of these mutations cooperated with N-RASG12D in hTERT-immortalized melanocytes to form tumors in immunodeficient mice. Interestingly, the mutations identified in *PREX2* are not clustered in hot-spots, but rather distributed evenly throughout the coding region (Berger et al., 2012).

P-REX2-PTEN interaction

We have previously reported that P-REX2 is a novel PTEN interacting protein. This interaction was identified by mass spectrometry analysis of PTEN binding proteins from cytoplasmic cell lysates purified over a glutathione S-transferase (GST) PTEN affinity column. Mutation analysis revealed that P-REX2 binding occurs in part through the C-terminal tail of PTEN, and that the DHPH domain of P-REX2 interacts with full-length PTEN. Most important, however, was the finding that P-REX2 inhibits the lipid phosphatase activity of PTEN in a non-competitive manner, and that the DHPH domain

of P-REX2 is sufficient for inhibition. P-REX2 rescues levels of phosphorylated AKT ablated by PTEN following insulin stimulation, but not EGF stimulation. Furthermore, P-REX2 and PTEN co-localize at the plasma membrane upon stimulation with insulin or PDGF, but not EGF. Knockdown of P-REX2 in PTEN positive breast cancer cells leads to decreased PI3K signaling and proliferation. Furthermore, P-REX2 associates significantly with PTEN status and P-REX2 expression was 3 times higher in those tumors that express PTEN (Fine et al. 2009).

Overall, these published results suggest that P-REX2 may be a critical regulator of PI3K signaling through inhibition of PTEN. Due to the frequency of P-REX2 mutations and genome copy number changes in cancer, it is possible that alterations in P-REX2 can disrupt the balance of PTEN regulation and AKT activation, resulting in the dysregulation of PI3K activated cellular activities including proliferation, migration and metabolism. This thesis focuses on understanding the importance of the P-REX2/PTEN inhibitory interaction in PI3K signaling transduction, in addition to uncovering how P-REX2 mediated PTEN inhibition itself is regulated.

FIGURE LEGENDS

Figure 1.1. **Generation of phosphorylated PtdIns.** Schematic of the interconversion of phosphorylated PtdIns by specific kinases and phosphatases.

Figure 1.2. **Downstream targets of activated AKT**. Receptor tyrosine kinase activation results in recruitment of the p110/p85 complex to either phosphorylated receptor or adaptor proteins where the catalytic subunit is activated to generate PIP3. AKT and PDK1 bind to PIP3, resulting in AKT phosphorylation at Thr-308, followed by phosphorylation at Ser-473 by the mTORC2 complex. AKT is now fully activated and can phosphorylate target protein including BAD, TSC2, MDM2, and GSK3.

Figure 1.3. **Crystal structure of PTEN**. Crystal structure of the N-terminal phosphatase domain, colored in blue, and C2 domain of PTEN, colored in red.

Figure 1.4. **PTEN "open" and "closed" conformations.** Phosphorylation of the C-terminal PTEN tail induces an intramolecular interaction between the C2/phosphatase domain and the C-terminal tail. This interaction blocks PTEN membrane recruitment and PIP3 dephosphorylation.

Figure 1.5. **Dbl-family guanine nucleotide exchange factors.** A phylogenic tree of human Dbl proteins based on the alignment of DH domains. Domain structures and Rho specificity is also summarized.

Figure 1.6. **Domain structure of P-REX2.** P-REX2 shares the same domain structure as P-REX1, which includes the DHPH tandem, two DEP domains, two PDZ domains, and an inositol-4 polyphosphate phosphatse domain with no known substrate. P-REX2b, a splice variant of P-REX2, has no C-terminal phosphatase domain.

FIGURE 1.1

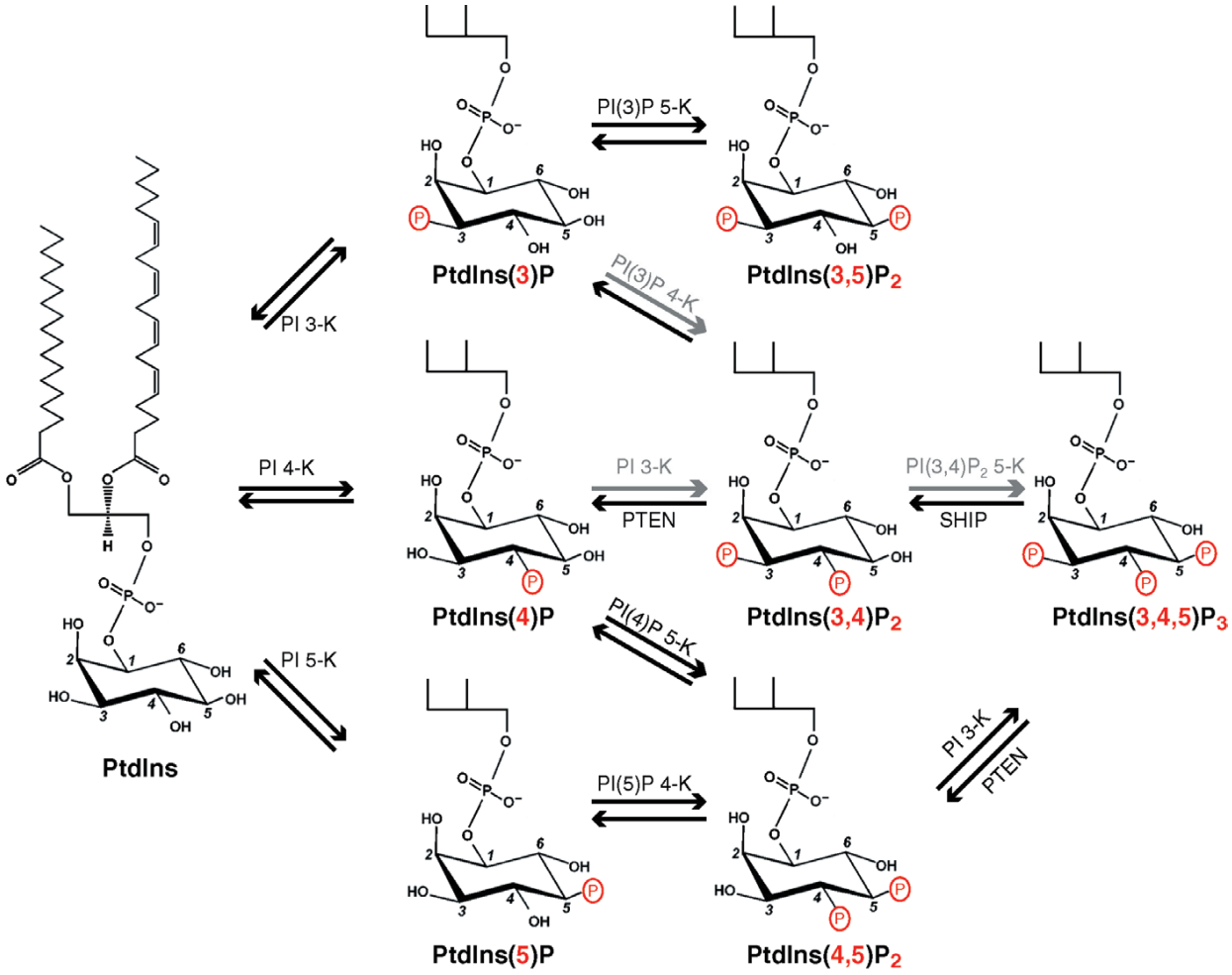

(Lemmon et al., 1995)

FIGURE 1.2

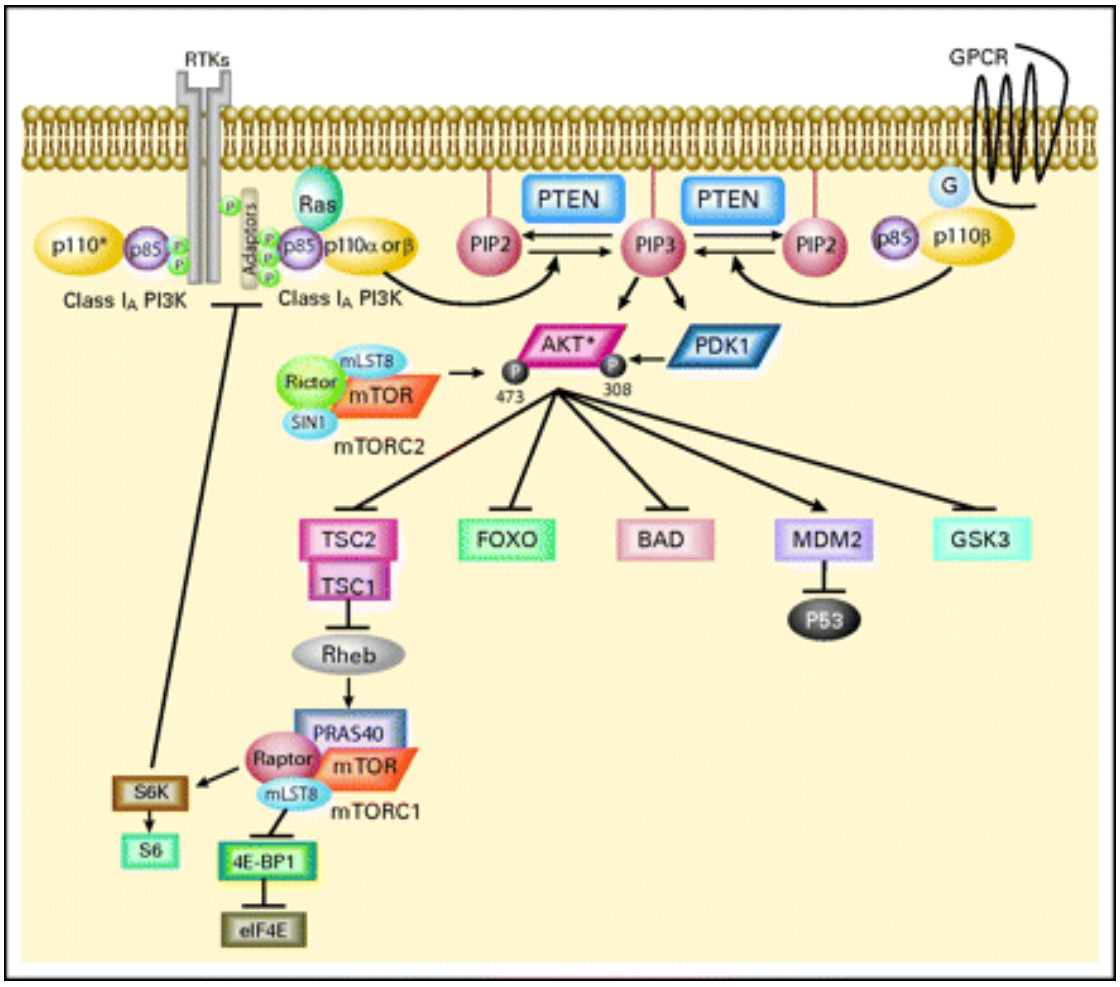

(Courtney et al., 2010)

FIGURE 1.3

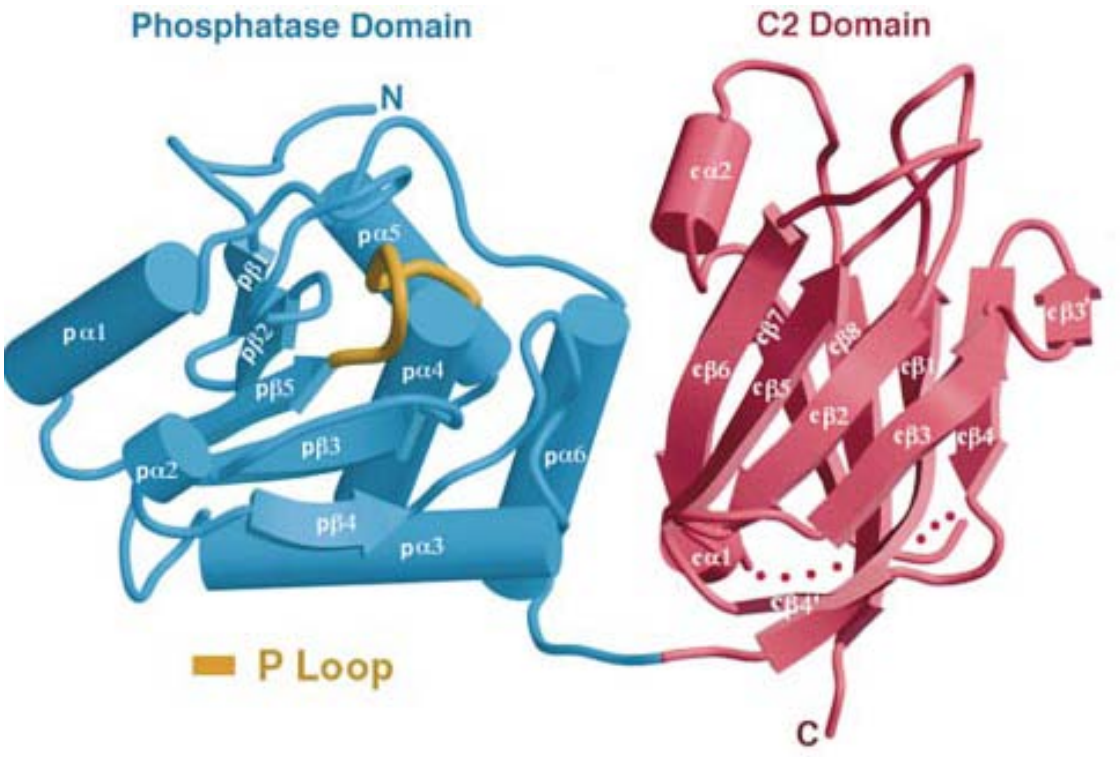

(Lee et al., 1999)

FIGURE 1.4

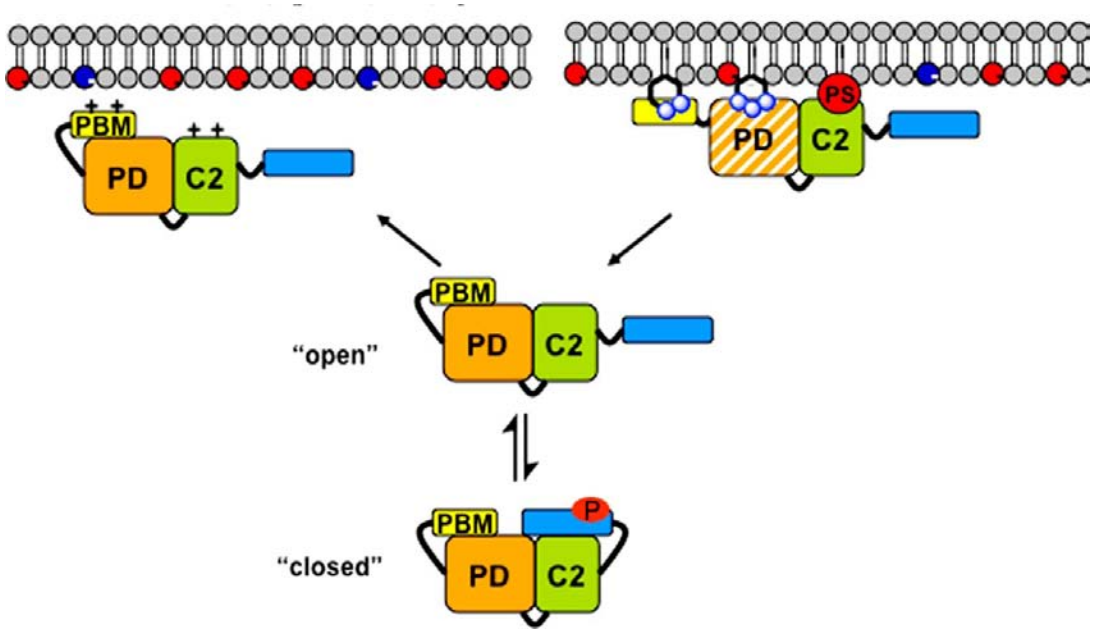

(Ross and Gericke, 2009)

FIGURE 1.5

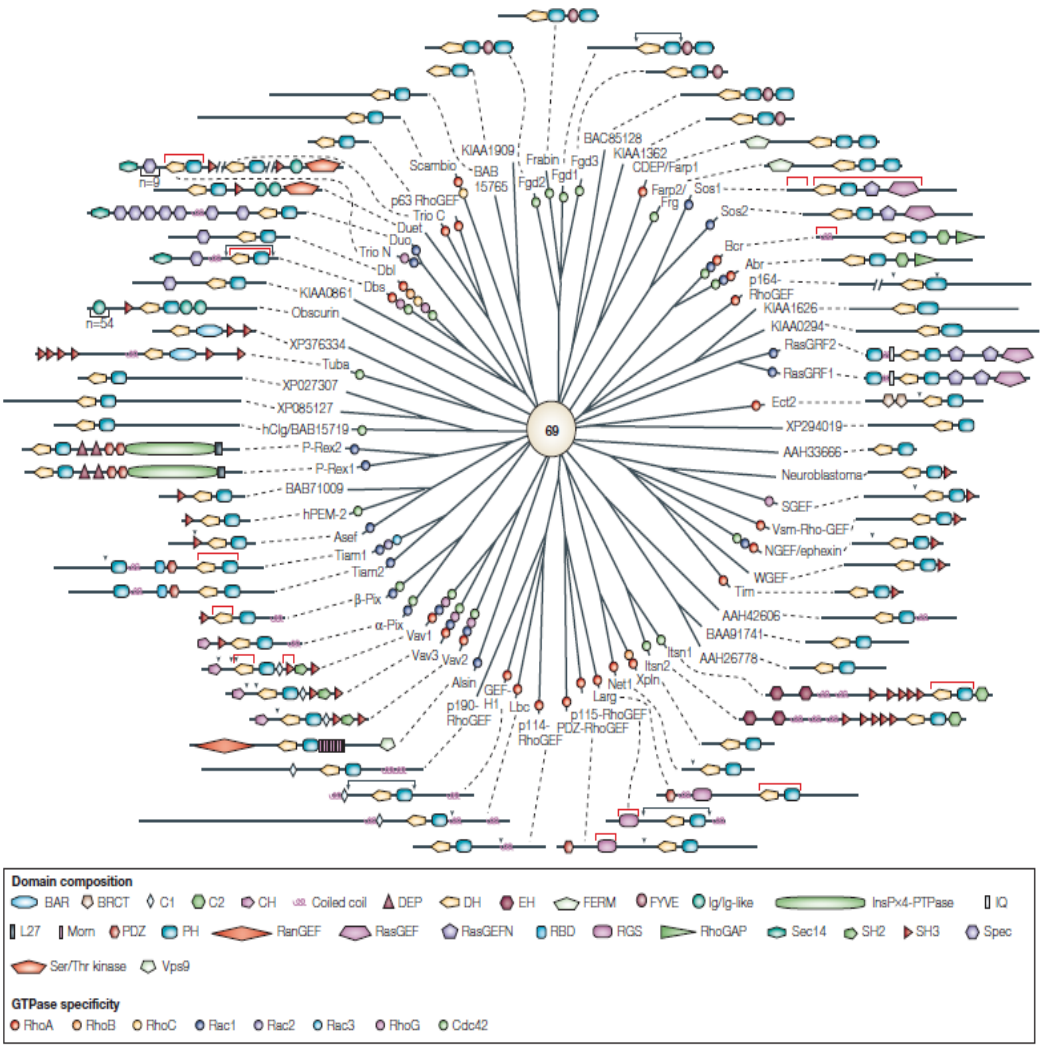

(Rossman et al., 2005)

FIGURE 1.6

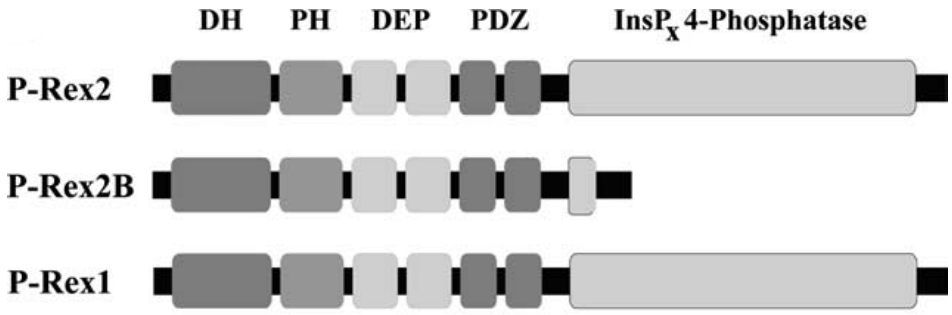

(Donald et al., 2004)

CHAPTER II

Expression of Wild-type P-REX2 and P-REX2 Cancer Mutants Increases PI3K Signaling and Proliferation, and Transforms Cells in Cooperation with Various Oncogenes

Cindy Hodakoski, Barry Fine, Benjamin Hopkins, Susan Koujak, Tao Su, Franklyn Fenton, Sarah Mense, Ramon Parsons

ABSTRACT

PTEN is a tumor suppressor that is lost in many cancers as well as cancer predisposition syndromes. PTEN dephosphorylates the second messenger phosphatidylinositol 3,4,5-triphosphate (PtdIns(3,4,5)P3), therefore antagonizing PI3K signaling, a pathway highly disrupted in cancer. We have recently identified a novel PTEN interacting protein, P-REX2, which inhibits PTEN phosphatase activity in a non-competitive manner. Here, we determined if P-REX2 Rac GEF activity was required for PTEN inhibition by using the GEF dead mutant N212A, and found that is could inhibit PTEN and rescue PTEN depleted AKT phosphorylation in culture. Due to its role in PTEN regulation, we determined if P-REX2 overexpression effected PI3K signaling activation in normal human epithelial cells. Expression of P-REX2 and the DHPH domain increased AKT phosphorylation and cellular proliferation. Expression analysis showed that increased *PREX2* correlated with *PIK3CA* mutations, Co-expression of P-REX2 and the oncogenic mutant PI3K E545K resulted in cellular transformation. Furthermore, *PREX2* and *CMYC* are located on the same chromosomal arm, which is increased in copy number in breast cancer. P-REX2 and c-MYC cooperated to promote proliferation and altered 3-D growth without increasing AKT activation. P-REX2 also cooperated with HER2 to form tumors in mice. *PREX2* is mutated in many cancer types, and signaling and growth analysis of these mutants revealed several transforming P-REX2 cancer mutants. Overall, these results suggest that P-REX2 has oncogenic properties and may cooperate with other oncogenes to promote tumorigensis, therefore serving as a potential target for anti-tumor therapy.

INTRODUCTION

The development of human cancer is a complex process that occurs through the accumulation of genetic events, mainly in tumor suppressors and proto-oncogenes, resulting in disrupted cell death, proliferation, and differentiation. One particular signal transduction pathway that is activated in many cancer types is the PI3K pathway. PI3K pathway activation occurs through the binding of growth factors to receptor tyrosine kinases, resulting in receptor autodephosphorylation and subsequent activation of the lipid kinase PI3K (Backer et al., 1992; Rordorf-Nikolic et al., 1995; Songyang et al., 1993; White, 1998). PI3K phosphorylates PI(4,5)P2 at the 3' position to generate PIP3 P3 (Downward, 1998; Toker and Cantley, 1997; Vanhaesebroeck et al., 1997), a second messenger that regulates cellular processes including growth, apoptosis, migration, and metabolism by recruiting and activating PH domain-containing proteins (Kavran et al., 1998). The most thoroughly described PIP3 effector is the threonine/serine kinase AKT (Frech et al., 1997, Klippel et al., 1997), but is PIP3 is also known to target PDK1, Arf GEFs including Grp1, and Btk1(Anderson et al., 1997; Fukuda et al., 1996; McManus et al., 2004; Salim et al., 1996; Venkateswarlu et al., 1998). Targets of activated AKT are involved in many cell processes including proliferation, survival, and migration. The lipid phosphatase PTEN opposes PI3K signaling by dephosphorylating PIP3 at the 3' position and converting it to PI(4,5)P2, (Maehama and Dixon, 1998), therefore inhibiting AKT activation.

Many genomic alterations in the PI3K pathway have been identified in human cancer. In fact, genetic aberrations have been found in all major components of this pathway. The receptor tyrosine kinases involved in PI3K pathway activation are often amplified in human cancer. Human epidermal growth factor receptor 2 (HER2), for example, is overexpressed in 25-30% of human breast cancers and ovarian cancers (Moasser, 2007), while EGFR is amplified often in gliomas, and mutated in non-small cell lung cancer (Arteaga, 2006; Sauter et al., 1996). PI3KCA, the gene encoding the p110α catalytic subunit of PI3K, is mutated in many cancer types including breast, brain, lung, and colon (Campbell et al., 2004; Samuels et al., 2004). These mutations mainly cluster in two regions including the kinase domain and helical domain. These hot spot mutations, H1047R, E545K, and E542K, result in constitutive activation of PI3K activity. Furthermore, KRAS, which is mutated in many cancers, binds to the p110α subunit of PI3K, resulting in increased PI3K activation (Rodriguez-Viciana et al., 1994). Amplification and overexpression AKT at both the message and protein level have been found in multiple cancers, and a activating missense mutation in the PH domain has been discovered in breast, colorectal, and ovarian cancer that increases AKT localization to the membrane (Bellacosa et al., 1995; Carpten et al., 2007; Cheng et al., 1992; Cheng et al., 1996; Miwa et al., 1996; Ruggeri et al., 1998; Stal et al., 2003). PTEN is deleted or mutated in many tumor types, such as advanced glial, breast, early endometrial, prostate, renal, melanomas, and small cell lung carcinomas (Ali et al., 1999). Furthermore, germline mutations in PTEN are associated with cancer predisposition syndromes such as Cowden's disease (Liaw et al., 1997). Discovering novel members of the PI3K pathway

that are altered in cancer would provide further insight into the deregulation of this pathway as well as new targets for cancer therapy.

We have recently identified a novel PTEN interacting protein, P-REX2, by utilizing an in-vitro screen for PTEN binding partners. Furthermore, we found that P-REX2 directly inhibits PTEN phosphatase activity in a non-competitive manner and rescues PI3K signaling ablated by PTEN expression in culture. Furthermore, knockdown of P-REX2 in PTEN positive breast cancer cell lines resulted in decreased PI3K signaling and proliferation (Fine et al, 2009). P-REX2 is a GEF for the small GTPase Rac, and was initially identified through a database search for proteins homologous to the leukocyte specific Rac-GEF P-REX1. P-REX2 is regulated by both PIP3 and the beta-gamma subunits of guanine nucleotide-binding proteins (Donald et al., 2004; Rosenfeldt et al., 2004). Interestingly, the gene encoding P-REX2 is located on chromosome 8q13, an area that is frequently amplified in breast, colorectal, and prostate cancers (Cher et al., 1994; Fejzo et al.; 1998, Nakao et at., 2004). Analysis of available genetic expression data sets revealed that *PREX2* mRNA was significantly elevated in breast, prostate, pancreatic, brain and ovarian tumors compared to normal tissues, and analysis of breast tumor samples revealed that P-REX2 associates significantly with PTEN status. By surveying publically available cancer mutation data sets, we also found non-synonymous *PREX2* mutations in many cancers, including those of the pancreas, lung, colon, and kidney (Fine et al, 2009). Furthermore, a recent report found that *PREX2* was mutated frequently in metastatic melanoma. Several of these mutations cooperated with N-RAS^{G12D} in human

telomerase reverse transcriptase (hTERT)-immortalized melanocytes to form tumors in immunodeficient mice (Berger et al., 2012).

Overall, these published results suggest that overexpression or mutation of P-REX2 may be important for cellular transformation and tumorigenesis through deregulation of PTEN inhibition and activation of PI3K signaling. By utilizing various cellular transformation assays, we report here that that overexpression of P-REX2 and the PTEN inhibitory DHPH domain activates PI3K signaling and increases proliferation. Furthermore, P-REX2 cooperates with oncogenic mutants of p110α, c-myc and Her2 to transform cells. We also identified cancer mutants of P-REX2 that increase its transformation potential.

EXPERIMENTAL PROCEDURES

Plasmids- NeuT-pBabe-puro expression vectors were a gift from Nancy Hynes, P110α(E545K)-pBabe-puro was a gift from Tom Roberts, and c-Myc-pBabe-neo was a gift from Ricardo Dalla-Favera. P-REX2a was cloned into pBabePuro via ligation BamHI/XhoI digest from pcDNA3.1 into BamHI/SalI digested pBabePuro. To generate MSCV-P-REX2, full length PREX2 was amplified by PCR and ligated into the MSCV-IRES-GFP vector backbone. DHPH-V5-pBabe-puro was generated by subcloning into the pBabe-puro vector backbone. To create the P-REX2A GEF inactive mutant, the QuikChange II XL Site-Directed mutagenesis kit was used to create the N212A mutation in the V5-tagged P-REX2 expression vector as per manufacturer instructions (Agilent, Santa Clara, CA). .

Antibodies- Antibodies against phospho-AKT (Thr308 and Ser473), total AKT, Her2/ErbB2 and anti-PTEN 138G6 were purchased from Cell Signaling (Danvers, MA). A P-REX2 rabbit polyclonal antibody to amino acids 960-973 was made by Zymed Laboratories (San Francisco, CA). Anti-vinculin and anti-βactin antibody was purchased from Sigma (St. Louis, MO), and monoclonal V5 antibody was from Invitrogen (Carlsbad, CA). Anti-c-Myc antibody clone 9E10 was purchased from Santa Cruz, CA, and anti-Rac was purchased from Millipore (Billerica, MA). Secondary antibodies directed against rabbit and mouse IgG conjugated to HRP were purchased from Pierce (Rockford IL).

Cell culture- MCF10A cells were grown in Dulbecco's Modified Eagle Medium (DMEM): Nutrient Mixture F-12 supplemented with 5% horse serum (Invitrogen), 10 µg/mL bovine insulin, 20ng/mL EGF, 0.5ug/mL hydrocortisone, 100ng/mL choleratoxin (Sigma), plus 100 IU penicillin and 100 µg/mL streptomycin (Cellgro, Herndon, VA). U87-MG cells were grown in minimal essential medium eagle supplemented with 10% FBS (Invitrogen) and 1% penicillin/streptomycin. HEK293 cells were grown in DMEM supplemented with 10% FBS and 1% penicillin/streptomycin. Cells were grown at 37 °C with 5% CO2.

Transfections and infections – Retrovirus was produced by transfection of either pBabe or MSCV-IRES-GFP based constructs into Phoenix HEK293 packaging cell line using Lipofecatime 2000 per the manufacturer's protocol (Invitrogen). Titers were collected 24 and 48 hours after transfection, filtered and frozen. For infection of cell lines, polybrene (Sigma) was added at a concentration of 6 µg/ml to increase infectivity. Cell lines were infected for 12 hours with 1:1 titer:growth media. For cells infected with pBabe puro, selection antibiotic was added to the media 48 hours after the initial point of infection. Cells expressing MSCV-IRES-GFP were isolated by flow cytometry.

Cell proliferation assay – 4000 cells were plated per well in a 48 well plate in at least triplicate for each experiment. Cells were allowed attach overnight, and media was changed to the indicated media 24 hours later. Cells were then allowed to proliferate and fixed at indicated time points in 0.05% crystal violet (Sigma) in 10% formalin. Each well was then washed multiple times with PBS. For relative quantification of cell density, the

crystal violet was re-solubilized in 10% acetic acid and the absorbance at 595nm was recorded by a MicroQuant plate spectrophotometer.

Soft Agar Colony Formation Assay - For soft agar colony formation assays, 1 X 10^5 cells from stable MCF10A cell lines were mixed with agar Noble (Becton Dickinson, Franklin Lakes, NJ) to form a top layer of 0.3% agarose. This layer was plated into a 35 X 10 mm plate on top of a solid layer of 0.5% agarose. Each assay was performed in triplicate. Colonies were stained with a 0.005% crystal violet solution after 14 days of incubation, and colony number was determined using ImageJ software.

Acini Formation Assay- Matrigel (Trevigen, Gaithersburg, MD) was spread evenly onto the bottom of the well of an 8-well chamber. MCF10A stable cell lines were resuspended into medium containing 2% Matrigel, 2% horse serum, and 5 ng/mL EGF, and plated at a density of $5X10^3$ cells per well. Each assay was performed in quadruplicate. Medium was changed every 4 days, and representative photographs were taken after 10 days of incubation (Debnath et al., 2003).

Xenograft assay- Mice were housed in the mouse facility of the Irving Cancer Research Center and were treated in accordance with IACUC protocol AAAB- 8776. Nude mice were obtained from Harlan Laboratories (NJ). Xenograft experiments were performed by injection of $1x10^6$ cells in matrigel and were monitored daily. For collection and staining of tumor samples, mice were euthanized via induction with CO2, at which point the

desired tissues were collected and stained with hematoxylin and eosin (H&E) to examine tumor histology.

GST-CRIB Preparation- BL21(DE3)pLysD bacteria (Invitrogen) were transformed with plasmids encoding GST-CRIB. 5 ml starter cultures were grown at 37°C overnight. Starter cultures were used to inoculate 500 ml LB cultures until OD =0.4. Protein expression was induced with 0.1 mM IPTG (Sigma) for 4 hours at 37°C. Bacterial cultures were centrifuged at 6000 x g and protein was extracted from the bacteria by sonication in a lysis buffer containing 400 mM NaCl, 50 mM Tris pH 7.2, 1% Triton X-100 and 1mM EDTA. Sonicated lysates were centrifuged at 20,000 x g for 45 minutes and the supernatant was passed through a 0.45 micron filter. The filtered supernatant was incubated overnight at 4°C with 0.5 ml GST-sepharose (GE Healthcare, Piscataway, NJ) and was then washed with GST-CRIB buffer containing 50 mM Tris pH 7.6, 50 mM NaCl and 5 mM MgCl2. Resin was assessed for purity and protein expression by SDS-PAGE followed by coomassie staining.

In vivo RAC-GEF assay- HEK293 cells were transfected with a myc-tagged RAC1 expression vector plus V5-tagged P-REX2A, P-REX2A N212A-V5, or control vector using Lipofectamine 2000 as per manufacturer protocol. After 36 hours, cells were lysed with buffer (500mM NaCl, 50mM MgCl2, 50mM Tris, 1% Triton X-100, 0.1% SDS and protease inhibitor cocktail) and incubated with GST-CRIB beads for 1 hour at 4^0C to pull down GTP-bound RAC1 (Sander et al., 1998). Beads were washed three times with lysis buffer without detergent and resuspended in 2X Laemlli sample buffer (125 mM Tris pH

6.8, 10% 2-mercaptoethanol, 4% SDS, 20% glycerol, 0.05% bromophenol blue). Rac was immunoblotted and quantitated using ImageJ software (version1.40g). Rac-GTP index is calculated by dividing the amount of RAC pulled down with GST-CRIB by the total amount of RAC multiplied by 100.

Immunoprecipitation PTEN phosphatase assay- PTEN and P-REX2-N212A were transfected into HEK293 cells as per manufacturer protocol at a ratio of 1:3 respectively. Cells were lysed 36 hours after transfection in Triton-containing lysis buffer (150 mM NaCl, 25 mM Tris pH 7.4, 1% Triton X-100, 1 mM EDTA) and precleared using agarose conjugated to mouse IgG (Santa Cruz, CA) for 1 hour. PTEN was immunoprecipitated using 138G6 antibody (Cell Signaling) and 20µl of Protein A/G Plus Agarose (Santa Cruz, CA). The sepharose was washed with cold phosphatase buffer (PB) (150 mM NaCl, 25 mM Tris-HCl pH 7.5) three times. PB, 1mM EGTA, 1mM EDTA, 5mM DTT and 20 µM soluble di-C8-D-myo-Phosphatidylinositol 3,4,5-trisphosphate (Echelon, Salt Lake City, UT) in a final volume of 50 µl was added to the beads and incubated for 30 minutes at 37^{o}C. The reactions were then added to 50µl of Biomol Green Reagent (Enzo, Farmingdale, NY) and allowed to incubate at room temperature for 30 minutes. Absorption at 620nm was quantitated in a Micro-QUANT microplate spectrophotometer (Biotek-Instrument Inc., Winooski, VT).

RESULTS

P-REX2 Rac-GEF activity is not required for PTEN inhibition

P-REX2 is an inhibitor of PTEN phosphatase activity; however, it is not known if P-REX2 GEF activity is required for PTEN inhibition and PI3K signaling activation. We therefore constructed a P-REX2 GEF-dead expression vector, P-REX2-N212A, based on a published P-REX1 GEF-dead mutant as well as the crystal structure of TIAM1 (Hill et al., 2005). First, we confirmed that this mutant was unable to activate Rac1 by determining levels of Rac-GTP loading in HEK293 cells overexpressing wild-type (WT) or mutant P-REX2. RAC-GTP loading was determined by binding to the CRIB domain of p21 activated kinase (PAK). As expected, P-REX2 expression led to increased Rac-GTP loading, whereas P-REX2-N212A Rac-GTP loading was comparable to control levels, confirming that this mutant was unable to activate Rac (Fig 2.1A).

We next determined if P-REX2-N212A was still able to inhibit PTEN activity. To test this, we transfected HEK293 cells with PTEN alone or in combination with P-REX2-V5 (WT) or P-REX2-N212A-V5. PTEN complexes were immunoprecipitated with anti-PTEN 138G6 antibody, and phosphatase assays were performed. Both wild-type P-REX2 and P-REX2-N212A inhibited PTEN phosphatase activity by 70%, suggesting the GEF activity is dispensable for PTEN inhibition (Fig 2.1B). Next, we examined if GEF activity was required to restore PI3K signaling blunted by PTEN expression. PTEN was transfected alone or in combination with WT P-REX2 or P-REX2-N212A into the PTEN deficient cell line U87-MG. As with PTEN inhibition, both P-REX2 and P-REX2-

N212A restored levels of pAKT308 and pAKT473 that were reduced by overexpression of PTEN, but had no effect on pAKT levels on their own (Fig 2.1C). In summary, loss of P-REX2 GEF activity does not affect PTEN phosphatase inhibition or PTEN dependent PI3K signaling activation. This suggests that P-REX2 induced transformation is likely due to its direct regulation of PTEN rather than through Rac activation.

P-REX2 overexpression results in increased PI3K signaling, proliferation, and disrupted morphology

We have shown that P-REX2 inhibits the activity of PTEN, a negative regulator of PI3K signaling and cell proliferation, and this does not require Rac GEF function. Therefore, we hypothesized that increased P-REX2 expression may enhance PTEN inhibition and PI3K signaling. We therefore investigated the effect of P-REX2 overexpression in the immortalized human mammary epithelial cell line MCF10A by retroviral infection of P-REX2, or a V5-tagged P-REX2 DHPH domain (DHPH-V5). Cells were lysed and PI3K signaling was analyzed by western blot analysis. Expression of both P-REX2 and the PTEN inhibitory domain, DHPH, resulted in increased levels of pAKT473, suggesting that PI3K activity is increased in these cells (Fig 2.2A).

Next, we determined whether expression of P-REX2 or the DHPH domain altered cellular proliferation of MCF10A cells. Cells were grown for several days in reduced growth factor and serum conditions, and proliferation was determined at the indicated time points by crystal violet staining. Indeed, P-REX2 and DHPH-V5 expression led to a significant increase in proliferation in growth factor-reduced medium (Fig 2.2B). We

then examined the effect of P-REX2 and DHPH-V5 expression on the 3-dimensional growth of MCF10A cells on a reconstituted basement membrane. Normally, when grown on matrigel, MCF10A cells form acini-like spheres with hollow centers resulting from the apoptosis of cells that no longer contact the membrane. However, the introduction of oncogenes disrupts the glandular morphology by deregulating proliferation and apoptosis (Debnath et at., 2003). P-REX2 and DHPH-V5 overexpression resulted in the disruption of acini morphology that is indicative of an oncogene. Cells formed large, disorganized clusters with no observed apoptosis (Fig 2.2C). The observed increase in cellular proliferation and disruption of 3-D morphology when P-REX2 and DHPH-V5 is expressed can be explained by the corresponding increase in PI3K signaling. However, cells expressing P-REX2 were not capable of anchorage independent growth (data not shown), suggesting that expression of P-REX2 alone is not sufficient for full cellular transformation. Since P-REX2 overexpression lead to increased AKT activation and proliferation in normal mammary epithelial cells, we next determined the levels of P-REX2 protein in various breast cancer derived cell lines. High levels of P-REX2, as well as the shorter isoform P-REX2b, was observed in many of the cell lines analyzed (Fig 2.2D), suggesting that upregulation of P-REX2 protein may be important in breast tumorigenesis.

P-REX2 cooperates with PI3Kα oncogenic mutants to transform MCF10A cells

Because P-REX2 overexpression did not fully transform cells, we next determined if P-REX2 could cooperate with other oncogenes to transform cells. Quantitative reverse transcription polymerase chain reaction (qRT-PCR) of P-REX2 mRNA in a cohort of

PTEN-expressing breast tumors showed that increased P-REX2 expression levels significantly correlated with the presence of activating mutations in PIK3CA (Fig. 2.3A). We therefore expressed P-REX2, a tumor derived mutant of p110α- E545K (PI3K[EK]), or both in combination in MCF10A and analyzed the effect of P-REX2 and PI3K[EK] expression on PI3K signaling by western blot. We saw that the expression of both proteins in combination resulted in increased phosphorylation of pAKT473 (Fig 2.3B).

We next determined the effect of P-REX2 and PI3K[EK] co-expression on cellular proliferation in the absence of growth factors and serum. Cells expressing P-REX2 or PI3K[EK] alone did not proliferate during starvation conditions, but over-expression of PI3K[EK] and P-REX2 in combination allowed for growth factor-independent cellular proliferation (Fig. 2.3C). We again utilized the ability of MCF10A cells to form acini during 3-D growth to further analyze the consequence of P-REX2 and PI3K[EK] overexpression. PI3K[EK] in combination with P-REX2 resulted in the formation of large, branched structures that resembled cellular invasion, and were significantly more disrupted compared to the structures formed with P-REX2 or PI3K[EK] expression alone (Fig 2.3D). We next performed soft agar assays to test whether co-expression of P-REX2 and PI3K[EK] allows cells to overcome anchorage dependent growth, a hallmark of transformation. While PI3K[EK] expressing cells formed a small number of colonies in soft agar, co-expression with P-REX2 resulted in three-times as many colonies formed, suggesting that P-REX2 and PI3K[EK] may cooperate to transform cells by increasing PI3K activation (Fig 2.3E). Surprisingly, injection of these cells into the mammary fat

pads of SCID mice did not result in tumor growth, suggesting that further pathway activation or activation of additional pathways is needed for tumor formation.

P-REX2 and c-Myc are amplified in cancer and promote cellular proliferation

The choromosome arm 8q containing *PREX2* also contains the *MYC* gene at 8q24.2, and like *PREX2*, is increased in copy number in breast cancer (Deming et al., 2000). Copy number anaylsis of our own breast tumor samples show increased copy number of *PREX2* and *MYC* within the same tumor samples (Fig 2.4A). Therefore, we hypothesized that because P-REX2 and c-Myc are often amplified, they may cooperate to transform cells. To examine this, we overexpressed P-REX2, the DHPH domain, and c-Myc alone or in combination by retroviral infection in MCF10A cells. As hypothesized, P-REX2 and the DHPH domain cooperated with c-Myc to increase cellular proliferation under starvation conditions (Fig 2.4C) and also disrupted normal acini formation when cells were grown in a 3-D culture (Fig 2.4D). Interestingly, western blot analysis of cell lysates showed that co-expression of c-Myc and P-REX2 resulted in down regeulation of PI3K signaling compared to expression of P-REX2 or the DHPH domain alone (Fig 2.4A), suggesting that P-REX2 and c-Myc cooperation likely involves other signaling pathways in addition to AKT activation.

Co-expression of P-REX2 with activated Her-2 leads to tumor formation

P-REX2 cooperated with oncogenic PI3K mutants to transform normal cells, but the increase in PI3K signaling was not sufficient to promote tumor growth. We therefore examined the oncogenic cooperation of P-REX2 and Her2, a RTK that activates PI3K

signaling as well other signaling pathways important for tumor formation. P-REX2 and oncogenic NeuT, the rat homolog of Her2, were expressed alone or in combination by retroviral infection in MCF10A cells. Western blot analysis of cell lysates showed a dramatic increase in PI3K signaling with NeuT expression alone and in combination with P-REX2 expression compared to P-REX2 alone (Fig 2.5A). We performed xenograft experiments by injecting these cells into the mammary fat pad of immunodeficient mice. Injection of P-REX2 or NeuT expressing cells did not result in tumor formation, while all mice injected with cells co-expressing P-REX2 and NeuT formed palpable tumors (Fig 2.5B). Tumor samples were collected and stained with hematoxylin and eosin to confirm tumor histology (Fig 2.5C).

Expression of P-REX2 cancer mutants causes increased proliferation and anchorage independent growth in combination with PI3K[EK]

We have surveyed publically available somatic mutation data sets and found non-synonymous mutations on *PREX2* in many cancers including those of the pancreas, lung, colon, and kidney (Fig 2.6A). We wanted to determine if any of these mutations increased the oncogenic potential of P-REX2, and therefore made retroviral expression vectors harboring many of these mutations including Y126H, V432M, R498I, K634E, S926Y, D1256N, S1488L, and A1571E. We expressed these mutants in MCF10A cells and tested whether these mutations affected protein stability. Y126H and A1571E were not stable, and were therefore not used in subsequent experiments (Fig 2.6B). Expression of stable mutants alone did not lead to any measurable increase in PI3K signaling or growth advantage. Because we previously found that co-expression of P-REX2 and

PI3K[EK] by retroviral infection causes cellular transformation, we next decided examine the oncogenic potential of wild-type (WT) P-REX2 compared to mutant P-REX2 in the presence of PI3K[EK]. We decided to express P-REX2 in MCF10A cells containing a targeted PI3KCA knock-in allele because they are less transformed compared to cells overexpressing PI3K[EK]. This allowed us to observe more subtle oncogenic effects that would otherwise be masked by high expression of PI3K[EK]. P-REX2 expression in knock out cells was observed by western blot (Fig 2.6C). PI3K[EK] knock-in cells formed a few number of colonies in soft agar, and co-expression of WT P-REX2 did not cooperate to induce colony formation. However, the mutants V432M and R498I, located in the DEP domain tandem, cooperated with PI3K[EK] to increase colony formation by 5.5 fold and 2.5 fold, respectively (Fig 2.6D). Proliferation analysis showed the expression of PI3K[EK] increased proliferation in reduced serum 2.3 fold compared to control cells. Co-expression of V432M and R498I mutants further increased proliferation 3.8 and 3.5 fold, respectively, while WT P-REX2 had no effect under these conditions (Fig 2.6E). This suggests that these two mutations have greater oncogenic potential that WT P-REX2 and may cooperate with other oncogenes to drive tumor formation.

DISCUSSION

The PI3K pathway is often perturbed in many cancer types through various mechanisms. Here, we show that overexpression of P-REX2, an inhibitor of PTEN phosphatase activity, increases PI3K signaling in normal cells, and causes increased proliferation and disrupted 3-D morphogenesis. We hypothesize that this increase in PI3K signaling is a result of increased PTEN inhibition by P-REX2; however, we cannot eliminate the possibility that P-REX2 expression affects other cellular processes that leads to increased signaling and proliferation. It has been reported that P-REX2 and P-REX1 both interact with the mTORC2 complex, which phosphorylates AKT on Ser473, and also regulates the actin cytoskeleton through activation of Rho-GTPases (Hernández-Negrete et al., 2007). It has also been shown that the mTORC2 complex regulates cancer cell migration, metastasis, and invasion by activating AKT1 phosphorylation. Interestingly, P-REX1 is necessary for cancer cell invasion through a direct interaction with AKT1 (Kim et al., 2011). Because P-REX2 also interacts with mTORC2, it is possible that it shares the same function as P-REX1 in mTORC2 activation and cancer cell migration, invasion, and metastasis.

P-REX2 is a well-established Rac-GEF, and therefore activation of Rac activity may also be playing a role in PI3K signaling activation. Rac1 controls many cellular functions including cellular migration, actin-reorganization, growth, and apoptosis and is therefore critical for the migration and invasion of certain cancer cells. Deregulation of Rac1 and Rac2 expression has been found in cancer of the breast, brain, head and neck, colon, and

blood, and domatic mutations in Rac2 have been identified in brain tumors (Bokoch, 2000; Dummler at al., 2009; Hwang et al., 2005; Rayala et al., 2006; Sneltzer et al., 2000; Sundaresan et al., 1996). Furthermore, there has been mounting evidence for the importance in GEFs in cancer. P-REX1 is overexpressed in breast cancers and derived cell lines with elevated ErbB2 and ER expression, and upregulation of P-REX1 in prostate cancer and melanoma plays a major role in metastasis (Lindsay et al., 2011; Montero et al., 2011; Qin et al., 2009; Sosa et al., 2010). Furthermore, other Rac-GEFs, including Vav3, Trio, and Tiam1 are overexpressed in human tumors (Lane et al., 2008; Lee et al., 2008). Therefore, it is possible that P-REX2 may drive tumorigenesis and metastasis through two cooperating mechanisms: activation of PI3K signaling through inhibition of PTEN and Rac1 activation.

Our results suggest that P-REX2 cooperates with other oncogenes, specifically those of the PI3K pathway including the PI3K hotspot mutation E545K and activated Her2 to transform cells and form tumors. Although mutations in genes in the same pathway are usually mutually exclusive in cancer, there are several cancer types where mutations in the PI3K pathway coexist. In endometrial, breast, and colon cancers, mutations in PI3K and PTEN are commonly found in the same tumor (Oda et al., 2005; Od et al., 2008; Yuan and Cantley, 2008). Furthermore, in breast cancer, ErBB2 amplification often coexists with PTEN loss or PIK3CA mutations (Fujita et al., 2006; Nagata et al., 2004; Saal et al., 2005), whereas Ras mutations and PIK3CA mutations occur together in colorectal cancer (Parsons et al., 2005). There are several explanations as to why these mutations coexist, and why P-REX2 cooperates with PIK3CA, c-myc, and Her2

activation. It is possible that multiple mutations in the same pathway may have a potentiating effect on the PI3K pathway by overcoming existing negative feedback loops. Indeed, when P-REX2 was co-expressed with a p110α mutant, we observed an additive increase in PI3K signaling which resulted in increased cellular proliferation. However, it is also possible that these cooperating mutations are not redundant, but rather activate additional pathways that are necessary for full cellular transformation. P-REX2 expression results in Rac activation, therefore, cells may require both PI3K pathway activated proliferation and Rac activated migration to fully transform. We observed that P-REX2 cooperated with c-Myc to increase cellular proliferation and disrupt acini morphogenesis without increasing AKT phosphorylation. It has previously been reported that PI3K and c-Myc cooperate to transform normal epithelial cells and fibroblasts through PI3K mediated transcriptional activation of Myc target genes, allowing for c-Myc induced transformation (Zhao et al., 2003). It is possible that increased PI3K signaling by P-REX2 also facilitates c-Myc transformation in a similar manner. Furthermore, P-REX2 cooperated with oncogenic Her2 to form tumors in mouse xenografts. In addition to the PI3K pathway, Her2 receptor activation also stimulates other signaling pathways, such as the RAS-MAPK pathway (Hendriks et al., 2003). Therefore, it is possible that P-REX2 and Her2 activation of PI3K signaling cooperates with Her2 stimulated MAPK activation to promote tumor growth.

Mutations in *PREX2* have been found in many cancer types, including cancer of the kidney, lung, colon, pancreas, and most recently, skin (Fine et al., 2009; Berger et al., 2012). We analyzed the transformation abilities of many of these mutants, and found two

mutations that cooperated with knock-in PI3K E545K cells to transform cells. Although these two activating mutations are located in the DEP domain tandem, it is intriguing that the mutations identified are distributed evenly across the coding region, and include several different truncating mutations. Furthermore, several of the mutations found in melanoma cooperated with an activating N-RAS mutant to form tumors in mouse xenograft experiments, yet none of these mutations clustered together (Berger et al, 2012). Therefore, because P-REX2 mutations are so varied, it seems that there are numerous ways in which P-REX2 can be activated in cancer. It will be important to uncover the mechanism of activation of these P-REX2 mutants in order to fully understand the cause of cellular transformation and tumor growth.

In summary, we have shown that P-REX2 increases PI3K signaling and proliferation, cooperates with other oncogenes to transform cells and promote tumor growth, and is mutated and activated in many different cancers. Previously published data has also shown that *PREX2* expression is increased in breast tumor samples that are positive for PTEN, as well as in cancers of the pancreas, brain, prostate, and ovary. Taken together, it appears that P-REX2 would be an effective anti-tumor target for tumors positive for PTEN. Furthermore, combining P-REX2 therapy and treatment with PI3K inhibitors may serve as an effective therapy in tumors that have coexisting mutations or amplifications of *PREX2*, *PIK3CA* or *ERBB2*.

FIGURE LEGENDS

Figure 2.1. **P-REX2 GEF activity is not required for PTEN inhibition.** *A)* RAC-GTP loading was determined by binding to the CRIB domain of p21 activated kinase (PAK) when overexpressed in HEK 293 cells with the indicated plasmids. Protein band intensity was quantified using ImageJ software. *B)* IP phosphatase assays were performed from HEK293 lysates using the 138G6 monoclonal PTEN antibody. The mean phosphatase activity is displayed along with +/- standard error (*$p<0.05$, t-test). *C)* P-REX2 or P-REX2-N212A was transfected alone or in combination with PTEN in U87-MG cells. Starved lysates were analyzed by western blot to determine levels of phosphorylated AKT.

Figure 2.2. **Effect of P-REX2 or the DHPH expression on signaling and proliferation**. *A)* Levels of phosphorylated AKT473 in MCF10A cells expressing P-REX2 or the DHPH by domain by retroviral infection, as measured by western blotting. The phosphorylation status of T308AKT was not detectable under normal growth conditions in MCF10A cells. *B)* Proliferation of MCF10A cells expressing P-REX2 or DHPH when cultured in reduced growth factor conditions (0.1% serum). Cell density was measured using crystal violet staining. *C)* Microscopy of acini morphology in MCF10A cells expressing P-REX2 or DHPH as indicated when grown in 3-D basement membrane culture. *D)* P-REX2 protein levels in breast cancer cell lines as determined by western blotting.

Figure 2.3. **P-REX2 cooperates with PI3K mutants.** *A)* P-REX2 expression levels in PTEN wild-type breast tumors without PIK3CA–activating mutations (left) and with them (right) (P = 0.014; two-tailed t test). *B)* Levels of phosphorylated AKT473 in MCF10A cells expressing combinations of P-REX2 or PI3K[EK] by retroviral infection determined by western blotting. *C)* Proliferation in the absence of all growth factors and serum in MCF10A cells expressing P-REX2 and PI3K[EK], as determined by crystal violet staining. *D)* Quantification of colony formation of MCF10A cells expressing P-REX2 and PI3K[EK] grown in soft agar after 14 days. (**P < 0.01; t test) (D) Microscopy of acini morphology of MCF10A cells expressing combinations of PI3K[EK] and P-REX2 as indicated when grown in a 3-D basement membrane culture.

Figure 2.4. **P-REX2 and c-Myc have increased copy number in breast cancer and cooperate to increase cellular proliferation.** *A)* Copy number analysis of chromosome 8q in breast tumor samples. *B)* Western blot analysis of pAKT473 levels in MCF10A cells overexpressing P-REX2 and c-Myc in combination by retroviral infection. *C)* Proliferation of MCF10A cells expressing P-REX2 and c-Myc alone or in combination as indicated when cultured in reduced growth factor conditions. Cell density was measured using crystal violet staining *D)* Microscopy of acini morphology of MCF10A cells expressing P-REX2 or c-Myc alone or in combination as indicated when grown in 3-D basement membrane culture.

Figure 2.5. **Cooperation of P-REX2 and NeuT results in tumor formation in xenograft experiments.** *A)* P-REX2 and NeuT were expressed by retroviral expression

and protein levels and pAKT473 levels were determined by western blotting. *B)* $1X10^6$ MCF10A cells expressing NeuT, P-REX2, or both in combination were injected into the mammary fat pad of immunodeficient mice. Tumors were allowed to reach and tumor samples were collected at that point, n=4. *C)* H&E staining of a representative tumor sample.

Figure 2.6. **Analysis of P-REX2 activating mutants.** *A)* A physical map of the P-REX2a mutations and their associated tumors. *B)* Expression of P-REX2 mutants in MCF10A cells determined by western blotting. *C)* Western blot analysis of P-REX2 mutant and pAKT473 expression levels in PI3KCA E545K knock-in MCF10A cells. *D)* Quantification of colony formation of PI3KCA E545K knock-in MCF10A cells expressing control vector, WT P-REX2 or P-REX2 mutants grown in soft agar after 14 days. *E)* Proliferation of E545K knock-in or control MCF10A cells expressing control vector, WT P-REX2 or mutant P-REX2 after three days of growth in reduced growth factor medium. Cell density was measured using crystal violet staining.

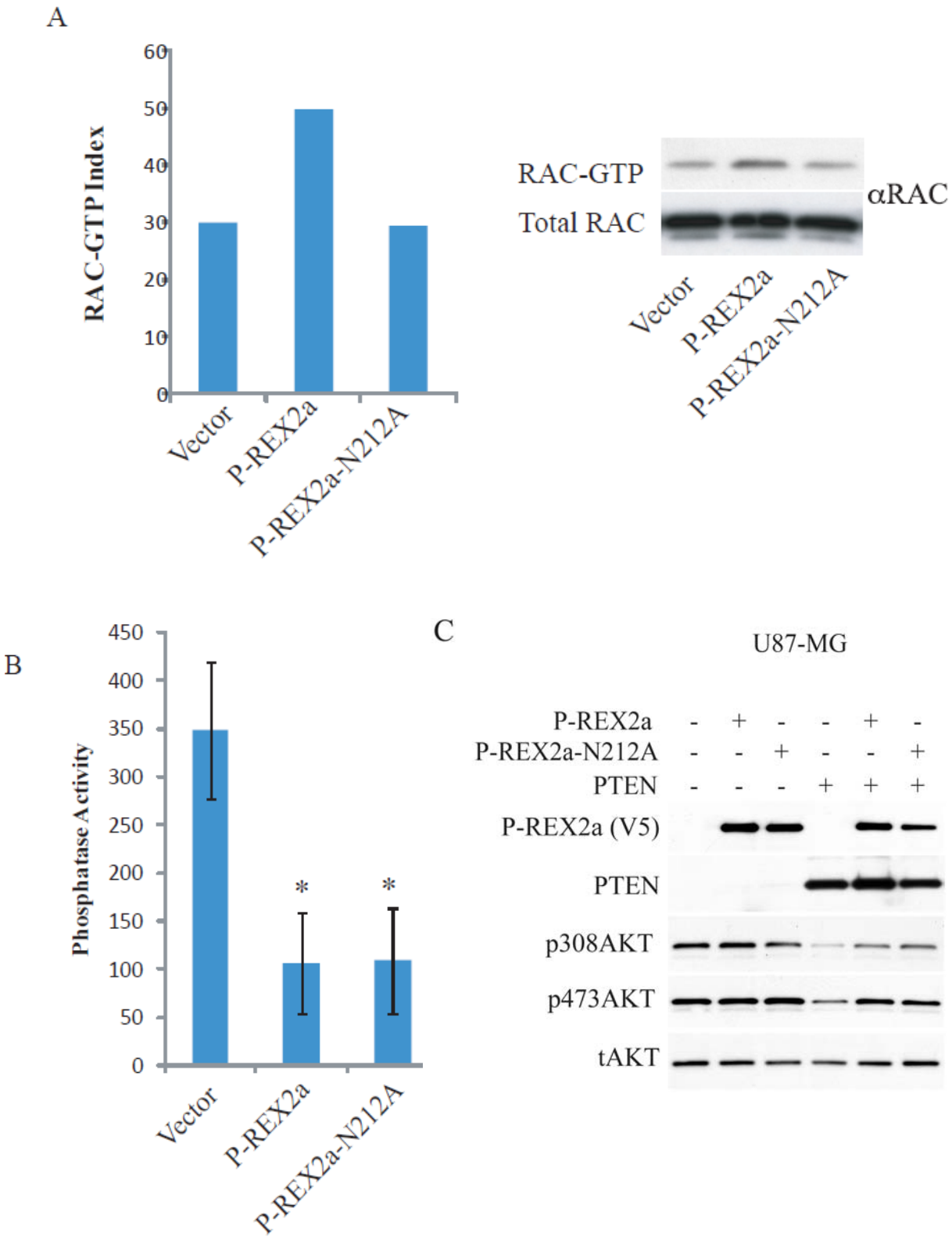
A
RAC-GTP Index
60
50
40
30
20
10
0
Vector
P-REX2a
P-REX2a-N212A
RAC-GTP
Total RAC
αRAC
Vector
P-REX2a
P-REX2a-N212A
B
Phosphatase Activity
450
400
350
300
250
200
150
100
50
0
*
*
Vector
P-REX2a
P-REX2a-N212A
C
U87-MG
P-REX2a - + - - + -
P-REX2a-N212A - - + - - +
PTEN - - - + + +
P-REX2a (V5)
PTEN
p308AKT
p473AKT
tAKT

FIGURE 2.1

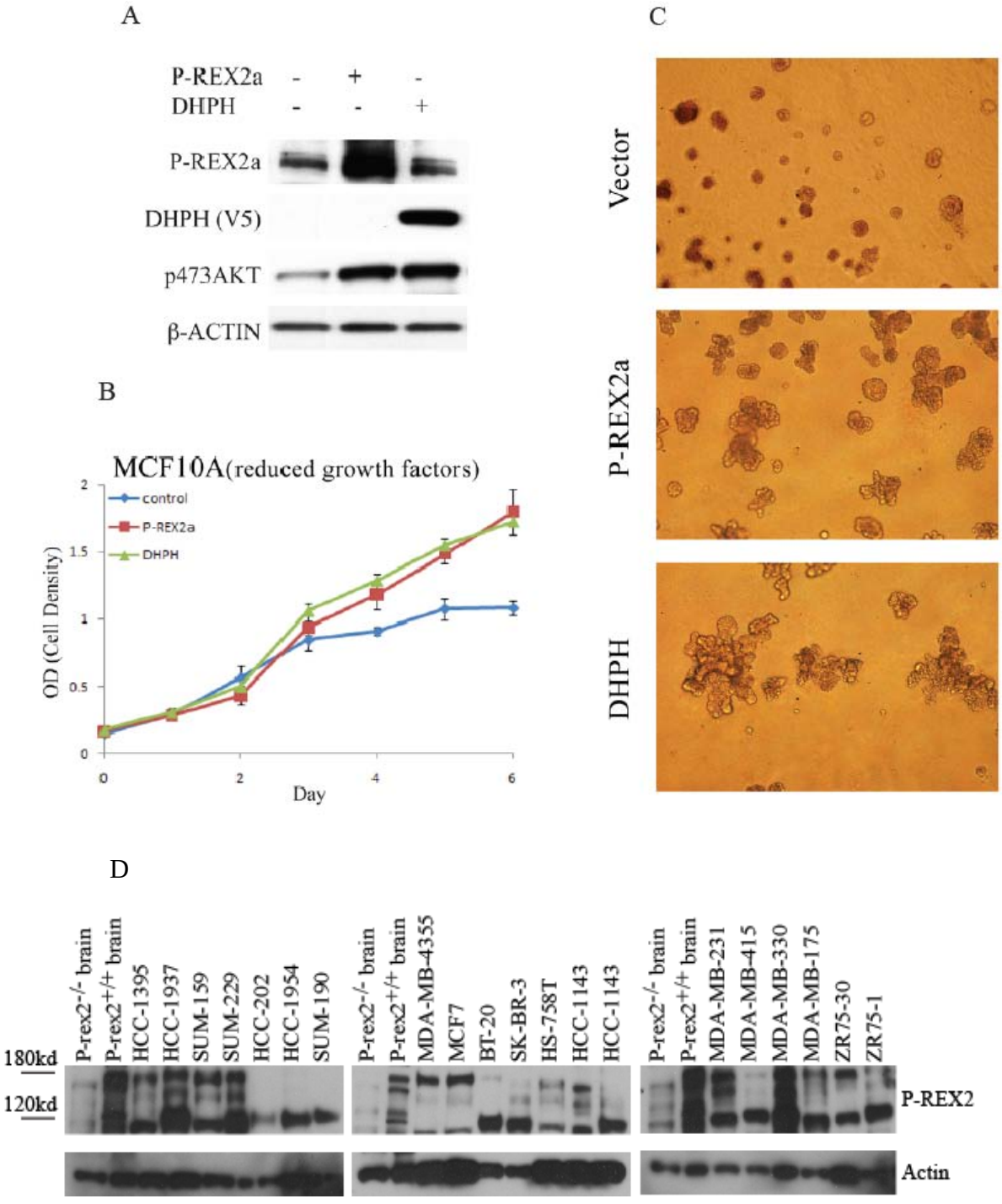
A
P-REX2a - + -
DHPH - - +
P-REX2a
DHPH (V5)
p473AKT
β-ACTIN
B
MCF10A(reduced growth factors)
control
P-REX2a
DHPH
OD (Cell Density)
Day
C
Vector
P-REX2a
DHPH
D
P-rex2-/- brain
P-rex2+/+ brain
HCC-1395
HCC-1937
SUM-159
SUM-229
HCC-202
HCC-1954
SUM-190
MDA-MB-4355
MCF7
BT-20
SK-BR-3
HS-758T
HCC-1143
MDA-MB-231
MDA-MB-415
MDA-MB-330
MDA-MB-175
ZR75-30
ZR75-1
180kd
120kd
P-REX2
Actin

FIGURE 2.2

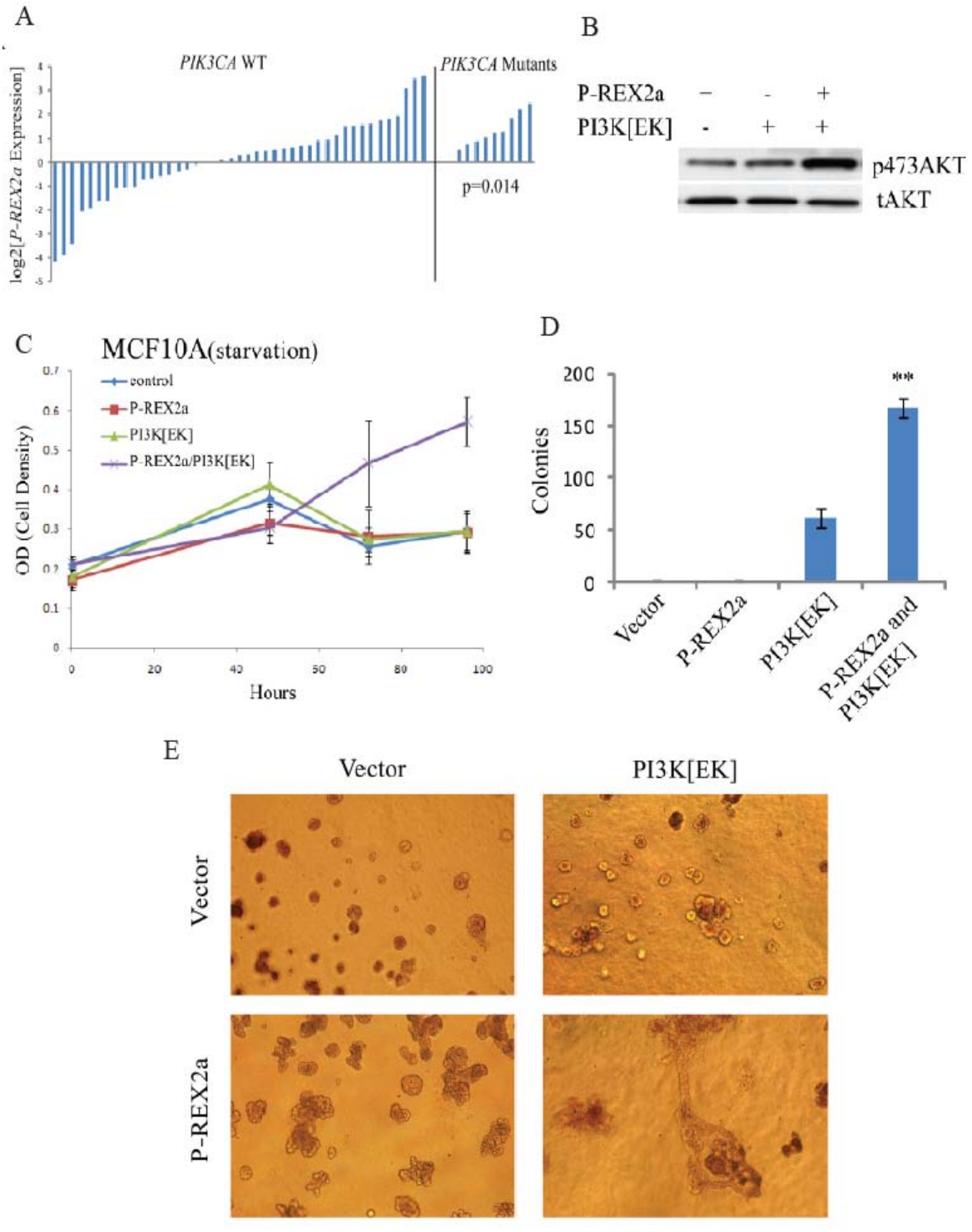
A
PIK3CA WT
PIK3CA Mutants
log2[P-REX2a Expression]
p=0.014
B
P-REX2a
PI3K[EK]
p473AKT
tAKT
C
MCF10A(starvation)
control
P-REX2a
PI3K[EK]
P-REX2a/PI3K[EK]
OD (Cell Density)
Hours
D
Colonies
***
Vector
P-REX2a
PI3K[EK]
P-REX2a and PI3K[EK]
E
Vector
PI3K[EK]
Vector
P-REX2a

FIGURE 2.3

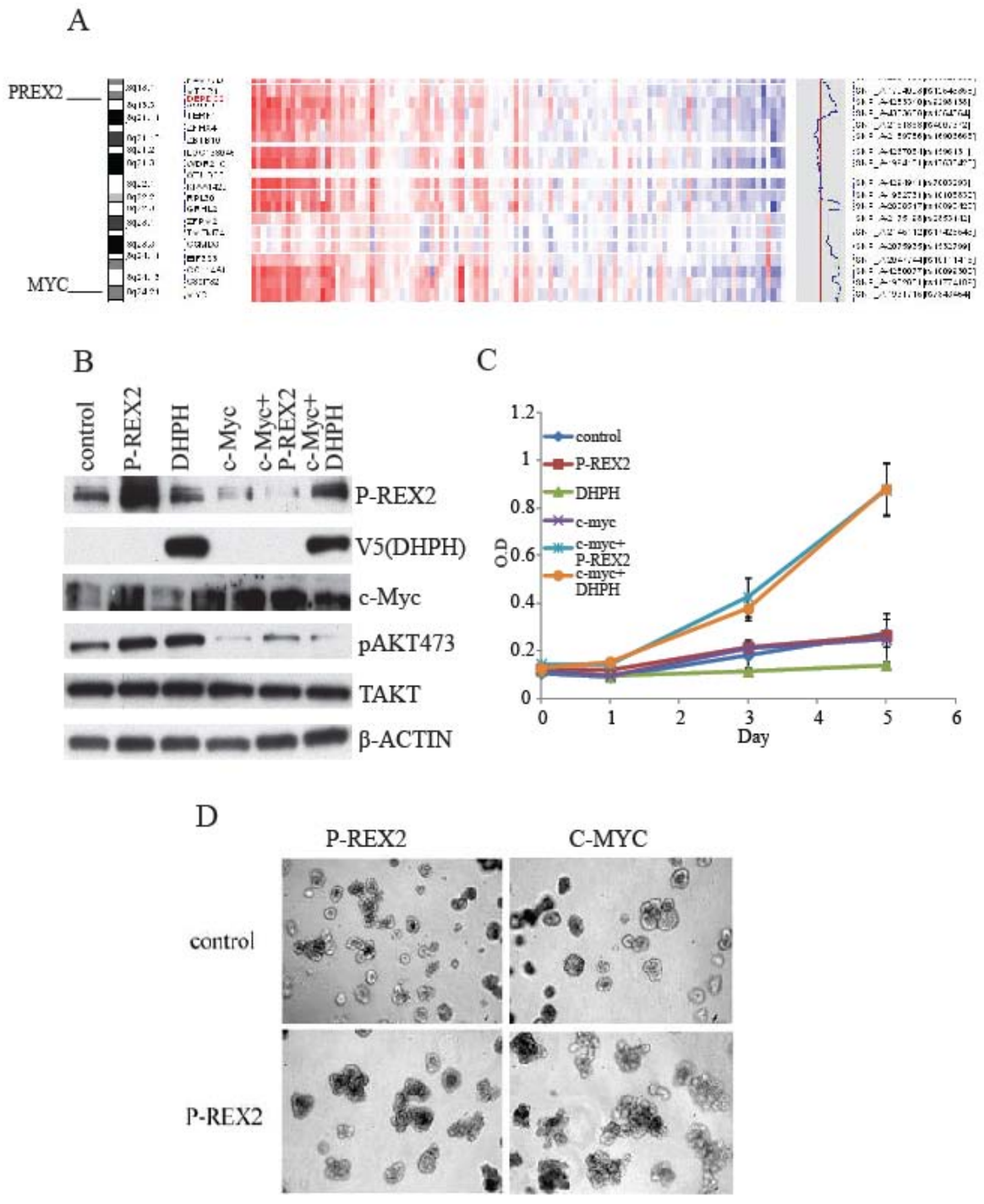
A
PREX2
MYC
B
control
P-REX2
DHPH
c-Myc
c-Myc+ P-REX2
c-Myc+ DHPH
P-REX2
V5(DHPH)
c-Myc
pAKT473
TAKT
β-ACTIN
C
O.D
Day
control
P-REX2
DHPH
c-myc
c-myc+ P-REX2
c-myc+ DHPH
D
P-REX2
C-MYC
control
P-REX2

FIGURE 2.4

A

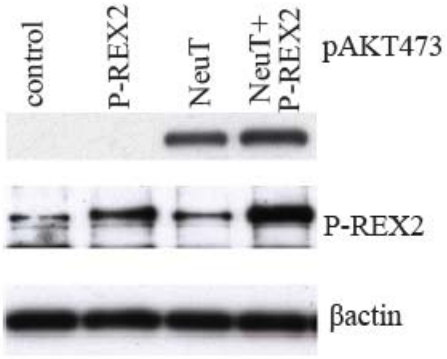

B

MCF10A Cell Line	
P-REX2	0/4
NeuT	0/4
P-REX2 + NeuT	4/4

C

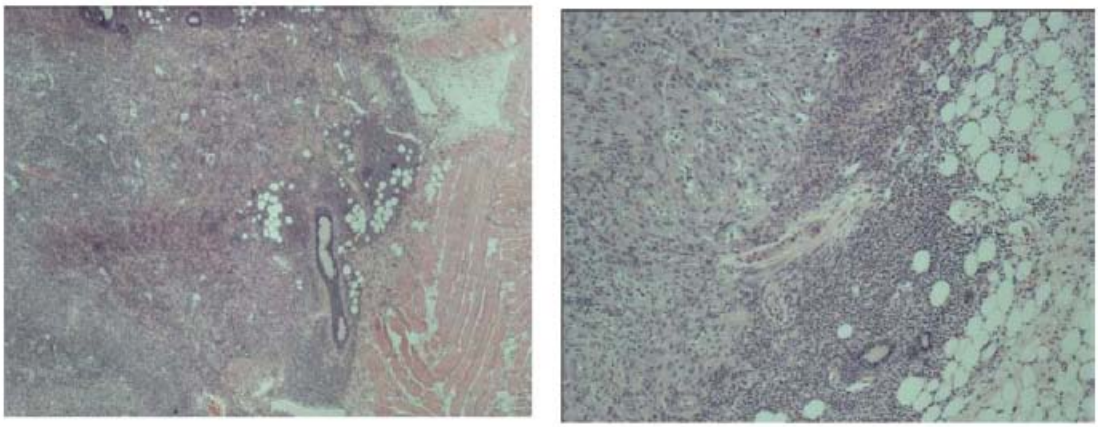

4X 10X

H&E

FIGURE 2.5

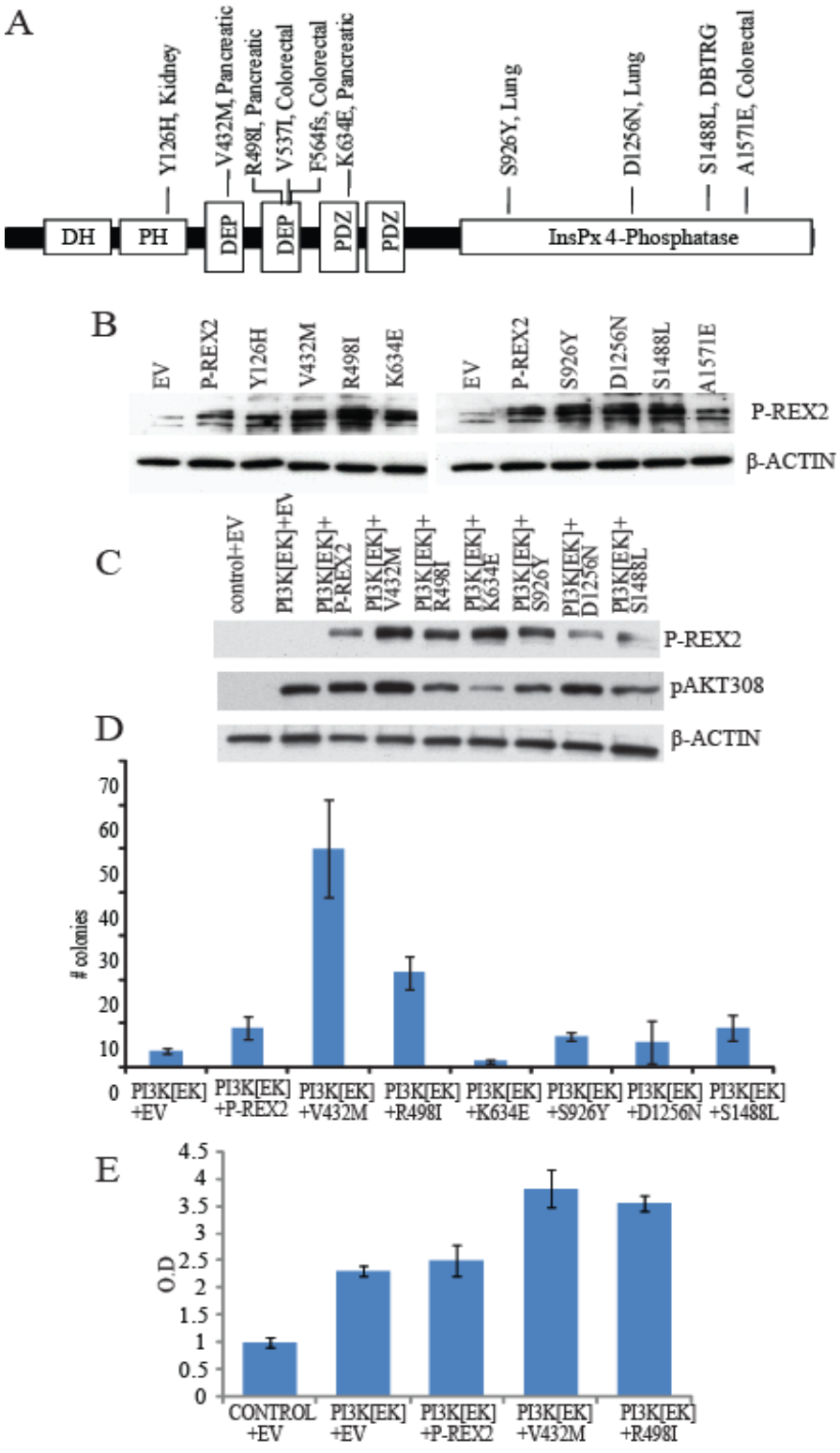
A
Y126H, Kidney
V432M, Pancreatic
R498I, Pancreatic
V537I, Colorectal
F564fs, Colorectal
K634E, Pancreatic
S926Y, Lung
D1256N, Lung
S1488L, DBTRG
A1571E, Colorectal
DH
PH
DEP
DEP
PDZ
PDZ
InsPx 4-Phosphatase
B
EV
P-REX2
Y126H
V432M
R498I
K634E
EV
P-REX2
S926Y
D1256N
S1488L
A1571E
P-REX2
β-ACTIN
C
control+EV
PI3K[EK]+EV
PI3K[EK]+ P-REX2
PI3K[EK]+ V432M
PI3K[EK]+ R498I
PI3K[EK]+ K634E
PI3K[EK]+ S926Y
PI3K[EK]+ D1256N
PI3K[EK]+ S1488L
P-REX2
pAKT308
β-ACTIN
D
colonies
70
60
50
40
30
20
10
0
PI3K[EK] +EV
PI3K[EK] +P-REX2
PI3K[EK] +V432M
PI3K[EK] +R498I
PI3K[EK] +K634E
PI3K[EK] +S926Y
PI3K[EK] +D1256N
PI3K[EK] +S1488L
E
O.D
4.5
4
3.5
3
2.5
2
1.5
1
0.5
0
CONTROL +EV
PI3K[EK] +EV
PI3K[EK] +P-REX2
PI3K[EK] +V432M
PI3K[EK] +R498I

FIGURE 2.6

CHAPTER III

P-REX2 Regulates Insulin Dependent PI3K Signaling and Glucose Metabolism *in vivo*

Cindy Hodakoski, Benjamin Hopkins, Nicole Steinbach, Karen Anderson, Phillip Hawkins, Len Stephens, Ramon Parsons

ABSTRACT

Insulin signaling regulates glucose metabolism by promoting glucose uptake in the muscle and fat and glucose production in the liver. PTEN negatively regulates insulin signaling by dephosphorylating PI(3,4,5) to PI(4,5), therefore reducing insulin stimulated AKT phosphorylation and activation of downstream targets. P-REX2 inhibits PTEN phosphatase activity, and we have shown that P-REX2 overexpression results in increased PI3K signaling and proliferation. However, it is not known in P-REX2 has a physiological role in insulin signaling. Here, we report that disruption of P-rex2 in fibroblasts results in reduced insulin and IGF-1 stimulated PI3K signaling. In addition, PTEN phosphatase activity is decreased following insulin stimulation, and this is dependent on P-rex2. We identified an interaction between P-REX2 and phosphorylated insulin, and observed P-REX2 mediated PTEN membrane localization following insulin stimulation. *In vivo*, deletion of P-rex2 leads to glucose and insulin intolerance, as well as reduced insulin stimulated PI3K signaling in liver and fat tissue. PTEN activity is increased in *Prex2* deleted liver samples and corresponds with decreased PIP3 levels. These results suggest that P-Rex2 regulates insulin stimulated PTEN inhibition, which in turn affects insulin signaling in the fat and liver and glucose metabolism *in vivo*.

INTRODUCTION

Insulin signaling is a key regulator of glucose homeostasis in the cell. Insulin stimulates glucose uptake in adipose and muscle tissue and regulates glucose production and uptake in the liver. Impaired glucose uptake and reduced insulin sensitivity results when cells do not respond to normal levels of circulating insulin, which contributes to the development of metabolic diseases such diabetes mellitus type 2 and obesity (White and Kahn, 1994; Kruszynska et al., 1996). After secretion by pancreatic β cells, insulin binds to the insulin receptor (IR) which is a member of the family of receptor tyrosine kinases. The PI3K pathway is then activated following receptor autodephophorylation and phosphorylation of substrates such as IRS1 and IRS2 (Holman et al., 1997; Shepard et al., 1998).

Insulin stimulated activation of the of the PI3K pathway results in the phosphorylation and activation of the serine/threonine kinase AKT. AKT has been shown to be a key regulator in the maintenance of proper glucose metabolism in the cell. Mice deficient for *Akt2* have elevated blood glucose and serum insulin levels and display reduced glucose tolerance and insulin resistance in skeletal muscle (Cho et al, 2001; Garofalo et al, 2003). Furthermore, loss of AKT1 and AKT2 in cultured adipocytes following expression of dominant negative AKT or siRNA targeting *Akt1* and *Akt2* results in decreased insulin stimulated translocation of GLUT4, reduced glucose uptake, and impaired glycogen synthesis (Katome et al., 2003; Jiang et al., 2003).

Insulin signaling and activation of downstream targets is negatively regulated by the dual specificity and lipid phosphatase PTEN. PTEN opposes insulin response by dephosphorylating PIP3 to PI(4,5)P2, inhibiting PIP3 mediated recruitment and activation of AKT (Maehama and Dixon, 1998; Stambolic et al., 1998). PTEN is a critical regulator of glucose homeostasis. *Pten* haploinsufficient mice are resistant to diabetes induced by loss of *Irs2*, as reduced *Pten* levels in these mice restored normal glucose metabolism and β cell islet function (Kushner et al., 2005). Furthermore, loss of *Pten* by antisense oligonucleotide delivery results in increased PI3K signaling in cultured liver cells, as well as increased insulin sensitivity in *db/db* and *ob/ob* mice (Butler et al., 2002). Tissue specific *Pten* knockout mice have also been utilized to examine the role of PTEN in insulin signaling and glucose metabolism. Specific loss of *Pten* in adipose tissue results in increased insulin sensitivity and glucose tolerance, as well as protection from streptozotocin-induced diabetes. Conversely, overexpression of PTEN in cultured adipocytes decreased insulin induced AKT phosphorylation, glucose uptake, and GLUT4 translocation. However, microinjection of anti-PTEN antibody had the inverse effect, increasing GLUT4 translocation (Nakashimi et al., 2000; Ono et al., 2001; Tang et al., 2005). *Pten* loss also affects insulin signaling in muscle. Specifically, muscle specific deletion of *Pten* protects mice from diabetes and insulin resistance induced by a high fat diet (Wijesekara et al., 2005; Kurlawalla-Martinez et al., 2005).

We have previously reported that the Rac-GEF P-REX2 directly interacts with PTEN and inhibits its phosphatase activity. Furthermore, knockdown of P-REX2 in PTEN positive cell lines results in decreased PI3K signaling and cellular proliferation, while

overexpression of P-REX2 in normal mammary epithelial cells causes increased PI3K signaling, increased growth and cellular transformation. Upon stimulation with serum, insulin, and PDGF, PTEN and P-REX2 co-localize at the plasma membrane (Fine et al., 2009). Loss of P-REX2 in endothelial cells results in decreased Rac1 activation and migration, and deletion of *Prex2* in-vivo results in disrupted Purkinje cell morphology and motor coordination (Donald et al., 2008; Li et al., 2005). However, the physiological role of P-REX2 mediated inhibition of PTEN in the PI3K pathway has yet to be thoroughly examined. Here, we used a gene-trap method to generate mice deleted for *Prex2*. We report that deletion of *Prex2* results in decreased insulin and IGF-1 stimulated PI3K signaling in MEFs and in-vivo, specifically in the liver and adipose tissue. A corresponding increase in PTEN phosphatase activity was also observed after insulin stimulation in the absence of P-rex2, and this results in intolerance to glucose and resistance to insulin.

EXPERIMENTAL PROCEDURES

Antibodies- Antibodies against phospho-AKT (Thr308 and Ser473), total AKT, phospho-GSK3-β (Ser9), phospho-FOXO1/3a (Thr24/Thr32), phospho-EGFR (Tyr1173), phospho-PDGFR (Tyr754), phospho-IGF-IRβ (Tyr1135/1136)/IRβ (Tyr1150/1151) and PTEN 138G6 were purchased from Cell Signaling (Danvers, MA). Anti-V5 antibody was obtained from Invitrogen (Carlsbad, CA). P-REX2 rabbit polyclonal antibody to amino acids 960-973 was made by Zymed Laboratories (San Francisco, CA). Vinculin antibody and actin antibody were purchased from Sigma (St. Louis, MO), and phosphotyrosine 4G10 was obtained from Millipore (Billerica, MA). Secondary antibodies directed against rabbit and mouse IgG conjugated to HRP were purchased from Pierce (Rockford IL).

Generation of Prex2 knockout mice and genotyping- To generate mice deleted for *Prex2*, the Sanger Institute Gene Trap Resource was utilized. In brief, the E14 embryonic stem cell (ES) line clone AH0440 was purchased from the Wellcome Trust Sanger Institute. In brief, this cell line was created by high throughput gene trapping, resulting in the insertion of a reporter gene containing a β-galactosidase and neomycin phosphotransferase II fusion between exons 4 and 5 of *Prex2*. The location of this reporter gene in the ES cells was confirmed by RT-PCR. The mutant allele was transmitted through the germline, and mice heterozygous for the mutant allele were intercrossed to generate homozygous mutant progeny. Mutant mice were then backcrossed with C57BL/6 mice for eight generations to generate mice of the same

background. Genomic DNA was for genotyping was isolated from tail samples from three week old mice. Genotyping the mutant allele was done by PCR using forward primer 5' TGA TAG GAT GCATGG GAC AA 3', which anneals to intron 4 outside of the reporter gene, and reverse primer 5' CAA CCT CCG CAA ACT CCT AT 3', which anneals to the reporter gene. Genotyping the wild-type allele was done using forward primer 5' TCG ACT CCT GAA GAT TTG ACC 3' and reverse primer 5' TGA CCA CGT TGC CTT GACTA 3', which amplified a region of intron 4 which is deleted in the mutant allele.

Harvest and culture of mouse embryonic fibroblasts- Fetuses were harvested between days 12.5-14.5. The head, which was used for genotyping, liver, and large blood clots were removed, and the embryo was washed in 2 mL of PBS. The tissue was minced with a razor blade, and 2 mL of 0.05% tryspin-EDTA (Cellgro, Herndon, VA) was added. Minced tissue was incubated at 37 ºC for 10 minutes, and then pipetted vigorously until cells were in a single suspension. I mL of cells was placed in a T25 flask. MEFs were cultured in Dulbecco's minimal essential medium (DMEM) supplemented with 10% FBS (Invitrogen), 1% of 200mM L-glutamine, plus 100 IU penicillin and 100 µg/mL streptomycin (Cellgro).

MEF Growth Factor Stimulation, lysate collection, and western blotting- For growth factor stimulation, MEFs were starved in DMEM for 3 hours and then incubated with 10 µg/mL bovine insulin, 20 ng/mL IGF-1, 20 ng/mL PDGF, and 20 ng/mL EGF as indicated (Sigma). Cells were lysed with 2X Laemlli sample buffer (125 mM Tris pH

6.8, 10% 2-mercaptoethanol, 4% SDS, 20% glycerol, 0.05% bromophenol blue). Lysates were analyzed by SDS-PAGE on 4-20% or 4-12% Tris-Gylcine gels (Invitrogen) and transferred onto PVDF using a semi-dry apparatus (Biorad, Hercules, CA). Membranes were blocked with 5% non fat milk in TBST and incubated with the appropriate antibody overnight at 4°C. Membranes were washed three times with TBST and the appropriate secondary antibody was added for 1 hour at room temperature. Blots were developed using ECL (Pierce) and audioradiography film (Denville Scientific).

Cell proliferation assay – 4000 cells were plated per well in a 48 well plate in at least triplicate for each experiment. Cells were then allowed to proliferate and fixed at indicated time points in 0.05% crystal violet in 10% formalin. Each well was then washed multiple times with PBS. For relative quantification of cell density, the crystal violet was re-solubilized in 10% acetic acid and the absorbance at 595nm was recorded by a MicroQuant plate spectrophotometer.

Transfection and immunoprecipitation of HEK293 cells – HEK293 cells were grown in Dulbecco's minimal essential medium supplemented with 10% FBS plus 100 IU penicillin and 100 µg/mL streptomycin. Transfections were performed using Lipofectamine 2000 (Invitrogen) following the protocol of the manufacturer. 24 hours after transfection, HEK293 cells were starved in unsupplimented DMEM overnight, and stimulated with either insulin (10 µg/mL) or EGF (20 ng/mL) for 15 minutes. Cells were then rinsed with cold PBS and lysed with Triton-containing lysis buffer (150 mM NaCl, 25 mM Tris pH 7.4, 1% Triton X-100, 1 mM EDTA) supplemented with eukaryotic

protease cocktail inhibitor (Sigma) and phosphatase inhibitors sodium orthovanate and sodium fluoride. Lysates were vortexed, sonicated, and clarified by high speed centrifugation for 30 minutes, and precleared with normal mouse IgG with protein A/G PLUS-agarose (Santa Cruz, CA) for 1 hour at 4°C. Protein complexes were then immunoprecipitated with V5-agarose plus 20 µL protein A/G PLUS- agarose overnight at 4°C and elute in 2X sample buffer.

Immunofluorescence- U87 cells were plated on gelatin coated glass coverslips and transfected with Lipofectamine 2000 with FLAG-PTEN plus pCDNA3.1 empty vector or PTEN-V5. 18 hours after transfection cells were starved for 6h and stimulated with Insulin (final concentration: 10µg/ml) for 15 min. Cells were fixed in 2% paraformaldehyde and permeablized/blocked in 0.1% Triton X-100/10% goat serum/PBS. Antibody dilutions (Anti-V5 antibody 1:500, and PTEN 1:200) were prepared in the permeabilization/blocking solution and incubated overnight. Secondary antibodies were used at 1:500 after washing. Coverslips were mounted with Prolong Gold Antifade with DAPI and visualized with a Nikon Eclipse 80i with a CoolSnap HQ2 CCD camera.

Glucose and insulin tolerance test- For glucose challenge tests, six week old male mice were starved overnight. After measuring fasting blood glucose levels using the OneTouch Ultra glucometer, mice were injected intraperitoneally with 30% glucose per kg. Blood glucose was measure at 15, 30, 45, 60, 90, and 120 minute time points. For insulin tolerance tests, eight week old fed male mice were injected intraperitoneally with

0.75 U/kg bovine insulin (Sigma), and blood glucose was measured before injection, and post injection at 15, 30, 45, 60, 90, and 120 minutes.

In-vivo insulin signaling and western blot analysis- Eight week old male mice were fasted overnight. For collection of starved tissue, fasted mice were sacrificed by cervical dislocation and liver, fat, and hind leg skeletal muscle was collected from the starved samples. For insulin stimulation, fasted mice were injected with 0.75 mU/g bovine insulin intraperitoneally and liver, fat, and skeletal muscle was collected 2 minutes or 15 minutes after stimulation. Tissues were flash frozen and stored at -80 ºC. For western blot analysis, frozen tissue was thawed on ice and homogenized for 30 seconds at high speed using a Tissuemiser (Fisher Scientific, Pittsburgh, PA) in Triton-containing lysis buffer supplemented with eukaryotic protease cocktail inhibitor.

PTEN phosphatase assays- For analysis of MEFs, cells were starved in plain DMEM for three hours and then stimulated with 10 µg/mL insulin for 10 minutes. Cells were washed with cold TBS and lysed with Triton-containing lysis buffer supplemented with eukaryotic protease cocktail inhibitor. For liver analysis, flash frozen liver tissue from mice fasted for 16 hours or stimulated with bovine insulin at 10 mU/g and homogenized in Triton-containing lysis buffer (150 mM NaCl, 25 mM Tris pH 7.4, 1% Triton X-100, 1 mM EDTA) for 30 seconds. Lysates were then sonicated and clarified by high speed centrifugation for 30 minutes, and precleared with normal rabbit IgG and protein A/G PLUS agarose for 1 hour at 4°C. 1 mg of total protein was next incubated with PTEN 138G6 antibody overnight at 4°C, and the beads were then washed extensively with

phosphatase buffer (PB) (150 mM NaCl, 25 mM Tris-HCl pH 7.5). The beads were preincubated in PB at 37°C for 10 minutes and then collected by centrifugation at low speed to remove the supernatant. Beads were then incubated with 20 µM soluble di-C8-D-myo-Phosphatidylinositol 3,4,5-trisphosphate (Echelon, Salt Lake City, UT) and PB at a final volume of 50 µL and incubated at 37°C for 30 minutes. The beads were removed from the reaction mixture by centrifugation at low speed, and the supernatant was added to 100 µL Biomol Green reagent (Enzo, Farmingdale, NY) which stopped the reaction and absorbance at 620 nm was read after 15 minutes.

Mass spectrometry measurements of inositol lipids

Mass spectrometry was used to measure inositol lipid levels essentially as described previously (Clark et al, Quantification of PtdInsP3 molecular species in cells and tissues by mass spectrometry, Nat Meth (2011),8:3. 267), using a QTRAP 4000 (AB Sciex) mass spectrometer and employing the lipid extraction method described for mouse liver tissue. Measured C18:0 C20:4 PIP3 signals from each sample were expressed as a ratio of the C18:0 C20:4 PIP2 signal to account for cell variation in each sample.

RESULTS

Generation of *Prex2* knockout mice

We used a gene trap method to generate a mouse line with a deletion of the *Prex2* gene. The ES cell clone AH0440 was purchased from the Sanger Institute Gene Trap Resource. These cells have a gene trap cassette containing a splice acceptor site, a β-galactosidase and neomycin phosphotransferase II fusion ending with a stop codon, and polyadenylation sequence. This cassette is inserted between exons 4 and 5 of *Prex2*, which is in the region that encodes the DH domain of P-rex2 (Fig 3.1A). The insertion of this reporter gene also results in a deletion of exons 5 and 6, as shown by PCR of genomic DNA from ES cells (Fig 3.1A). The mutant allele was transmitted through the germline, and heterozygous mutant mice were intercrossed to generate *Prex2*$^{-/-}$ mice, which were then backcrossed with C57BL/6 mice for eight generations. PCR genotyping is shown (Fig 3.1B). We confirmed loss of P-rex2 protein in various tissue samples by western blot analysis (Fig 3.1C). Alternative splicing may result in a transcript spliced directly from exon 4 to exon 7, therefore bypassing the gene-trap vector. However, the absence of a protein band at the predicted size of 170kd suggests that this is likely not occuring. Furthermore, due to the deletion of exons 5 and 6, this truncated protein would be expected to be nonfunctional. *Prex2*$^{-/-}$ mice were born with the expected mendelian frequency, were fertile and appeared healthy.

Insulin and IGF-1 stimulated PI3K signaling is decreased in *Prex2*$^{-/-}$ MEFs

It is well established that PTEN is a negative regulator of PI3K signaling. Given that P-REX2 inhibits PTEN function, it may also be important for PI3K regulation. To test this possibility, we generated *Prex2*$^{+/+}$ and *Prex2*$^{-/-}$ MEFs harvested from E12.5-14.5 embryos from backcrossed mice. We first determined the level of P-rex2 expression in MEFs to ensure that they were appropriate for the study of P-rex2. Analysis of lysates from a wild-type and mutant pair revealed that P-rex2 was indeed expressed in wild-type cells, and confirmed that P-rex2 was lost at the protein level in mutant cells. Next, to examine the effects of *Prex2* deletion on baseline PI3K signaling, we collected lysates from normally proliferating cells. Western blot analysis showed that there was no difference in the AKT phosphorylation between *Prex2*$^{+/+}$ and *Prex2*$^{-/-}$MEFs, suggesting that P-REX2 does not regulate baseline PI3K signaling (Fig 3.2A). Furthermore, loss of *Prex2* in MEFs did not affect cellular proliferation in normal growth medium (Fig 3.2B), further suggesting that baseline PI3K signaling and proliferation are not altered by *Prex2* deletion .

Next, we decided to look more specifically at PI3K signaling in response to certain growth factors over an extended time period. MEFs were starved for 3 hours in DMEM without FBS or L-glutamine, and then stimulated at the indicated time points with insulin, IGF-1, PDGF, or EGF. Western blot analysis revealed that insulin stimulated PI3K signaling was diminished in *Prex2*$^{-/-}$ MEFs. Specifically, a reduction of phosphorylated Akt at Thr308 and Ser473 (pAKT308 and pAKT473) was observed in *Prex2*$^{-/-}$ MEFs at each time point. Phophorlyated Akt levels returned to baseline levels after 30 minutes in *Prex2*$^{-/-}$ MEFs, whereas Akt was still phosphorylated and active 60

minutes after stimulation in *Prex2*$^{+/+}$ MEFs. Downstream targets of insulin activated AKT were similarly affected by P-rex2 loss. Reduced phosphorylation of GSK3-B at Ser9 and FOXO1 and FOXO3 at Thr24 and Thr32 was observed in *Prex2* knockout cells compared to wild-type. However, levels of phosphorylated insulin receptor (IR) were not significantly altered, suggesting that PI3K signaling is being affected downstream of receptor activation. Similarly, *Prex2* loss resulted in disrupted IGF-1 stimulated PI3K signaling. Phosphorylation of AKT308, as well as FOXO1/3a and GSK3-β peaked after 10 minutes of IGF-1 stimulation in wild-type MEFs, and began to regress at 60 minutes. In contrast, knockout MEFs maintained low levels of phosphorylated Akt, GSK3B, and FOXO1/3a during all analyzed time points. IGF-1R phosphorylation remained elevated at 60 minutes in *Prex2*$^{-/-}$ MEFs, perhaps due to a lack negative feedback regulation. Deletion of P-rex2 had no effect on PI3K signaling stimulated by EGF or PDGF (Fig 3.2C). Overall, our data suggest that P-REX2 loss results in reduced PI3K signaling specifically in response to insulin and IGF-1 in MEFs.

Insulin stimulated PTEN inhibition is dependent on P-rex2

We have shown that disruption of P-REX2 results in decreased PI3K pathway activation only in response to insulin and IGF-1. We next wanted to determine if reduced signaling observed was due to disrupted P-REX2 inhibition of PTEN. To this end, we collected lysates from starved or insulin stimulated primary *Prex2*$^{+/+}$ or *Prex2*$^{-/-}$ MEFs and immunoprecipitated PTEN complexes with anti-PTEN 138G6 antibody conjugated to Protein A/G beads. After extensive washes with PB buffer, we performed PTEN phosphatase assays by incubating protein-bound beads with soluble di-C8 PIP3 substrate

at 37°C for 30 minutes. After quantifying free phosphate using malachite green, we observed that PTEN was equally active in *Prex2*$^{+/+}$ or *Prex2*$^{-/-}$ MEFs under starvation conditions. Interestingly, when MEFs were stimulated with insulin, PTEN activity was reduced by 45.3% in *Prex2*$^{+/+}$ MEFs, but was unchanged in *Prex2*$^{-/-}$ MEFs (Fig 3.3A). This result provides insight into insulin dependent PTEN regulation in MEFs. Following insulin stimulation, it appears that PTEN activity is reduced, allowing for high PIP3 levels in the cell and therefore, increased activation of AKT. Furthermore, this mode of regulation is dependent on P-REX2, because this reduction in phosphatase activity does not occur when P-REX2 is absent.

P-REX2 interacts with phosphorylated insulin receptor following insulin stimulation

P-REX2 mediated inhibition of PTEN appears to be important for the regulation of insulin stimulated PI3K signaling specifically. To further understand this growth factor specificity, we examined the affinity of P-REX2 for activated membrane receptors. HEK293 cells were transfected with P-REX2-V5, and then stimulated with insulin or EGF following overnight starvation. Lysates were immunoprecipitated with V5-agarose, and eluted protein complexes were analyzed by western blotting. P-REX2 interacted with phosphorylated-IR from insulin stimulated cells, but showed no affinity for phospho-EGFR from cells stimulated with EGF (Fig 3.3B). This result suggests that P-REX2 interacts with phosphorylated IR following receptor activation, but we cannot rule out a possible interaction with unphosphorylated IR as well.

To determine if PTEN is transported with P-REX2 to activated IR at the cell membrane, we analyzed PTEN localization alone or in combination with P-REX2 following insulin stimulation by immunofluorescence. P-REX2 expression led to an increase in the number of cells with PTEN membrane localization compared to cells expressing PTEN alone. The cell shown is representative of average localization observed (Fig 3.4). This result suggests that following insulin stimulated IR autophosphorylation, the P-REX2-PTEN complex is recruited to the membrane through the interaction of P-REX2 with activated IR, allowing for P-REX2 inhibition of PTEN and full activation of PI3K signaling.

Deletion of *Prex2* leads to decreased glucose uptake and insulin resistance *in-vivo*

Increased PTEN phosphatase activity due to P-REX2 deletion results in decreased insulin stimulated PI3K downstream signaling in MEFs. Because insulin signaling tightly regulates glucose homeostasis, we next tested whether *Prex2* null mice were defective for glucose uptake. Six week old $Prex2^{+/+}$ and $Prex2^{-/-}$ mice were fasted overnight and then injected intraperitoneally with a bolus of glucose. Blood glucose levels were recorded over time and normalized to the levels before glucose injection. Blood glucose levels peaked 15 minutes after glucose delivery, and $Prex2^{-/-}$ mice exhibited 22% higher blood glucose levels compared to $Prex2^{+/+}$ mice at this time. Blood glucose levels of $Prex2^{-/-}$ remained elevated throughout the entire time course, and after 120 minutes, were 222.6% higher than baseline, compared to 11.5% for $Prex2^{+/+}$ mice (Fig 3.5A). Insulin tolerance tests were also performed. Eight week old fed mice were injected intraperitoneally with insulin and blood glucose levels were measured over time. As expected, insulin injection resulted in an initial drop in blood glucose levels, whcih slowly began to return to

baseline levels. At 120 minutes post injection, *Prex2*$^{+/+}$ low blood glucose levels were 29.6% below baseline, whereas blood glucose levels in *Prex2*$^{-/-}$ mice were 8.4% above baseline (Fig 3.5). These data suggest that *Prex2* loss causes decreased glucose tolerance as well as increased insulin resistance. Despite differences in glucose homeostasis, there was no significant difference in body weight between *Prex2*$^{+/+}$ and *Prex2*$^{-/-}$ mice at eight weeks. Furthermore, *Prex2*$^{-/-}$ mice did not exhibit fasting hyperglycemia, as fasting glucose levels were the same (Fig 3.5C).

Prex2 deletion results in decreased insulin stimulated PI3K signaling in liver and adipose tissue

Due to decreased glucose tolerance and insulin resistance observed in *Prex2*$^{-/-}$ mice, we decided to examine if P-rex2 loss disrupted insulin stimulated PI3K signaling in liver and adipose tissue, which are highly responsive to insulin and also express high levels of P-rex2. We stimulated starved mice with insulin by intraperitoneal injection and collected tissue samples at the indicated time points. There was a marked decrease in phosphorylated Akt at Thr308 in *Prex2*$^{-/-}$ adipose tissue following insulin stimulation. There was also a corresponding decrease in the phosphorylation of downstream AKT targets, including phosphorylated Foxo1/3a at Thr24/Thr32 as well as phosphorylated Gsk3-β at Ser9. However, despite differences in downstream PI3K signaling, there was no difference in IR phosphorylation between *Prex2*$^{+/+}$ and *Prex2*$^{-/-}$ which suggests that diminished insulin stimulated PI3K signaling occurs downstream of insulin receptor activation (Fig 3.6A).

We next examined insulin signaling in the liver, which regulates glucose metabolism by increasing glycogen synthesis and decreasing gluconeogenesis in response to insulin, resulting in lower circulating blood glucose. After 15 minutes post insulin injection, there was a considerable decrease in phosphorylated Akt at Thr308 in *Prex2*$^{-/-}$ liver during stimulated conditions. There was also a decrease in the phosphorylation of the Akt target protein Gsk3-β at Ser9 in *Prex2*$^{-/-}$ samples, while levels of phosphorylated IR were comparable. While Akt was robustly activated following 2 minutes of insulin stimulation, liver tissue exhibited low levels of Akt activation; however there was still an observed decrease in Akt and Gsk3-β phosphorylation *Prex2*$^{-/-}$ samples. Interestingly, a decrease in phosphorylation was also observed in *Prex2*$^{-/-}$ starved livers (Fig 3.6C).

PTEN activity is increased and PIP3 levels are decreased in insulin stimulated liver from *Prex2*$^{-/-}$ mice

P-Rex2 regulates insulin signaling *in vivo* in specific tissues, however it is unclear whether this occurs through inhibition of PTEN phosphatase activity. We suspected that P-Rex2 ablation would release PTEN from inhibition, resulting in higher phosphatase activity. Therefore, we compared the phosphatase activity of PTEN purified from *Prex2*$^{+/+}$ and *Prex2*$^{-/-}$ livers harvested during fasted and insulin stimulated conditions. Lysates from livers of fasted or insulin stimulated *Prex2*$^{+/+}$ and *Prex2*$^{-/-}$ mice were incubated with either normal rabbit IgG (negative control) or anti-PTEN 138G6 antibody conjugated to protein A/G beads to immunprecipitate PTEN complexes. Phosphatase assays were then performed on protein-bound beads. As expected, PTEN purified from from *Prex2*$^{-/-}$ livers displayed significantly higher phosphatase activity relative to *Prex2*$^{-/-}$

livers. PTEN activity was increased 52% and 38% during fasted and stimulated conditions, respectively (Fig 3.7A). This correlates with our analysis of PI3K signaling in the liver, which showed decreased PI3K downstream signaling in *Prex2*$^{-/-}$ samples during both starvation and stimulation. We can speculate that disrupted insulin stimulation and glucose homeostasis in *Prex2*$^{-/-}$ mice are due increased PTEN activity.

To further examine the effects of P-rex2 loss on PTEN activity in liver, we measured PIP3 levels in liver samples collected following insulin stimulation. If PTEN is indeed more active, we would expect to see lower levels of PIP3 in *Prex2* null tissue samples compared to wild-type. Liver PIP3 levels were measured using high performance liquid chromatography–mass spectrometry, and were then normalized to levels of PIP2. There was no significant difference in PIP3 levels during fasting conditions (Fig 3.7C); however following insulin stimulation, *Prex2*$^{-/-}$ liver had a 37.4% less PIP3 compared to *Prex2*$^{+/+}$ liver (Fig 3.7B). This reduction in liver PIP3 can in part be explained by higher PTEN activity, and supports our finding that PTEN in the liver is more active in the absence of P-REX2.

DISCUSSION

Type II non-insulin dependent diabetes mellitus is a common metabolic disease caused mainly by two specific events, including the inability of liver, tissue, and fat to respond to normal levels of insulin as well as the lack of insulin production by pancreatic β cells to compensate for this insulin resistance (White and Kahn, 1994; Kruszynska et al., 1998). Insulin stimulation of PI3K signaling is regulated in part by the PTEN, as loss of PTEN in specific tissues, including liver, fat, and muscle results in increased insulin sensitivity and glucose metabolism as well as protection from diabetes. Here, we show that P-REX2 mediated inhibition of PTEN is important for the regulation of insulin signaling and the maintenance of glucose homeostasis.

It is well known that PTEN opposes the action of insulin signaling and PI3K activation by converting PIP3 to PIP2. However, the ability of insulin to regulate PTEN activity has not been established. We show here in Figure 2 that in MEFs, the phosphatase activity of PTEN is decreased following insulin stimulation. Furthermore, this inhibition is dependent on P-REX2, as this decrease is not observed in *Prex2*$^{-/-}$ MEFs. Insulin regulation of PTEN was not observed in the liver, likely due to the presence of circulating insulin in the body and PI3K pathway activation by other growth factors including IGF-1 during fasting conditions. Insulin stimulated phosphatase regulation has been demonstrated for other phosphatases, including the protein tyrosine phosphatase 1B (PTP1B). PTP1B is an established negative regulator of insulin signaling by binding to and dephosphorylating IR, inhibiting receptor autophosphorylation. Following insulin

stimulation, activated insulin receptor regulates PTP1B phosphatase activity through direct phosphorylation of tyrosine residues, although reports are conflicting as to whether this leads to activation or inhibition of PTP1B (Dadke et al., 2001; Tao et al., 2001). Therefore, there is precedence for a mechanism of insulin stimulated phosphatase regulation.

In addition to our model of insulin simulated PTEN regulation presented here, it has been shown that PTEN can also be regulated by the hormone leptin. Leptin and insulin are crucial regulators of food intake and energy expenditure, and disruptions in these processes strongly associate with diabetes and obesity. Leptin and insulin bind to receptors on arcuate neurons of the hypothalamus that regulate body weight. (Niswender et al, 2004; O'Rahilly et al., 2007; Schwartz et al., 2005). Leptin and insulin lead to increased PIP3 levels in arcuate neurons and hypothalamic cell lines (Niswender et al, 2003; Xu et al, 2005), and PI3K inhibition prevents leptin and insulin reduction of food intake and neuronal hyperpolarization (Mirshamsi et a1., 2004; Niswender et al, 2001). While insulin stimulates PI3K signaling by activating IR, leptin increases PI3K signaling specifically by inhibiting the activity of PTEN without affecting IRS-1/2 phosphorylation or PI3K activity (Ning et al., 2006). Moreover, it has been demonstrated that leptin, but not insulin, stimulates the phosphorylation and inhibition of PTEN in hypothalamic cell lines and pancreatic β cells (Ning et al., 2009). P-REX2 inhibition of PTEN may therefore be regulated by hormone stimulation in a cell-type specific manner, depending on which contributes most to PI3K pathway activation. In hypothalamic neurons, leptin

may stimulate P-REX2 inhibition of PTEN, whereas insulin regulates PTEN inhibition in the liver and fat.

We have shown in Figure 5 that loss of *Prex2* results in decreased glucose uptake and insulin tolerance. Furthermore, in Figure 6 and 7, we show that this is, at least in part, due to reduced insulin stimulated PI3K signaling in liver adipose tissue and increased PTEN activity. However, we cannot ignore that P-REX2 is also a Rac GEF, and altered Rac activation may contribute to altered glucose metabolism. Indeed, Rac1 is activated by insulin and regulates glucose uptake independent of Akt activation in the muscle. It has been shown that Rac1 is activated in both cultured muscle cells and muscle tissue following insulin stimulation (Ishikura et al., 2008; Jebailey et al., 2004). Furthermore, overexpression of constitutively active Rac1 in muscle cells increased GLUT4 translocation in the absence of insulin, whereas expression of a dominant negative Rac1 or siRNA depletion of Rac1 resulted in decreased insulin stimulated GLUT4 translocation and decreased glucose uptake (Jebailey et al., 2007; Ueda et al., 2008). It has also been reported that Rac-GEFs can affect glucose metabolism. For instance, expression of the PI3K activated Rac-GEF FLJ00068 increases insulin stimulated GLUT4 translocation in muscle cells, whereas GLUT4 translocation was decreased following knockdown of FLJ00068 (Ueda et al., 2008). These findings suggest that in the muscle, Rac1 activation by insulin and the translocation of GLUT4 may be the primary mechanism of glucose uptake. Furthermore, it has been shown that IR deletion in muscle results in increased mass, serum free fatty acids, and triglycerides, but does not affect glucose metabolism or insulin sensitivity, suggesting that other tissues may be

more critical for insulin stimulated glucose uptake (Brüning et al., 1998). Therefore, even though muscle does not seem to express appreciable levels of P-rex2, it is not surprising that insulin resistance in the liver and fat sufficiently disrupts glucose metabolism. It is also possible that the combination of reduced Rac1 activation in muscle and decreased AKT phosphorylation in adipose tissue cooperate to disrupt glucose uptake in *Prex2* deficient mice.

It will also be interesting to analyze insulin signaling and glucose metabolism in older *Prex2*$^{-/-}$ mice. In many mouse models of diabetes, glucose homeostasis deteriorates as mice age. For instance, mice heterozygous for both *Ir* and *Irs1* show significant increases in blood glucose levels and plasma insulin levels from 2 months to 6 months of age (Kito et a., 2000). Therefore, examining diabetic phenotypes at 6 months may reveal a more dramatic diabetic phenotype in *Prex2*$^{-/-}$ mice.

Our results show that P-REX2 mediated PTEN inhibition is an important regulator of PI3K signaling *in vivo* and consequently affects glucose metabolism; however other cellular processes not examined here may also be regulated through this manner. For instance, reports have shown that loss of *Prex2 in-viv*o results in disrupted Purkinje cell dendrite morphology as well as motor coordination defects (Donald et al., 2008). This phenotype could be explained by the loss of P-REX2 mediated PTEN inhibition. This is supported by reports showing that PTEN is highly expressed in the Purkinje cells of mice (Li et al., 2002; Li et al., 2003). Furthermore, loss of PTEN and activation of AKT results in increased dendritic branching and length in cultivated neurons. Conversely,

inhibition of PI3K signaling reduces dendritic growth, similar to the phenotype observed when *Prex2* is lost (Jaworski et al., 2005, Kumar et al., 2005). Therefore, it is possible that disruption of *Prex2 in-vivo* releases PTEN from inhibition, allowing it to inhibit PI3K pathway dependent dendritic growth.

FIGURE LEGENDS

Figure 3.1. **Generation of *Prex2* deficient mice.** *A)* Wild-type and mutant alleles of *Prex2*. ES cells with with a gene trap containing a splice acceptor site (SA), β-galactosidase and neomycin phosphotransferase II fusion (βgeo), and polyadenylation sequence (pA) in intron 4 were used to generate chimeras. Primers (p) used for genotyping are depicted by arrows (pA-pD), and PCR genotyping using these primers is shown. *B)* Insertion of the βgeo reporter gene resulted in a deletion of exons 5 and 6, as shown by PCR. *C)* Expression of P-REX2 and P-REX2b, a shorter spice variant, in various tissue.

Figure 3.2. **PI3K signaling in *Prex2* deficient fibroblasts**. *A)* Western blot analysis of P-Rex2 and p-Akt(Thr308) expression in MEFs during normal growth conditions. *B)* Proliferation of *Prex2*$^{+/+}$, *Prex2*$^{+/-}$, and *Prex2*$^{-/-}$ MEFs in regular growth medium as quantified by crystal violet staining. *C)* Analysis of growth factor stimulated PI3K signaling. *Prex2*$^{+/+}$ and *Prex2*$^{-/-}$ MEFs were starved for three hours and then stimulated with indicated growth factors. Levels of phosphorylated Akt and downstream targets were analyzed over time by western blot.

Figure 3.3. **P-REX2 interacts with phosphorylated IR to inhibit PTEN following insulin stimulation.** *A) Prex2*$^{+/+}$ and *Prex2*$^{-/-}$ MEFs were starved for three hours and then stimulated with insulin for 15 minutes. Lysates were incubated with a rabbit monoclonal PTEN antibody conjugated to agarose beads overnight. Phosphatase assays were performed on immunoprecipitated protein complexes by incubating the beads with 20

μM soluble di-C8-D-myo-phosphatidylinositol 3,4,5-trisphosphate (PIP3) at 37°C for 30 minutes. Levels of immunoprecipitated PTEN were determine by western blot analysis. *B)* The interaction between P-REX2 and activated RTKs was analyzed by co-immunoprecipitation. P-REX2-V5 was transfected into HEK293 cells and lysates were incubated with V5- agarose beads overnight at 4ºC. Total lysates and V5-immunoprecipitated protein complexes were analyzed by western blot.

Figure 3.4. **P-REX2 recuits PTEN to the membrane following insulin stimulation.** U87 cells expressing PTEN alone or with P-REX2 were starved overnight and stimulated with 10 μg/mL insulin. PTEN and P-REX2 were visualized using indirect immunofluorescence. PTEN was stained with the rabbit monoclonal antibody 138G6 and Alexa Fluor-568. P-REX2a was stained the V5 monoclonal antibody and AlexaFluor-488. Nuclei were stained with 4',6-Diamidino-2-phenylindole dihydrochloride (DAPI) (Invitrogen).

Figure 3.5. **Effect of P-rex2 loss on glucose metabolism and insulin sensitivity.** *A)* Intraperitoneal glucose tolerance tests were performed by measuring blood glucose levels following intraperitoneal glucose injection at the indicated time points (n=6). *B)* Insulin tolerance tests were performed by measuring blood glucose levels following intraperitoneal injection of insulin (0.75 mU/g) at the indicated time points. Red diamonds represent *Prex2*$^{+/+}$ mice (n=5) and blue squares represent *Prex2*$^{-/-}$ mice (n=6). *C)* Blood glucose levels from 8 week old *Prex2*$^{+/+}$ mice (n=20) and *Prex2*$^{-/-}$ mice (n=14) fasted for 16 hours. Weights were also determined, (*Prex2*$^{+/+}$,n=14; *Prex2*$^{-/-}$, n=10).

Data are presented as means and error bars represent standard error of the mean (SEM). **, $P < 0.05$.

Figure 3.6. **P-REX2 regulates insulin signaling in liver and fat tissue.** *A-C)* Analysis of insulin stimulation *in-vivo*. *Prex2*$^{+/+}$ and *Prex2*$^{-/-}$ mice were fasted overnight and then injected intraperitoneally with insulin (0.75 mU/g) for 2 minutes or 15 minutes. Levels of phosphorylated Akt, Foxo1/3, Gsk3-β, and IR in collected fat and liver tissue were analyzed by western blot.

Figure 3.7. **P-REX2 inhibits PTEN activity in starved and insulin stimulated liver.** *A)* PTEN phosphatase assay from liver samples. *Prex2*$^{+/+}$ and *Prex2*$^{-/-}$ mice were fasted overnight and then injected with insulin (10 mU/g) for 8 minutes. Lysates from collected starved and stimulated livers were incubated with rabbit monoclonal PTEN antibody conjugated to agarose beads overnight. Phosphatase assays were performed on immunoprecipitated protein complexes by incubating the beads with 20 μM PIP3 at 37°C for 30 minutes. *B)* Analysis of PIP3 levels. Liver samples collected for the above phosphatase assays were used to compare PIP3 levels from insulin stimulated mice. Lipids were measured using mass spec and PIP3 values are represented as a ratio of PIP3/PIP2 to account for cell number variability.

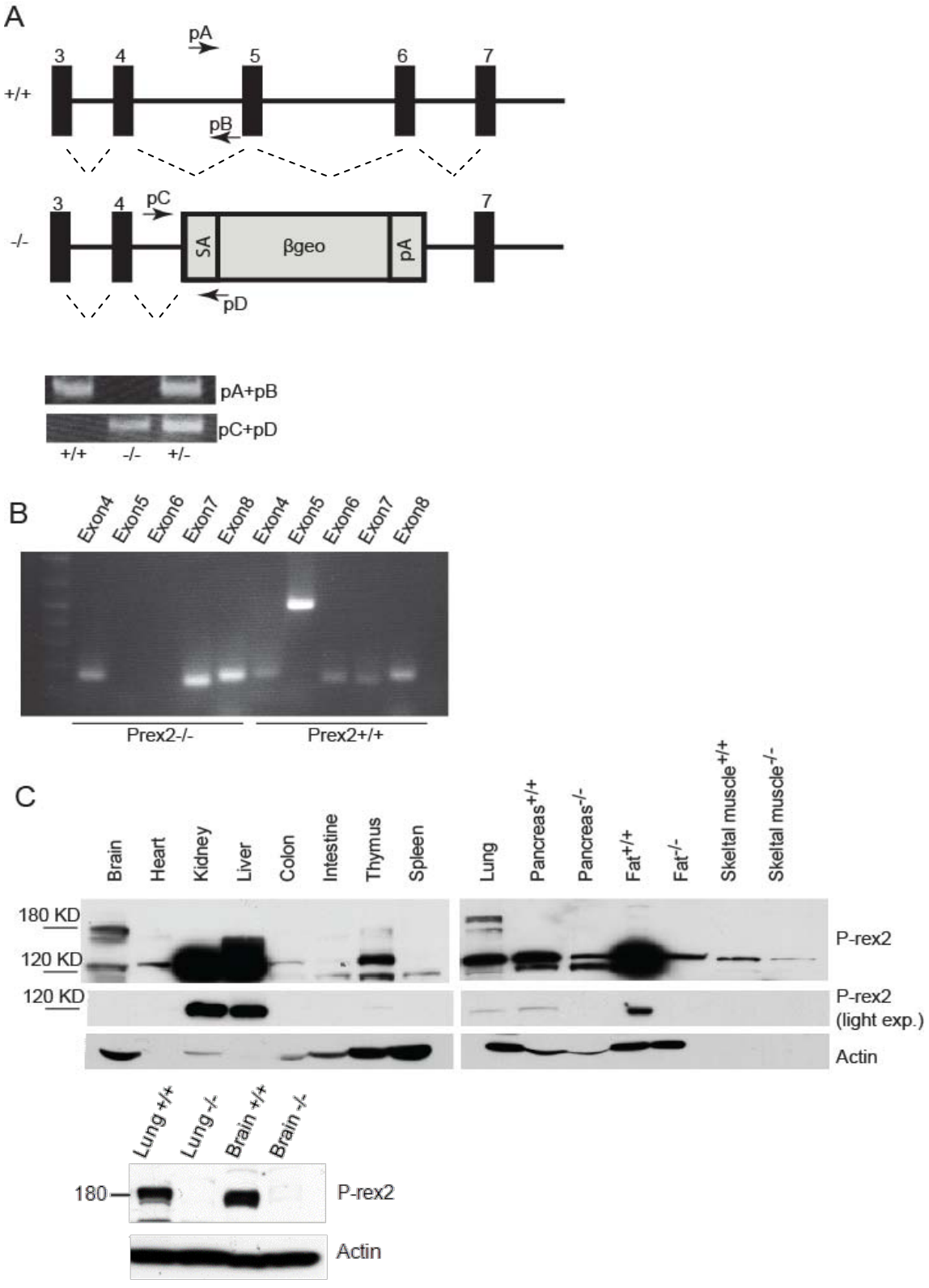
A
pA
3
4
5
6
7
+/+
pB
3
4
pC
7
-/-
SA
βgeo
pA
pD
pA+pB
pC+pD
+/+
-/-
+/-
B
Exon4
Exon5
Exon6
Exon7
Exon8
Exon4
Exon5
Exon6
Exon7
Exon8
Prex2-/-
Prex2+/+
C
Brain
Heart
Kidney
Liver
Colon
Intestine
Thymus
Spleen
Lung
Pancreas+/+
Pancreas-/-
Fat+/+
Fat-/-
Skeltal muscle+/+
Skeltal muscle-/-
180 KD
120 KD
120 KD
P-rex2
P-rex2
(light exp.)
Actin
Lung +/+
Lung -/-
Brain +/+
Brain -/-
180
P-rex2
Actin

FIGURE 3.1

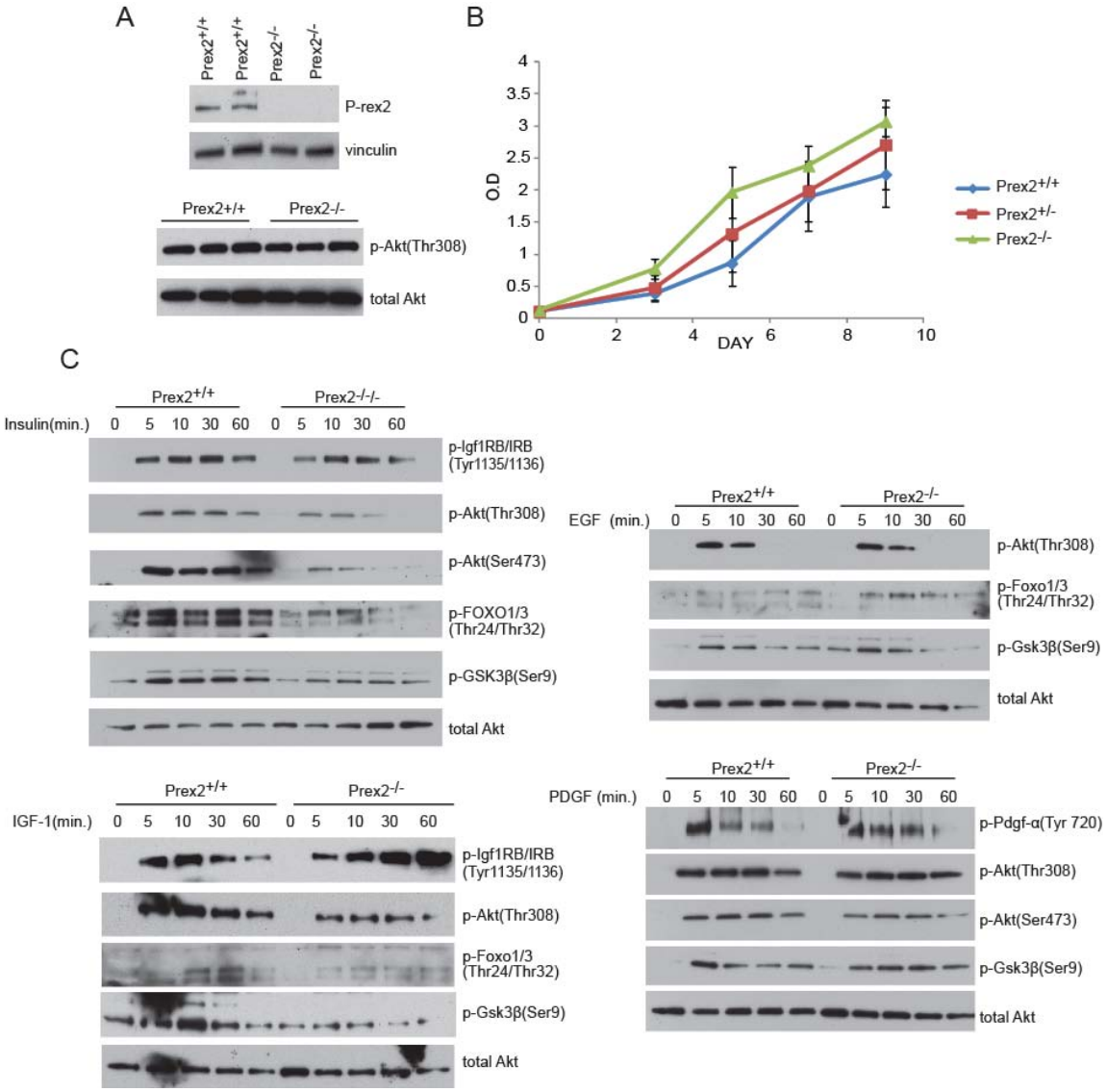
A
Prex2+/+
Prex2+/+
Prex2-/-
Prex2-/-
P-rex2
vinculin
Prex2+/+
Prex2-/-
p-Akt(Thr308)
total Akt
B
O.D
DAY
Prex2+/+
Prex2+/-
Prex2-/-
C
Prex2+/+
Prex2-/-/-
Insulin(min.)
0 5 10 30 60 0 5 10 30 60
p-Igf1RB/IRB (Tyr1135/1136)
p-Akt(Thr308)
p-Akt(Ser473)
p-FOXO1/3 (Thr24/Thr32)
p-GSK3β(Ser9)
total Akt
Prex2+/+
Prex2-/-
EGF (min.)
0 5 10 30 60 0 5 10 30 60
p-Akt(Thr308)
p-Foxo1/3 (Thr24/Thr32)
p-Gsk3β(Ser9)
total Akt
Prex2+/+
Prex2-/-
IGF-1(min.)
0 5 10 30 60 0 5 10 30 60
p-Igf1RB/IRB (Tyr1135/1136)
p-Akt(Thr308)
p-Foxo1/3 (Thr24/Thr32)
p-Gsk3β(Ser9)
total Akt
Prex2+/+
Prex2-/-
PDGF (min.)
0 5 10 30 60 0 5 10 30 60
p-Pdgf-α(Tyr 720)
p-Akt(Thr308)
p-Akt(Ser473)
p-Gsk3β(Ser9)
total Akt

FIGURE 3.2

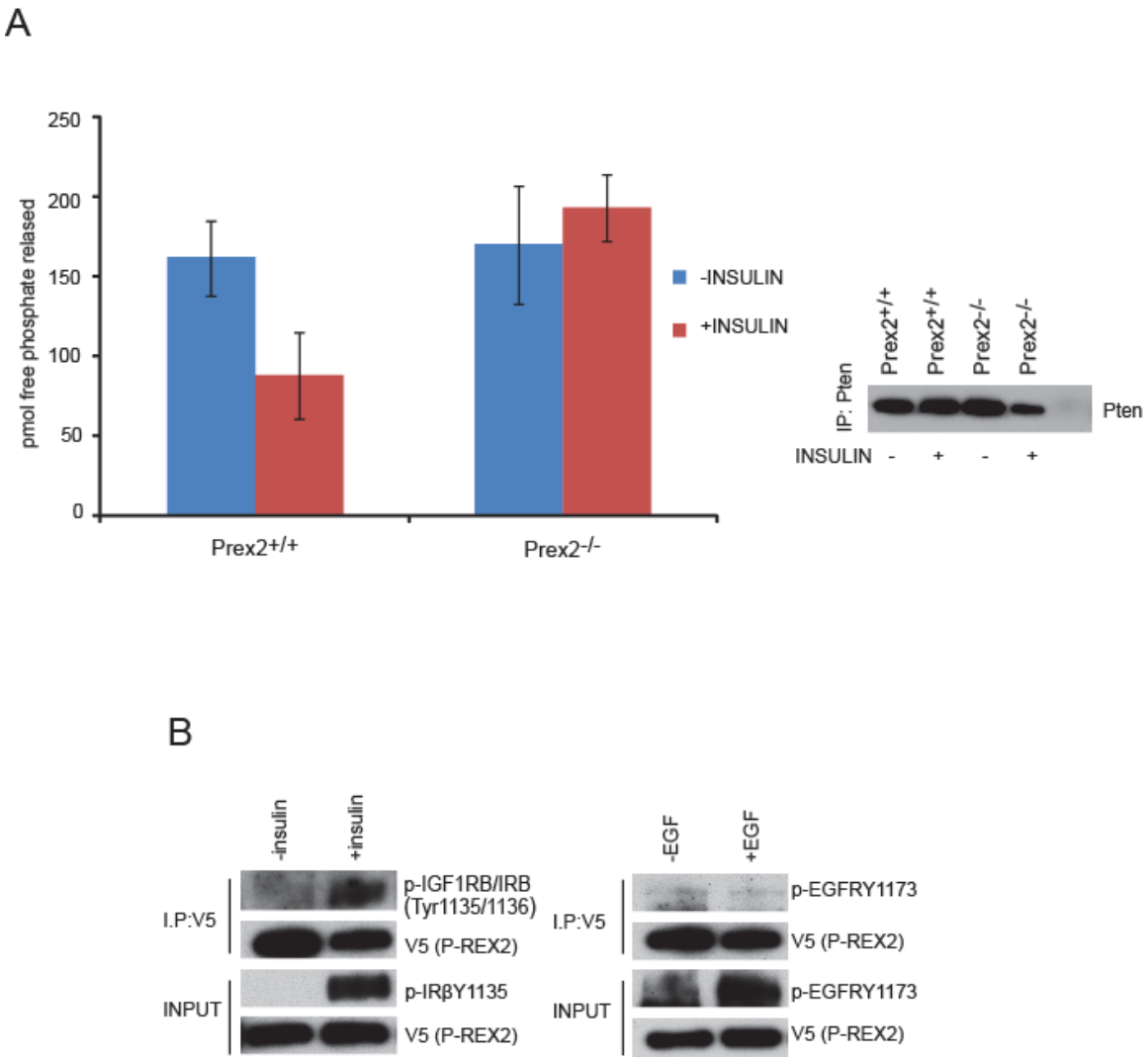
A
250
200
150
100
50
0
pmol free phosphate relased
-INSULIN
+INSULIN
Prex2+/+
Prex2-/-
IP: Pten
Prex2+/+
Prex2+/+
Prex2-/-
Prex2-/-
Pten
INSULIN - + - +
B
-insulin
+insulin
I.P:V5
p-IGF1RB/IRB (Tyr1135/1136)
V5 (P-REX2)
INPUT
p-IRβY1135
V5 (P-REX2)
-EGF
+EGF
I.P:V5
p-EGFRY1173
V5 (P-REX2)
INPUT
p-EGFRY1173
V5 (P-REX2)

FIGURE 3.3

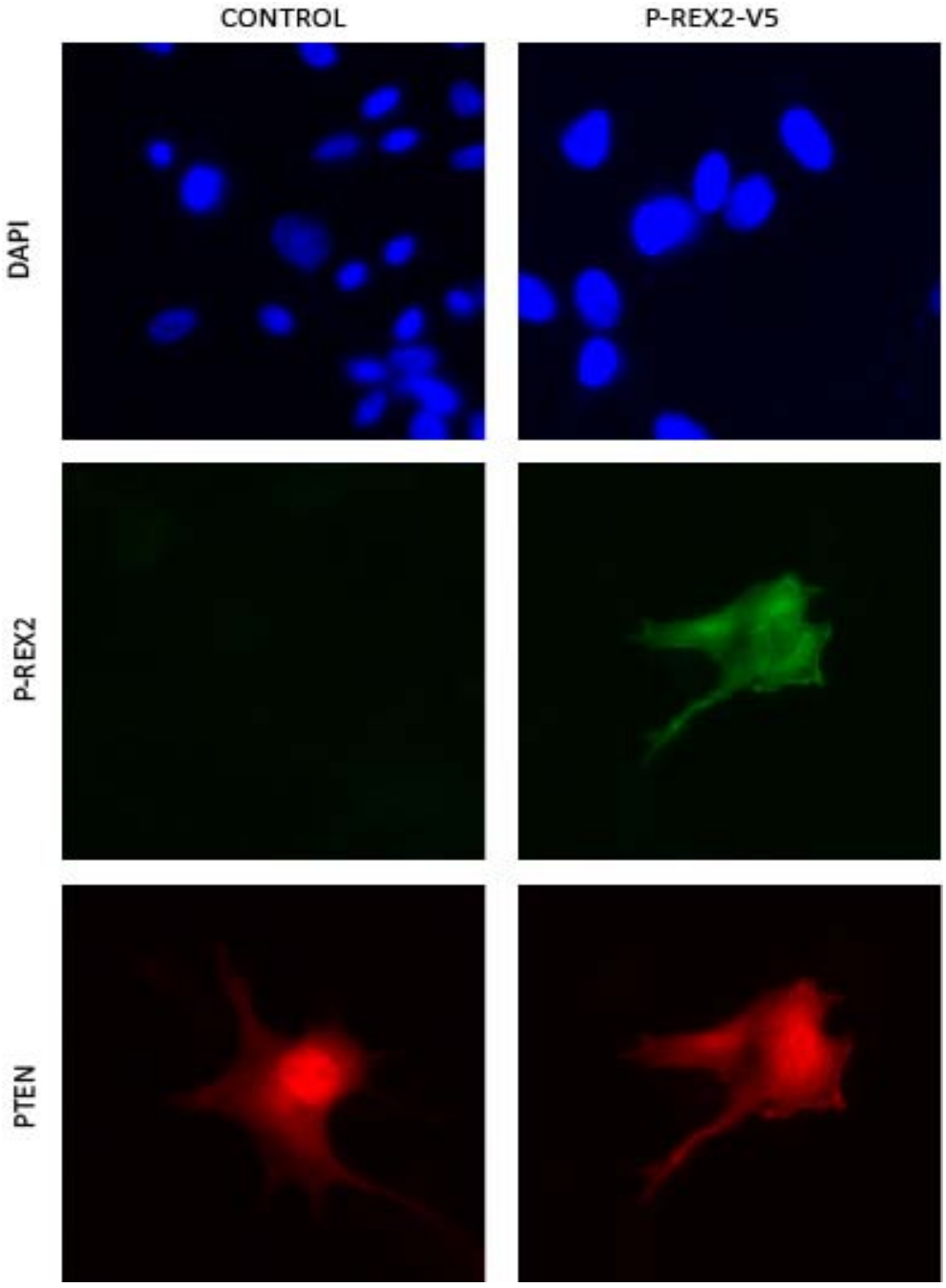

FIGURE 3.4

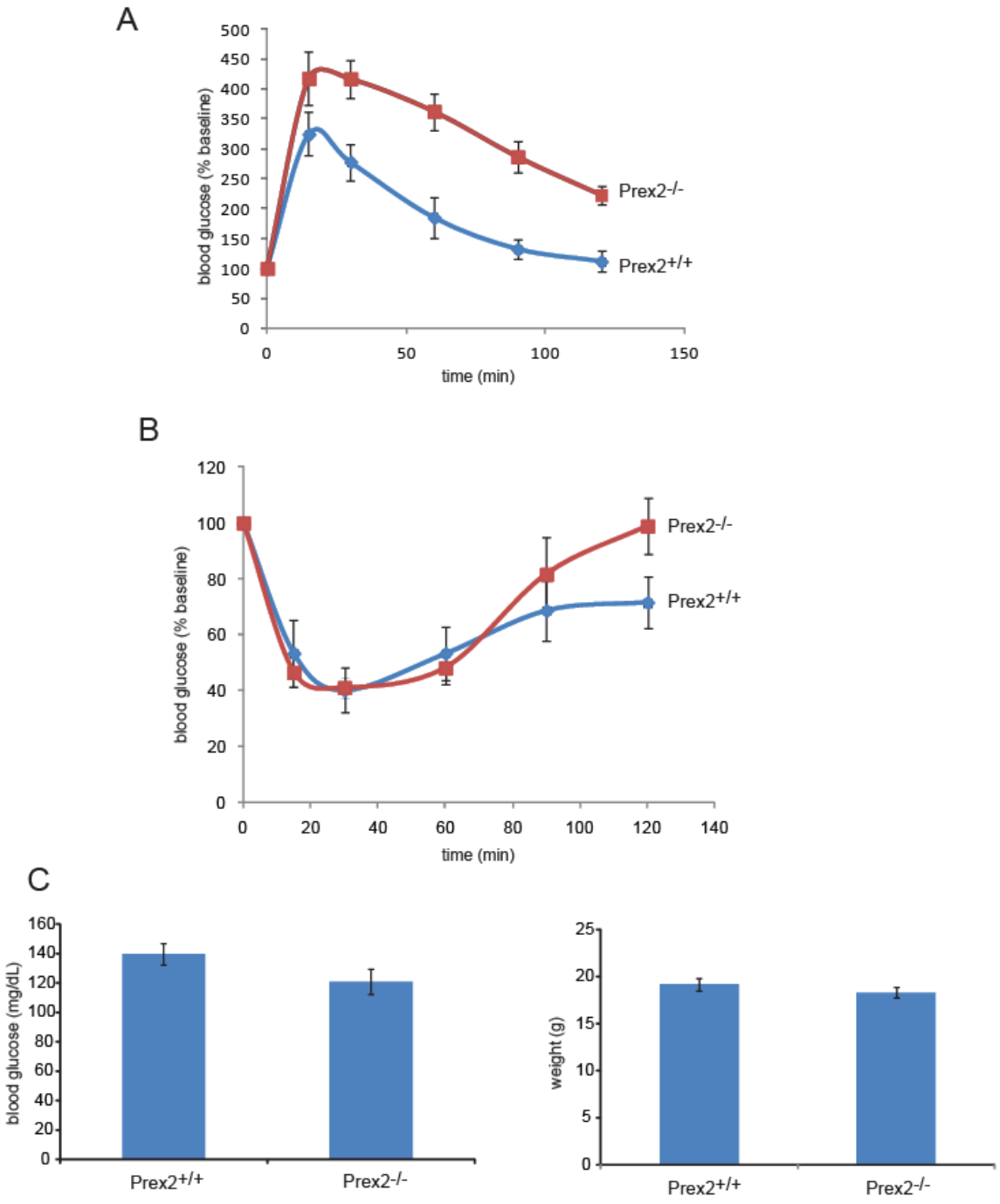
A
blood glucose (% baseline)
500
450
400
350
300
250
200
150
100
50
0
0
50
100
150
time (min)
Prex2-/-
Prex2+/+
B
blood glucose (% baseline)
120
100
80
60
40
20
0
0
20
40
60
80
100
120
140
time (min)
Prex2-/-
Prex2+/+
C
blood glucose (mg/dL)
160
140
120
100
80
60
40
20
0
Prex2+/+
Prex2-/-
weight (g)
25
20
15
10
5
0
Prex2+/+
Prex2-/-

FIGURE 3.5

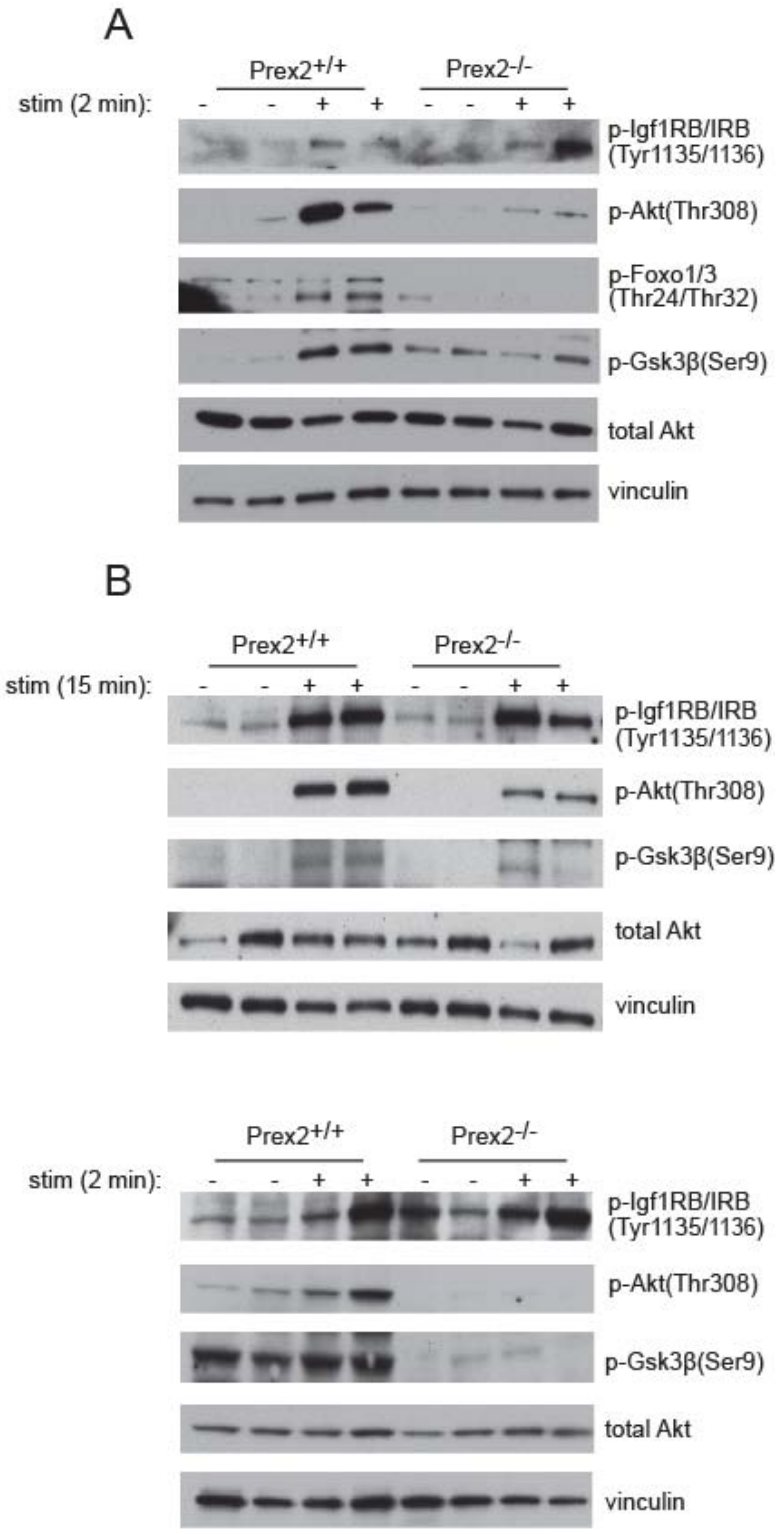
A
Prex2+/+
Prex2-/-
stim (2 min):
- - + + - - + +
p-Igf1RB/IRB (Tyr1135/1136)
p-Akt(Thr308)
p-Foxo1/3 (Thr24/Thr32)
p-Gsk3β(Ser9)
total Akt
vinculin
B
Prex2+/+
Prex2-/-
stim (15 min):
- - + + - - + +
p-Igf1RB/IRB (Tyr1135/1136)
p-Akt(Thr308)
p-Gsk3β(Ser9)
total Akt
vinculin
Prex2+/+
Prex2-/-
stim (2 min):
- - + + - - + +
p-Igf1RB/IRB (Tyr1135/1136)
p-Akt(Thr308)
p-Gsk3β(Ser9)
total Akt
vinculin

FIGURE 3.6

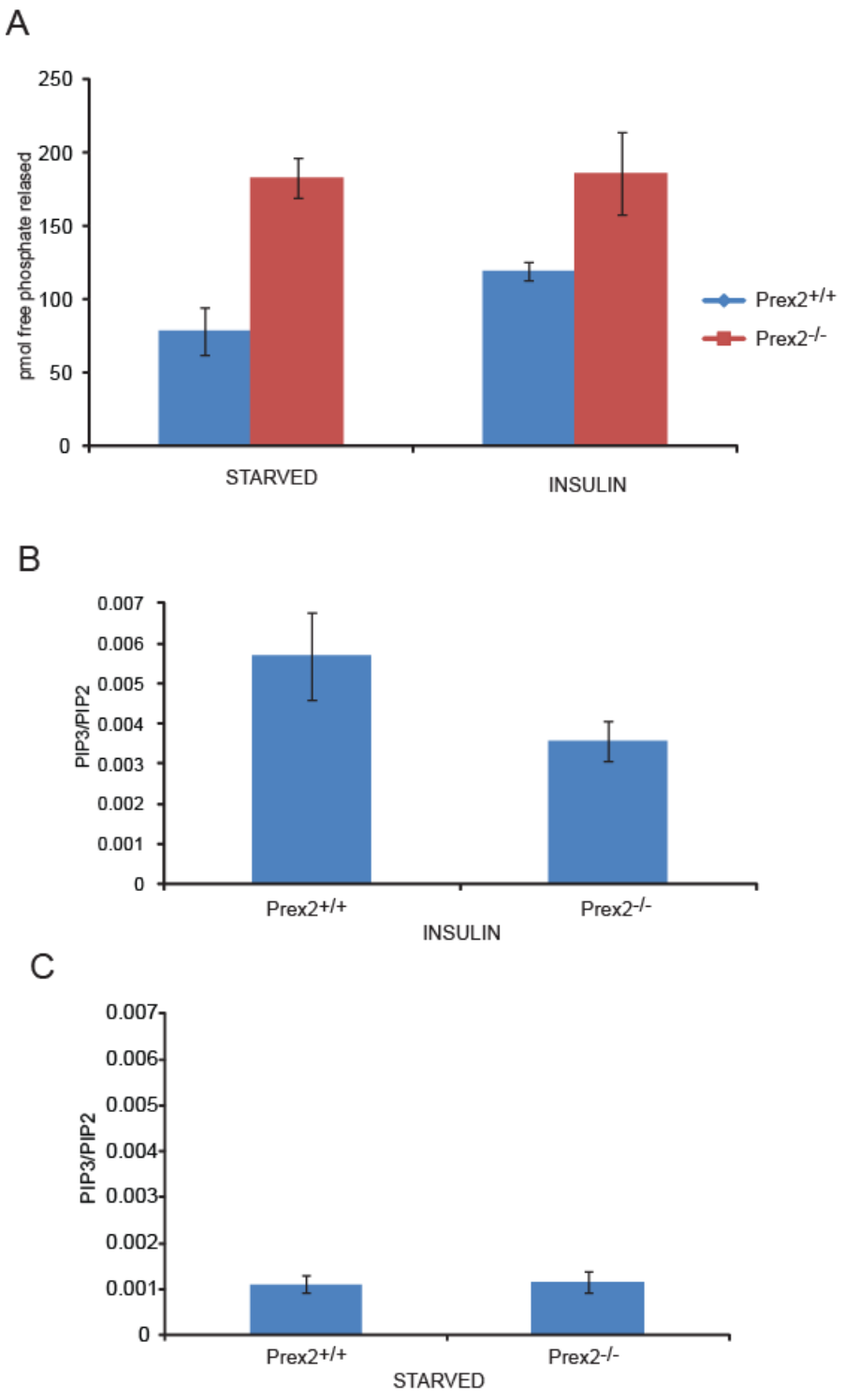
A
250
200
150
100
50
0
pmol free phosphate relased
STARVED
INSULIN
Prex2+/+
Prex2-/-
B
0.007
0.006
0.005
0.004
0.003
0.002
0.001
0
PIP3/PIP2
Prex2+/+
Prex2-/-
INSULIN
C
0.007
0.006
0.005
0.004
0.003
0.002
0.001
0
PIP3/PIP2
Prex2+/+
Prex2-/-
STARVED

FIGURE 3.7

CHAPTER IV

Phosphorylation of the PTEN carboxyl-terminal tail domain regulates P-REX2 Pleckstrin Homology domain-mediated inhibition of PTEN

Cindy Hodakoski, Douglas Barrows, Sarah M. Mense, Megan Keniry, Ramon Parsons

ABSTRACT

Appropriate levels of phosphorylation events in the cell are maintained by balancing kinase and phosphatase regulation. Phosphatase activity is dynamically regulated through various mechanisms including phosphorylation and protein-protein interaction to control cell cycle progression. The phosphatase activity of the dual-specificity PTEN is inhibited through its interaction with P-REX2. We have shown that P-REX2 regulates cellular transformation, and is required for insulin stimulated PTEN inhibition and glucose homeostasis. Therefore it is important to understand how P-REX2 mediated inhibition of PTEN is regulated. Here, we report that P-REX2 interacts with PTEN though multiple interfaces, resulting in highly regulated PTEN inhibition. The pleckstrin homology (PH) domain of P-REX2 inhibits PTEN by interacting with the catalytic region of PTEN, whereas the inositol polyphosphate 4-phosphatase domain of P-REX2 provides high affinity binding to the PDZ-binding domain of PTEN. Regulation of P-REX2 PH domain-dependent inhibition of PTEN requires C-terminal phosphorylation of PTEN to unleash the PH domain from its neighboring Dbl homology domain. This suggests that like regulation of phosphatase activity during cell cycle progression, P-REX2 inhibition of PTEN may be dynamically regulated.

INTRODUCTION

Phosphatases are a large and diverse family of enzymes that counteract the action of kinases by dephosphorylating specific molecular substrates. Phosphatases are essential for the regulation of many signal transduction pathways and altered phosphatase activity can result in the disruption of various cellular processes. Most protein phosphorylation events in eukaryotic cells occur on tyrosine, threonine, and serine residues (Olsen et al., 2006). Phosphatases that reverse these events are grouped into families based on substrate specificity and signature sequences. These families include the serine/threonine phosphatases and the tyrosine phosphatases, each of which are further divided into many different subfamilies based on specific function.

The serine/threonine phosphatases are the most ancient family of protein phosphatases and evolved through the interaction of novel regulatory complexes with an ancestral catalytic domain (Moorhead et al., 2009). The predominant mechanism of serine/threonine phosphatase regulation occurs via the formation of these protein complexes. For example, protein phosphatase (PP) 1 and PP2B form regulatory complexes with inhibitors that block substrate access to the active site. More specifically, PP1 interacts with inhibitors C-kinase-activated PP1 inhibitor of 17 kDa (CPI-17), and inhibitor 1, while PP2A interacts with inhibitors including I2PP2A (Endo et al., 1996; Eto et al., 1997). Direct phosphorylation has also been implicated in serine/threonine phosphatase regulation. PP1 activity is diminished after phosphorylation by multiple cyclin-dependent kinases, and phosphorylation by specific growth factors and

tyrosine kinases inactivates PP2A (Chen et al., 1994; Dohadwala et al., 1994; Kwon et al., 1997). Interestingly, many inhibitory proteins are activated by phosphorylation, adding another layer of complexity to phosphatase regulation (Endo et al., 1996; Eto et al., 1997; Foulkes et al., 1983).

The family of protein tyrosine phosphatases, which appeared later than the serine/threonine phosphatases, first evolved most likely due to promiscuity of serine/threonine kinases towards tyrosine residues. They then diversified after the emergence of tyrosine kinases through the fusion of regulatory domains to its ancestral catalytic core (Moorhead et al., 2009). The protein tyrosine phosphatases family includes the large subgroup of dual-specificity phosphatase and is regulated largely through the reversible oxidation of their catalytic cysteine residue (Ostman et al., 2011). Similar to the serine/threonine phosphatases, direct phosphorylation is also a mechanism of regulation. SH2 domain containing protein tyrosine phosphatase-1 and -2 (SHP-1/2) and protein tyrosine phosphtase IB (PTP1B) (Dadke et al., 2001; Lu et al., 2001; Tao et al., 2001; Zhang et al., 2003) exhibit altered phosphatase activity after phosphorylation. More specifically, the activity of the *S. pombe* Cdc14 related dual specificity phosphatase Cdc14 like protein-1 (Clp1) is inhibited through direct phosphorylation by Cdk1 in a cell cycle dependent manner (Wolfe et al., 2006).

PTEN was discovered by multiple groups through the mapping of homozygous deletions in cancer (Li et al., 1997; Steck et al., 1997). PTEN has the conserved PTP catalytic motif, a C2 domain which are both required to dephosphorylate its main substrate, PIP3,

to PI(4,5)P2, therefore inhibiting PIP3 mediated recruitment and activation of the serine/threonine kinase AKT (Franke et al., 1997; Lee et al., 1999; Maehama and Dixon, 1998; Stambolic et al., 1998; Wu et al., 1998). Beyond these domains, the C-terminal tail of PTEN is also critical for proper protein function. The C-terminal tail of PTEN is phosphorylated mainly on Ser-370 and on a cluster consisting of Ser-380, Thr-382, Thr-383, and Ser-385. Dephosphoryation of these sites results in increased phosphatase activity and decreased protein half-life (Vazquez et al., 2002). C-terminal tail phosphorylation also regulates an intramolecular interaction that occurs between the tail and the catalytic region of PTEN, and this interaction inhibits PTEN membrane recruitment and PIP3 access (Odriozola et al., 2007; Rahdar et al., 2009). In addition to sites of phosphorylation, the C-terminus of PTEN contains a PDZ-binding domain (PDZ-BD) that interacts with proteins containing PDZ domains such as MAGI-1/2/3, MAST205, and hDLG. Interestingly, PTEN interaction with PDZ domains leads to increased protein stability and phosphorylation, suggesting that PDZ domain containing proteins can directly regulate PTEN function (Kim and Mak, 2006; Valiente et al., 2005). PTEN is also inactivated by acetylation by the histone deacetyltransferase p300/CBP-associated factor (PCAF) (Okumura et al., 2006) and by reversible oxidation of the catalytic cysteine (Cho et al., 2004; Lee et al., 2002). In addition, PTEN regulation by nuclear localization is mediated by monoubiquitination by neural precursor cell expressed, developmentally downregulated-4-1 (Nedd4-1) (Trotman et al., 2007).

Recently, we identified a novel PTEN interacting protein, P-REX2 (Fine et al., 2009). We have reported that P-REX2 interacts with PTEN and directly inhibits its phosphatase

activity in a non-competitive manner. It was also found that *PREX2* message levels are increased and missense mutations exist in a variety of different cancers. Furthermore, it has been reported that *PREX2* is significantly mutated in metastatic melanoma (Berger et al., 2012). Expression leads to increased PI3K signaling and proliferation in normal mammary epithelial cells, and loss of P-REX2 in endothelial cells results in decreased Rac1 activation and migration. In mice, deletion of *Prex2* results in disrupted Purkinje cell morphology and motor coordination (Donald et al., 2008) and disrupted insulin signaling and glucose metabolism, as discussed in Chapter III.. Here, we examine the mechanism by which P-REX2 inhibits PTEN and find that the pleckstrin homology (PH) domain of P-REX2 is responsible for inhibiting PTEN phosphatase activity. PH domain mediated inhibition is highly regulated by the Dbl homology (DH) domain of P-REX2 and PTEN C-terminal tail phosphorylation.

EXPERIMENTAL PROCEDURES

Plasmids and antibodies - Construction of a majority of the PTEN and P-REX2 plasmids used has been reported previously (Fine et al., 2009). Bacterial expression plasmids encoding GST-PTEN domains were made by polymerase chain reaction of the full length GST-PTEN plasmid and subcloning into the PGEX-2TK vector. GST-PTEN-3E and FLAG-PTEN-3E mutants were made by amino acid substitution using site directed mutagenesis (Agilent, Santa Clara, CA). FLAG-PTEN deletion mutants were constructed by substitution of a stop codon at the desired amino acid by site directed mutagenesis. PTEN antibodies were purchased from Cell Signaling (Danvers, MA). Monoclonal M2 FLAG and actin antibodies were purchased from Sigma (St. Louis, MO) and a monoclonal V5 antibody was from Invitrogen (Carlsbad, CA). V5-resin was obtained from Sigma. Antibodies against phosphorylated AKT threonine 308 and total AKT were purchased from Cell Signaling. A P-REX2 rabbit polyclonal antibody to amino acids 960-973 was made by Zymed Laboratories (San Francisco, CA). Secondary antibodies directed against rabbit and mouse IgG conjugated to HRP were purchased from Pierce (Rockford IL).

Cell culture, transfections- HEK293 cells were grown in Dulbecco's minimal essential medium supplemented with 10% FBS plus 100 IU penicillin and 100 µg/mL streptomycin (Cellgro, Herndon, VA). U87-MG cells were grown in minimal essential medium eagle (Cellgro) supplemented with 10% FBS and 1% penicillin/streptomycin. For signaling experiments, cells were starved in medium without FBS for 16 hours before

lysing. Transfections were performed using Lipofectamine 2000 (Invitrogen) following the protocol of the manufacturer.

Immunoblotting- Samples lysed in 2X Laemlli sample buffer (125 mM Tris pH 6.8, 10% 2-mercaptoethanol, 4% SDS, 20% glycerol, 0.05% bromophenol blue) are boiled for 5 minutes. Samples were separated by SDS-PAGE on 4-20% Tris-Gylcine gels (Invitrogen) and transferred onto PVDF using a semi-dry apparatus (Millipore, Billerica, MA). Membranes were blocked with 5% non fat milk in TBST and incubated with the appropriate antibody overnight at 4°C. Membranes were washed three times with TBST and the appropriate secondary antibody was added for 1 hour at room temperature. Blots were developed using ECL (Pierce) and audioradiography film (Denville, Metuchen, NJ).
GST fusion proteins- Recombinant GST fusion proteins were transformed into BL21(DE3) pLyseE bacterial cells (Invitrogen) and protein was purified as described previously (31). Briefly, expression of protein was induced in bacterial cultures at growing at log phase with 0.1mM IPTG (Sigma) at room temperature for 16 hours. Protein was extracted by sonication in lysis buffer (400 mM NaCl, 50 mM Tris pH 7.2, 1% Triton X-100, 1 mM EDTA) and incubated with glutathione sepharose beads (Sigma) overnight and washed excessively with either BC200 buffer (25 mm Tris-HCl buffer, pH 7.4, 200 mm KCl, 0.2% Triton, 1 mm EDTA, and 10% glycerol) or phosphatase buffer (150 mM NaCl, 25 mM Tris-HCl pH 7.5) (PB) if it was to be eluted. To elute, beads were incubated with an equal volume of glutathione elution buffer (150 mM NaCl, 25 mM Tris-HCl, 50 mM glutathione, pH 8.0) for 30 minutes at room temperature. Purified proteins were dialyzed in 5 L elution buffer without glutathione over night at 4°C using

SnakeSkin dialysis tubing (Pierce). Proteins conjugated to beads and purified proteins were quantified by coomassie staining.

In-vitro transcription and translation- V5-tagged P-REX2 domains were in-vitro transcribed and translated using the TnT T7 Quick Coupled Rabbit Reticulocyte Lysate Kit (Promega, Madison, WI) per the manufacturer's protocol.

Protein purification- V5-tagged P-REX2 domains were purified from 293 cells as previously described (Fine et al., 2009) with a few modifications . Briefly, HEK293 cells growing in 15 cm dishes were transfected with pCDNA3.1/ V5/His plasmids and incubated with MG132 16 hours prior to lysing. 36 hours after transfection, cells were washed with cold TBS and lysed with high salt lysis buffer (500 mM NaCl, 25 mM Tris pH 7.4, 1% Triton X-100, 1 mM EDTA) plus eukaryotic protease inhibitor cocktail. Clarified lysate was precleared with mouse IgG and protein A/G PLUS-agarose for 1 hour at 4°C and protein was then immunoprecipitated using V5-agarose overnight at 4°C. Beads were washed on a poly-prep column (BioRad, Hercules, CA) once with lysis buffer and 5 times with PB. Protein was eluted with V5 peptide in PB at a concentration of 150 µg/mL. Protein was quantified with spectrophotometry A280 and visualized by western blot.

Immunoprecipitation- Transfected cells were rinsed with cold PBS and lysed with Triton-containing lysis buffer (150 mM NaCl, 25 mM Tris pH 7.4, 0.1% Triton X-100, 1 mM EDTA) supplemented with eukaryotic protease cocktail inhibitor (Sigma, St. Louis, MO)

36 hours after transfection. Lysates were vortexed, sonicated, and clarified by high speed centrifugation for 30 minutes, and precleared with normal mouse IgG with protein A/G PLUS-agarose (Santa Cruz, CA) for 1 hour at 4°C. Protein complexes were then immunoprecipitated using either V5-agarose or FLAG antibody (Sigma) with 20 µL protein A/G PLUS- agarose overnight at 4°C. Beads were washed extensively with lysis buffer and eluted in 2X sample buffer (125 mM Tris pH 6.8, 10% 2-mercaptoethanol, 4% SDS, 20% glycerol, 0.05% bromophenol blue).

GST-pull down assay– Rabbit reticulocyte lysates (10 µL) were incubated with purified GST sepharose or GST PTEN sepharose in BC200 (25 mm Tris-HCl buffer, pH 7.4, 200 mm KCl, 0.2% Triton, 1 mm EDTA, and 10% glycerol) at 4ºC for 4 hours. The sepharose was then washed extensively with BC200 and eluted with sample buffer.

PTEN phosphatase assay- Equimolar concentrations of purified V5-tagged P-REX2 protein and recombinant GST fusion protein were incubated in phosphatase buffer (150 mM NaCl, 25 mM Tris-HCl pH 7.5) (PB) at a total volume of 48 µL. The protein mixture was pre-incubated at 37°C for 10 minutes before 20 µM soluble di-C8-D-myo-Phosphatidylinositol 3,4,5-trisphosphate (Echelon, Salt Lake City, UT) was added. The reactions were incubated at 37°C for 30 minutes, and stopped with 100 µL Biomol green reagent (Enzo, Farmingdale, NY). The colorimetric reaction developed for 15 minutes before being read on a plate reader at an absorbance of 620 nm. For immunoprecipitation phosphatase assays, 10 cm plates of HEK293 or U87-MG cells were co-transfected in triplicate with either 5 µg of V5 or FLAG-tagged PTEN plasmid and 15 µg of control or

V5-tagged P-REX2 constructs using Lipofectamine 2000 (Invitrogen, Carlsbad, CA). After 36 hours, cells were lysed with Triton-containing lysis buffer, vortexed, sonicated, and centrifuged at high speed for 30 minutes. Clarified lysates were precleared with normal mouse or rabbit IgG and protein A/G PLUS agarose for 1 hour at 4°C. 1 mg of total protein was next incubated with either V5-agarose or PTEN 138G6 antibody (Cell Signaling, Danvers, MA) overnight at 4°C, and the beads were then washed twice with lysis buffer and 4 times with PB. The beads were preincubated in PB at 37°C for 10 minutes and then collected by centrifugation at low speed to remove the supernatant. Beads were then incubated with 20 µM PIP3 and PB at a final volume of 50 µL and incubated at 37°C for 30 minutes. The beads were removed from the reaction mixture by centrifugation at low speed, and the supernatant was added to 100 µL Biomol green reagent which stopped the reaction and absorbance was read at 620 nm after 15 minutes. Detectible background levels of activity were subtracted from measured levels of PTEN activity for both *in-vitro* and immunoprecipitation phosphatase assays

Stable shRNA infection- Lentirviral Prex1 shRNA knockdown viruses were produced by transfection of HEK293T cells with a ratio of 1.3:1:0.1 of shRNA vector to CMVD8.9 packaging vector to VSV-G envelope vector, using Fugene 6 (Roche, Indianapolis, IN) at a ratio of fugene:DNA of 3:2. Lentiviral titers were collected at 48 hours and 72 hoursafter transfection. For infection MCF7 cells, polybrene (1,5-dimethyl-1,5-diazaundecamethylene- polymethobromide, hexadimethrine bromide) was added at a concentration of 6 µg/ml to increase infectivity. Cell lines were infected for 12 hours with 1:1 titer:growth media. Selection antibiotic was added to the media 48 hours after the

initial point of infection. Cell lines were allowed to select for 1 week and were subsequently maintained in selection antibiotic for the course of experiments.

Cell proliferation assay – 4,000 MFC-7 cells were plated per well in a 48 well plate in at least triplicate for each experiment. Cells were then allowed to proliferate and fixed at indicated time points in 0.05% crystal violet in 10% formalin. Each well was then washed multiple times with PBS. For relative quantification of cell density, the crystal violet was re-solubilized in 10% acetic acid and the absorbance at 595nm was recorded by a MicroQuant plate spectrophotometer.

Soft Agar Colony Formation Assay - For soft agar colony formation assays, 1 X 10^5 cells from stable MCF7 cell lines were mixed with agarose to form a top layer of 0.3% agarose. This layer was plated into a 35 X 10 mm plate on top of a solid layer of 0.5% agarose. Each assay was performed in triplicate. Colonies were stained with a 0.005% crystal violet solution after 14 days of incubation, and colony number was determined using ImageJ software.

RESULTS

P-REX2 inhibition of PTEN is regulated by C-terminal tail phosphorylation.

We have previously reported that the carboxy-terminal 50 amino acids (tail) of PTEN is required for interaction with P-REX2 (Fine et al., 2009). Due to the presence of critical phosphorylation sites located on the tail, we were interested in determining if phosphorylation of the tail affected P-REX2 binding. To do this, a FLAG-PTEN mutant was constructed containing unphosphorylatable alanine substitutions at amino acids T380, T382, and S383 (FLAG-PTEN-3A). Wild type FLAG-PTEN and FLAG-PTEN-3A were co-transfected in 293 cells with control vector or P-REX2-V5, and the FLAG-PTEN/P-REX2-V5 complex was immunoprecipitated using FLAG-M2 antibody. SDS-PAGE analysis of eluted proteins showed P-REX2 bound equally to FLAG-PTEN and FLAG-PTEN-3A (Fig 4.2A). This suggested that lack of tail phosphorylation at these sites does not affect the physical interaction between P-REX2 and PTEN. This did not rule out the possibility, however, that phosphorylation of the tail regulates P-REX2 mediated PTEN inhibition. To investigate this, we co-transfected FLAG-PTEN or FLAG-PTEN-3A with or without P-REX2 into U87-MG cells and immunoprecipitated protein complexes with anti-PTEN 138G6 antibody. Protein-bound beads were incubated with soluble di-C8 PIP3 substrate at 37°C for 30 minutes. After quantifying free phosphate using malachite green, we observed that P-REX2 inhibited FLAG-PTEN by 53%, but did not inhibit FLAG-PTEN-3A (Fig 4.2B). This result indicates that PTEN tail phosphorylation can regulate P-REX2 inhibition without affecting binding.

To verify this result, we construced a recombinant GST-PTEN vector to make a mutant containing phospho-mimicking glutamatic acid substitutions at amino acids T380, T382, and S383 (GST-PTEN-3E). We purified recombinant GST-PTEN and GST-PTEN-3E from bacteria (Fig. 4.1A) and performed phosphatase assays with equimolar concentrations of purified P-REX2-V5 and PTEN protein. In accordance with our previous results, P-REX2-V5 inhibited GST-PTEN-3E by 46%, but did not inhibit GST-PTEN (Fig. 4.2C). Taken together, our results strongly suggest that P-REX2 can recognize the phosphorylation status of the PTEN tail, and only inhibits when PTEN is phosphorylated, despite its ability to interact with the unphosphorylated form of PTEN.

P-REX2 binds to multiple sites on PTEN.

Because the tail regulates P-REX2 inhibition of PTEN as well as P-REX2 binding, we sought to understand the P-REX2-PTEN tail interaction in more detail. To further examine this, we created N-terminal FLAG-tagged PTEN constructs containing step-wise deletions into the tail of PTEN, including a truncation of the PDZ-BD, in order to determine the region of the tail required for P-REX2 binding (Fig 4.1A). We next co-transfected V5-tagged P-REX2 with full length FLAG-tagged PTEN or PTEN deletion mutants into HEK293 cells. Cells were lysed and subsequent co-immunoprecipitation analysis revealed that a two amino acid deletion at the C-terminus of the PDZ-BD led to a major reduction of P-REX2 binding. Furthermore, as the tail domain mutants became progressively shorter, P-REX2 binding increased, but was still significantly weaker than binding to full length PTEN (Fig 4.3A). This result suggests that P-REX2 binds strongly to the PDZ-BD of PTEN, and also binds weakly to a region of PTEN outside of the tail.

To confirm that P-REX2 binds to site on PTEN separate of the tail, we performed co-immunoprecipitation experiments with P-REX2-V5 and FLAG-NC2, containing amino acids 1-353 encompassing the phosphatase and C2 domains, and compared their binding affinity to that seen with FLAG-Δ361. SDS-PAGE analysis revealed that P-REX2 bound to FLAG-NC2 with higher affinity than FLAG-Δ361 (Fig 4.3B), validating P-REX2 binding to an additional site on PTEN. Overall, these results suggest that P-REX2 binds with high affinity to the PDZ-BD, and also interacts with a region of PTEN located outside of the PTEN tail.

The IP4P domain of P-REX2 docks to the PDZ-BD of PTEN.

The above data suggests that there are multiple binding sites for P-REX2 located on PTEN. One site is the PDZ-BD, and the other site is located N-terminally of the tail. To first determine how P-REX2 interacts with the PDZ-BD, we first performed pull-down experiments using recombinant GST-PTEN mutants bound to gluthatione sepharose beads and P-REX2-V5 deletion mutants (Fig 4.1A-B) expressed in HEK293 cells. Lysates from the transfected cells were incubated with either GST-NC2 or GST-TAIL, which only contains the tail region (amino acids 353-403), and eluates were analyzed by western blot. CP-REX2, a mutant lacking the DHPH domain, had strong affinity for the tail, but not the phosphatase and C2 domains (Fig. 4.4A), suggesting that this region of P-REX2 may be interacting with the PDZ-BD of PTEN.

We next wanted to confirm this interaction by co-immunoprecipitation. CP-REX2-V5 was expressed in HEK293 cells with FLAG-C2TAIL or FLAG-C2TAILΔ402 (Fig. 4.1A)

and complexes were immunoprecipitated with anti-FLAG antibody. Western blot analysis showed that CP-REX2 co-immunoprecipitated well with FLAG-C2TAIL, and that this interaction was dependent on the PDZ-BD (Fig. 4.4B). To further map this interaction, we performed similar immunoprecipitation experiments using smaller P-REX2 fragments. Specifically, we co-transfected the inositol polyphosphate 4-phosphatase domain (IP4P-V5) and the DEP PDZ tandem (DEPPDZ-V5) (Fig. 4.1A) with FLAG-C2TAIL or FLAG-C2TAILΔ402, and immunoprecipitated protein complexes with anti-FLAG antibody. We had predicted that binding to the PDZ-BD would occur through the DEPPDZ domain; however that was not what we observed. Surprisingly, it was the IP4P domain that interacted with the C2TAIL domain of PTEN in a PDZ-BD dependent manner (Fig. 4.4C). We therefore conclude that one mechanism of P-REX2 and PTEN interaction is through the binding of the IP4P domain of P-REX2 with the PDZ-BD of PTEN.

The PH domain of P-REX2 directly interacts with the Phosphatase and C2 Domains of PTEN.

We have shown P-REX2 interacts with a region of PTEN separate from the tail and PDZ-BD. In addition, prior work showed that the DHPH domain bound to PTEN *in-vitro* (Fine et al., 2009). To further investigate the nature of the DHPH domain interaction with PTEN, we performed pull-down experiments by mixing recombinant GST-PTEN mutants bound to gluthatione sepharose beads with DHPH-V5 (Fig 4.1A-B) expressed in HEK293 cells. Cell lysates were incubated with either GST-NC2 (phosphatase and C2 domain) or GST-TAIL, and eluates were analyzed by western blot. The DHPH domain

bound to GST-NC2, but not to GST-CTAIL (Fig. 4.5A), demonstrating that it interacts with PTEN in a different manner from the C-terminal domain. To determine the region of the DHPH domain required for this interaction, DH-V5 and PH-V5 (Fig. 4.1A) were *in-vitro* translated using rabbit reticulocyte lysate. The translated proteins were incubated with various GST-PTEN domain constructs bound to glutathione sepharose and the eluates of the resulting pull-down reactions were analyzed by western blot. We observed that the PH domain bound well to GST-NC2 and GST-C2, but not to GST-CTAIL, which followed the pattern seen with the DHPH domain. The DH domain, however, did not bind to any region of PTEN (Fig 4.5B). These results suggest that the PH domain alone is necessary for P-REX2 binding to the phosphatase and C2 domains, and that this binding is independent of the tail. To analyze binding of the PH domain in more detail, we *in-vitro* translated DHPH-V5 and PH-V5 and incubated the protein lysates with several GST-PTEN deletion constructs, including GST-N (phosphatase domain) and GST-C2 (C2 domain) (Fig 4.1A). SDS-PAGE analysis of pulled-down proteins showed that the DHPH and PH domains bound strongly to both GST-N and GST-C2 (Fig. 4.5 C). Therefore, the PH domain does not bind exclusively to one particular domain, but rather interacts with the interface of both the phosphatase and C2 domain, which together makes up the minimal catalytic region of PTEN.

We next confirmed these results by co-immunoprecipitation. PH-V5 and FLAG-NC2 were co-transfected into HEK293 cells and complexes were immunoprecipitated using anti-FLAG antibody. SDS-PAGE analysis of protein eluates showed that the PH domain of P-REX2 successfully bound FLAG-NC2 (Fig. 4.5D). We performed similar co-

immunoprecipitation experiments to validate binding of the DHPH domain to NC2. Co-transfection of FLAG-NC2 and DHPH-V5 and subsequent immunoprecipitation using anti-V5 antibody revealed that the FLAG-NC2 also interacted with the DHPH domain (Fig. 4.4D). In summary, both the DHPH and PH domains of P-REX2 directly interact *in- vitro* and in culture with the catalytic region of PTEN which includes both the phosphatase and C2 domains.

The PH domain of P-REX2 inhibits PTEN phosphatase activity in the absence of the tail.

Because both the DHPH and PH domains of P-REX2 bind to the phosphatase and C2 domains of PTEN, we hypothesized that these domains could inhibit PTEN in the absence of the C-terminal tail. We assessed this possibility by performing phosphatase assays with recombinant GST-NC2 protein and purified V5-tagged P-REX2 domains. PH-V5 inhibited GST-NC2 phosphatase activity by 64%, while the DH domain, and surprisingly, the DHPH domain did not (Fig. 4.6A). This suggests that the tail and PDZ-BD of PTEN is dispensable for PH domain inhibition of PTEN. Next, we determined if the PH domain was capable of inhibiting full length unphosphorylated GST-PTEN. Again, the PH domain, but not the DH or DHPH domain, was able to inhibit GST-PTEN phosphatase activity by 51% (Fig 4.6B), indicating that the PH domain inhibits PTEN regardless of its phosphorylation state.

The PH domain is unleashed from DH domain inhibition through the reading of tail phosphorylation by the DH domain

We suspected that phosphoryation of the tail may be regulating DHPH domain mediated PTEN inhibition. We therefore performed phosphatase assays using the GST-PTEN-3E mutant, and in accordance with our hypothesis, DHPH-V5 was now able to inhibit PTEN phosphatase activity along with PH-V5, by 27% and 61%, respectively (Fig. 4.6C). In summary, the PH domain is unique in its ability to inhibit PTEN activity independently of the tail and its phosphorylation status. Our results suggest that the DH domain blocks the function of the PH domain, as PH-V5 but not DHPH-V5 was able to inhibit unphosphorylated PTEN. Furthermore, the DH domain must be "reading" PTEN tail phosphorylation, unleashing the PH domain for PTEN inhibition when the tail is phosphorylated.

The PH domain inhibits PTEN activity in culture while the C-terminal region behaves in a dominant negative manner.

We next wanted to determine if PH domain inhibition of PTEN occurred under more physiological conditions. Therefore, we determined if the PH domain could inhibit PTEN when co-expressed in mammalian cells. HEK293 cells were co-transfected with PTEN-V5 and control vector, PH-V5 or CP-REX2-V5, which served as a negative control. Proteins were immunoprecipitated with anti-V5-agarose, and phosphatase assays were performed. We used a shared V5 epitope to immunoprecipitate protein complexes due of the weak interaction between PTEN and the DHPH and PH domains. The PH domain successfully inhibited eukaryotic PTEN activity by 63%, and surprisingly, CP-REX2 led to a significant 40% increase in PTEN activity (Fig. 4.7A). Western blotting revealed that PTEN was immunoprecipitated at equal levels in each sample (Fig. 4.7A).

These results demonstrate that the PH domain can inhibit not only bacterially produced PTEN, but also PTEN produced from mammalian cells. Conversely, CP-REX2 may act as a dominant negative form of P-REX2, as it caused an increase in PTEN activity. We can therefore speculate that C-P-REX2 may act as a dominant negative mutant by blocking the formation of the wild-type inhibitory complex.

Based on our data, we hypothesized that DHPH and PH mediated PTEN inhibition may affect signaling to AKT in cells. To examine this, signaling experiments were performed in the PTEN deficient cell line U87-MG. PTEN was expressed in these cells and PI3K pathway activation was determined by analysis of phosphorylated AKT (pAKT) levels. Expression of PTEN resulted in a significant decrease in pAKT at threonine 308, and expression of either the DHPH or PH domain with PTEN rescued pAKT308 levels (Fig. 4.7B). Furthermore, co-expression of CP-REX2 with PTEN did not result in rescued pAKT308 levels, but rather resulted in a greater decrease in pAKT308 compared to that observed with PTEN alone (Fig. 4.7B), supporting our claim that it behaves in a dominant negative manner. These results imply that the PH domain is the minimal domain required for PTEN inhibition, and docking of the C-terminal region of P-REX2 to the PDZ-BD increases PTEN activity through a dominant negative mechanism.

The PH domain of P-REX2 but not P-REX1 inhibits PTEN phosphatase activity

We next wanted to determine if inhibition of PTEN activity was specific to the PH domain of P-REX2, or if another PH domain, specifically that of its closest homolog P-REX1, could also inhibit PTEN. To determine this, we co-transfected PTEN-V5 with

control vector, P-REX2 PH-V5, or P-REX1 PH-V5. Lysates were incubated with anti-V5 agarose beads to immunoprecipitate the expressed proteins and phosphatase assays were performed. In accordance with our previous data, the PH domain of P-REX2 was able to inhibit PTEN phosphatase activity, but interestingly, the PH domain of P-REX1 was not (Fig. 4.8A). In support of this observation, co-transfection and immunoprecipitation of FLAG-PTEN with MYC-P-REX1 revealed that P-REX1 does not interact with PTEN, and therefore lacks the ability to dock via the PDZ-BD (Fig. 4.8B).

In addition, we have previously shown that loss of P-REX2 in the PTEN positive breast cancer cell line MCF-7 results in decreased PI3K signaling and cellular proliferation. We therefore determined if P-REX1 loss had a similar affect. P-REX1 expression was decreased in MCF-7 cells by stable shRNA infection. Western blot analysis of cell lysates showed no difference in AKT phosphorylation at Thr-308 following P-REX1 depletion (Fig. 4.8C). Furthermore, P-REX1 knockdown cells proliferated at the same rate as control cells (Fig. 4.8D), and P-REX1 loss did not lead to a reduction in soft agar colony formation (Fig. 4.8E). Taken together, these results suggest that unlike P-REX2, P-REX1 does not inhibit PTEN, decrease PI3K signaling or inhibit cellular transformation in PTEN positive cells. Therefore, it is likely that there is a level of specificity involved in P-REX2 PH domain mediated phosphatase inhibition and binding.

DISCUSSION

The Dbl family of Rho guanine nucleotide exchange factors consists of approximately 70 different proteins which create a highly specific network of Rho-family GTPase activation. GEFs exhibit varying degrees of GTPase selectivity, but a large number only activate a single GTPase. This specificity is due to the presence of non-conserved residues located at the interface between the DH and GTPase (Rossman et al., 2005). Activation of Rho-GTPases by the Dbl family of GEFs is coordinated by the integration of various signaling inputs. P-REX2 and P-REX1, for example, are activated by direct interaction with PIP3 and Gβγ generated by GPCR and PI3K signaling (Donald et al., 2004; Welch et al., 2002). For other GEFs, phosphorylation of regions outside the DH-PH domain by various kinases such as receptor tyrosine kinases blocks intramolecular autoinhibition and allows for GTPase activation (Aghazadeh et al., 2000; Das et al., 2000). Changes in subcellular localization also regulate their ability to activate GTPases. For example, the Rho GEF Ect2 is normally sequestered in the nucleus during interphase, but is activated by phosphorylation and localized to the cleavage furrow during G2/M phase, resulting in activation of Rho GTPases needed for cell division (Schmidt et al., 2002; Tatsumoto et al., 1999).

Here we present a novel mechanism of GEF mediated phosphatase inhibition that appears to be as highly regulated as GEF activation of Rho-GTPases. An illustrated model of this mechanism can be found in Figure 9. To summarize, P-REX2 docks to the PTEN PDZ-BD through its C-terminal domain, determines the phosphorylation site of the tail via the

DH domain, and inhibits PTEN activity through the unleashing of the PH domain, allowing for allosteric inhibition of the PTEN catalytic domain. Previous reports suggest that DH and PH domains of GEFs are capable of forming intramolecular auto-inhibitory interactions (Aghazadeh et al., 2000). We therefore hypothesize that negatively charged residues within the DH domain can interact with positive charges on the PH domain, blocking the phosphatase-inhibitory region of the PH domain (star in Fig. 9) from inhibiting PTEN, as demonstrated in Figures 2 and 6. However, phosphorylation of the C-terminal tail of PTEN could create a cluster of negative charges that competes with the DH domain for binding to positive charges on the PH domain, thereby unleashing the PH domain from the DH domain and allowing for allosteric inhibition of PTEN catalysis (Figure 9, bottom panel, and Figures 5 and 6). Docking of the IP4P domain of P-REX2 to the PDZ-BD of PTEN (Figure 4) is likely necessary for ensuring that the PH domain is in close proximity to PTEN so that it is positioned to inhibit phosphatase activity once PTEN is phosphorylated. Alternative explanations for the mechanism of unleashing the PH domain for PTEN inhibition cannot be excluded.

These findings are illuminating in several ways. First, we had never previously observed this secondary interaction between P-REX2 and PTEN using our original immunoprecipitation conditions. However, by lysing the cells in lysis buffer containing 1% Triton rather than NP-40 and SDS and exposing the immunoblots for longer time periods, we were able to see this weaker interaction. Also, we were surprised to find the P-REX2 bound strongly to the PDZ-BD. We believed that the PDZ-BD was not a binding site for P-REX2 based on our previous results that indicated a strong interaction

between P-REX2 and a PTEN mutant lacking the last three amino acids. However, deletion of the last three amino acids of PTEN creates another predicted PDZ-binding domain, a situation that has been observed to generate a functional PDZ-binding domain for PTEN (Valiente et al., 2005). We therefore used a PTEN mutant lacking the last two amino acids, eliminating both PDZ-BDs, to reveal the importance of this domain for binding to P-REX2. We also observed that PTEN phosphatase activity was never inhibited 100% by full length P-REX2 or any of the inhibitory domains, but rather decreased by approximately half. This could be due to the fact that not all PTEN is in a conformation that is amenable to PREX2 inhibition. Alternatively, P-REX2 may exhibit various degrees of PTEN inhibition based on its own post-translational modifications. It is also possible that there are specific pools of PTEN that are regulated by P-REX2 based upon its sub-cellular localization. For example, PTEN at the membrane may be inhibited by P-REX2 through its interaction with insulin receptor, whereas cytosolic and nuclear PTEN may not be inhibited. Performing phosphatase assays on PTEN from different cellular fractions would shed light on this possibility. Measuring the percentage of PTEN that is bound to P-REX2 in the cell, as well as determining where this interaction occurs will also be informative.

The above mechanism of PTEN regulation is illuminating because it reveals a novel function for a PH domain. The PH domain is highly represented in the human genome and is found in proteins of various functions (Ingley et al., 1994). Therefore, phosphatase inhibition by a PH domain may be broadly relevant to signaling pathway regulation because other PH domains may share a similar function. Furthermore, we show in Figure

6 and 7 that the PH domain of P-REX1, a close homolog of P-REX2 known to bind PIP3, does not inhibit PTEN phosphatase activity or effect PI3K signaling and transformation, suggesting that a specific PH domain may only be able to regulate the activity of a specific phosphatase, similar to GEF regulation of GTPases. Although P-REX1 did not inhibit PTEN, we cannot eliminate the possibility that there are other PH domains that share the ability to inhibit PTEN. In addition, some other PH domains could regulate other phosphatases, tightly controlling different signaling pathways.

A family of proteins that functions very similarly to PTEN is the myotubularins. Like PTEN, they contain a PTP active site motif, but mainly dephosphorylate lipid substrates, specifically at the 3' position (Blondeau et al., 2000; Taylor et al., 2000). All myotubularins contain a PH-GRAM domain, which is very similar to the PH domain of pleckstrin (Begley et al., 2003), and several, including MTMR13 and MTMR5 have PH domains (Begley and Dixon, 2005). Also, many myotubularins contain PDZ-binding domains. Interestingly, about half of the known myotubularins are inactive due to mutations in their catalytic domain, and it has been shown that the direct interaction between inactive and active myotubularins results in regulation of phosphatase activity (Kim et al., 2003; Robinson and Dixon, 2005). Therefore, it is possible that, similar to P-REX2 PH domain regulation of PTEN, myotubularins may also be regulated through direct interaction with PH or PH-GRAM domains.

It was originally thought that the maintenance of proper levels of phosphorylation events, especially those that direct cell cycle progression, occurred largely through the regulation

of kinase activity. However, it is clear that the activity of both kinases and phosphatases are tightly regulated in order to control cell-cycle dependent phosphorylation. There are many cases where phosphatase inhibition is dependent of the cellular environment. For instance, Clp1, a Cdc14 family phosphatase in *S. pombe* with strong homology to PTEN, is an activator of mitotic exit through its dephosphorylation and activating Cdk1 inhibitors. However, before mitotic exit, Clp1 is inactivated and sequestered to the nucleolus until mitotic entry begins. It is then released into the cytoplasm but remains inactive until mitotic exit. During this period of inactivation, Clp1 is phosphorylated by Cdk1, however during mitotic exit, Clp1 autodephosphorylates itself, allowing for phosphorylation and activation of Cdk1 inhibitor proteins and anaphase-promoting complex (Wolfe et al., 2006). Another example includes the protein phosphatase PP1. Like Clp1, PP1 is specifically required during mitotic exit to dephosphorylate mitotic phosphoproteins. It has been shown that PP1 is inactivated during early mitosis through both phosphorylation at Thr320 by Cdc2 and though the binding of inhibitor-1. However, at the onset of mitotic exit, Cdc2 is degraded, allowing for autodephosphorylation of PP1 at Thr320 and partial activation of phosphatase activity. PP1 then dephosphorylates inhibitor-1 at Thr35, releasing it from inhibitor-1 mediated inhibition and allowing for full PP1 activation and progression through mitotic exit (Wu et al., 2009). Therefore, as in the cell cycle, we present a model of PTEN inhibition by P-REX2 that is regulated by PTEN C-terminal phosphorylation. Phosphatase activity and GEF activation are dynamically regulated by various inputs, and likewise, P-REX2 inhibition of PTEN is likely not static, but rather responsive to specific cellular cues.

FIGURE LEGENDS

Figure 4.1. *A)* Illustration of deletion mutants used in experiments. *B)* Coomassie stain of recombinant GST-PTEN WT and mutant vectors purified from BL21(DE3) pLyseE bacterial cells using glutathione sepharose beads. BSA standards were used to quantify the protein.

Figure 4.2. **P-REX2 inhibition of PTEN is regulated by PTEN tail phosphorylation.** *A)* HEK293 cell lysates co-expressing empty vector, FLAG-PTEN, or FLAG-PTEN-3A with empty vector or P-REX2-V5 were incubated with FLAG-M2 antibody conjugated to agarose beads. Immunoprecipitated protein complexes were analyzed by immunoblotting. *B)* U87-MG cell lysates co-expressing FLAG-PTEN or FLAG-PTEN3A with empty vector or P-REX2-V5 were incubated with a rabbit monoclonal PTEN antibody conjugated to agarose beads. Phosphatase assays were performed on immunoprecipitated protein complexes by incubating the beads with 20 µM soluble di-C8-D-myo-phosphatidylinositol 3,4,5-trisphosphate (PIP3) at 37°C for 30 minutes. *C) In vitro* phosphatase assays were performed by incubating equimolar amounts of purified GST-PTEN WT or GST-PTEN-3E and purified P-REX2-V5 in the presence of PIP3 at 37°C for 30 minutes. Error bars represent standard deviation (SD), n=3, ** $P < 0.01$.

Figure 4.3. **P-REX2 interacts with multiple sites on PTEN.** *A)* The interaction between P-REX2 and PTEN deletion mutants was analyzed by co-immunoprecipitation. P-REX2-V5, FLAG- PTEN mutants, or empty vectors were co-transfected into HEK293 cells and

lysates were incubated with FLAG-M2 antibody conjugated to agarose beads overnight at 4ºC. Total lysates and FLAG-immunoprecipitated proteins were analyzed by western blot.

Figure 4.4. **The C-terminal region of P-REX2 interacts with the PDZ-BD of PTEN.** *A)* HEK293 cell lysates expressing C-P-REX2-V5 was incubated with recombinant GST-PTEN deletion mutants or control GST sepharose beads. Pulled-down proteins were analyzed by immunoblotting. *B-C)* HEK293 cells co-expressing P-REX2 C-terminal domains and FLAG-tagged PTEN deletion mutants were incubated with FLAG-M2 antibody or normal mouse IgG (control). Immunoprecipitated protein complexes were analyzed by immunoblotting.

Figure 4.5. **P-REX2 DHPH and PH domains interact with the catalytic domain of PTEN.** *A)* HEK293 cell lysates co-expressing DHPH-V5 were incubated with recombinant GST-PTEN deletion mutants or GST control sepharose beads. Pulled-down proteins complexes were analyzed by immunoblotting. *B-C)* PH-V5, DH-V5, or DHPH-V5 were in-vitro translated and 10 µL of protein lysate was incubated with GST control or GST-PTEN sepharose beads in BC200 buffer. Pulled-down proteins complexes were analyzed by immunoblotting. *D)* Immunoprecipitation experiments were performed by co-transfection of PH-V5 or DHPH-V5 with FLAG-NC2 into HEK293 cells. Protein lysates were incubated with FLAG-M2 antibody, V5-agarose beads, or normal mouse IgG (control) conjugated to agarose beads overnight. Total lysates and FLAG-immunoprecipitated proteins were analyzed by western blot.

Figure 4.6. **The PH domain inhibits PTEN in-vitro.** *A-C)* For *in-vitro* phosphatase assays, purified recombinant GST-PTEN WT or GST-PTEN mutants was incubated with equimolar amounts of purified V5-tagged P-REX2 domains as indicated in the presence of PIP3 at 37°C for 30 minutes. Error bars represent SD, n=3, ** and *, $P < 0.01$ and $P<0.05$, respectively.

Figure 4.7. **The PH domain inhibits PTEN produced in mammalian cells.** *A)* Lysates from HEK293 cells co-expressing PTEN-V5 with empty vector, PH-V5, or C-P-REX2-V5 were incubated with V5 agarose beads. Phosphatase assays were then performed on the immunoprecipitated protein. Levels of immunoprecipitated proteins were analyzed by immunoblotting. Error bars represent SD, n=3, **, $P < 0.01$.*B)* DHPH-V5, PH-V5 or CPREX2-V5 and untagged PTEN were transfected alone or in combination into U87MG cells. 24 hours after transfection, cells were starved with DMEM without FBS for 16 hours and then lysed in 2X sample buffer. Equal concentrations of lysate were resolved on SDS-polyacrylamide gels and levels of pAKT-Thr308 were analyzed by western blot.

Figure 4.8. **The PH domain of P-REX1 does not inhibit PTEN and does not affect cellular proliferation or transformation.** *A)* Lysates from HEK293 cells expressing PTEN-V5 with empty vector, P-REX2-PH-V5, or P-REX1-PH-V5 were incubated with V5-agarose beads, and phosphatase assays were performed on immunoprecipitated proteins. Levels of immunoprecipitated proteins were analyzed by immunoblotting. Error bars represent SD, n=3, **, $P < 0.01$. *B)* Immunoprecipitation of PTEN and full length P-REX1. FLAG-PTEN and MYC-P-REX1 were transfected into HEK293 cells.

Cells were lysed and incubated with FLAG-M2 antibody plus agarose beads overnight and eluted proteins were analyzed by western blot. *C)* Western blot analysis of pAKT308 levels in MCF-7 cells depleted for P-REX1 by shRNA *D)* Proliferation of control or P-REX1 depleted MCF-7 cells, as determined by crystal violet staining. *E)* Quantification of colony formation of control or P-REX1 depleted MCF-7 cells grown in soft agar after 14 days.

Figure 4.9. **Model of PTEN inhibition by P-REX2.** The DH domain of P-REX2 restricts PH domain inhibition of PTEN phosphatase activity when the C-terminal tail of PTEN is unphosphorylated (upper panel). However, phosphorylation of the tail is "read" by the DH domain, switching the ionic interaction to the phospho-tail, and unleashing the PH domain inhibitory region (star labeled "I") of P-REX2 through interaction with the phosphatase and C2 domains of PTEN on its non-lipid-binding surface (lower panel).

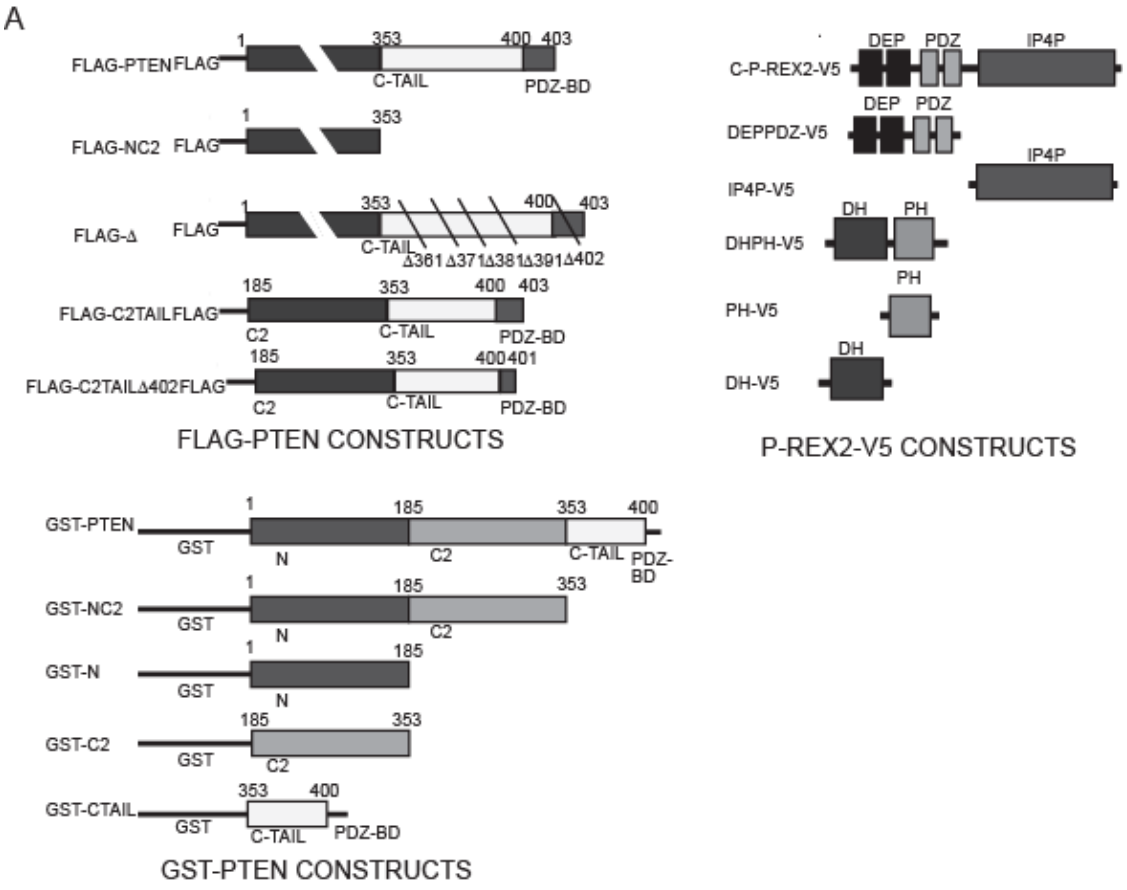
A
FLAG-PTEN
FLAG-NC2
FLAG-Δ
FLAG-C2TAIL
FLAG-C2TAILΔ402
FLAG
C-TAIL
PDZ-BD
C2
Δ361 Δ371 Δ381 Δ391 Δ402
FLAG-PTEN CONSTRUCTS
C-P-REX2-V5
DEPPDZ-V5
IP4P-V5
DHPH-V5
PH-V5
DH-V5
DEP
PDZ
IP4P
DH
PH
P-REX2-V5 CONSTRUCTS
GST-PTEN
GST-NC2
GST-N
GST-C2
GST-CTAIL
GST
N
C2
C-TAIL
PDZ-BD
GST-PTEN CONSTRUCTS

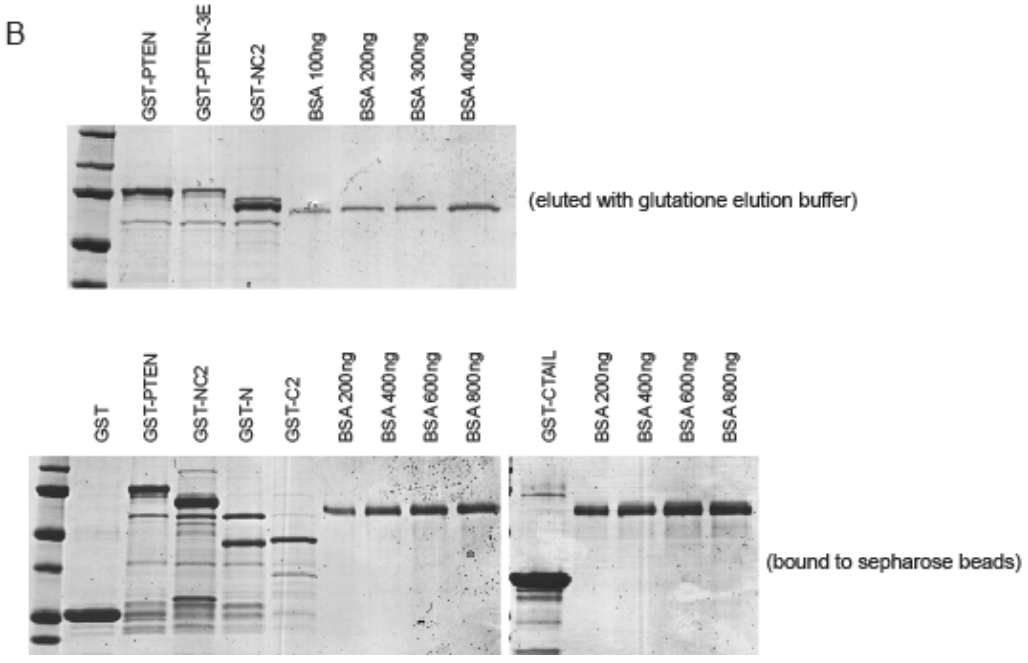
B
GST-PTEN
GST-PTEN-3E
GST-NC2
BSA 100ng
BSA 200ng
BSA 300ng
BSA 400ng
(eluted with glutatione elution buffer)
GST
GST-PTEN
GST-NC2
GST-N
GST-C2
BSA 200ng
BSA 400ng
BSA 600ng
BSA 800ng
GST-CTAIL
BSA 200ng
BSA 400ng
BSA 600ng
BSA 800ng
(bound to sepharose beads)

FIGURE 4.1

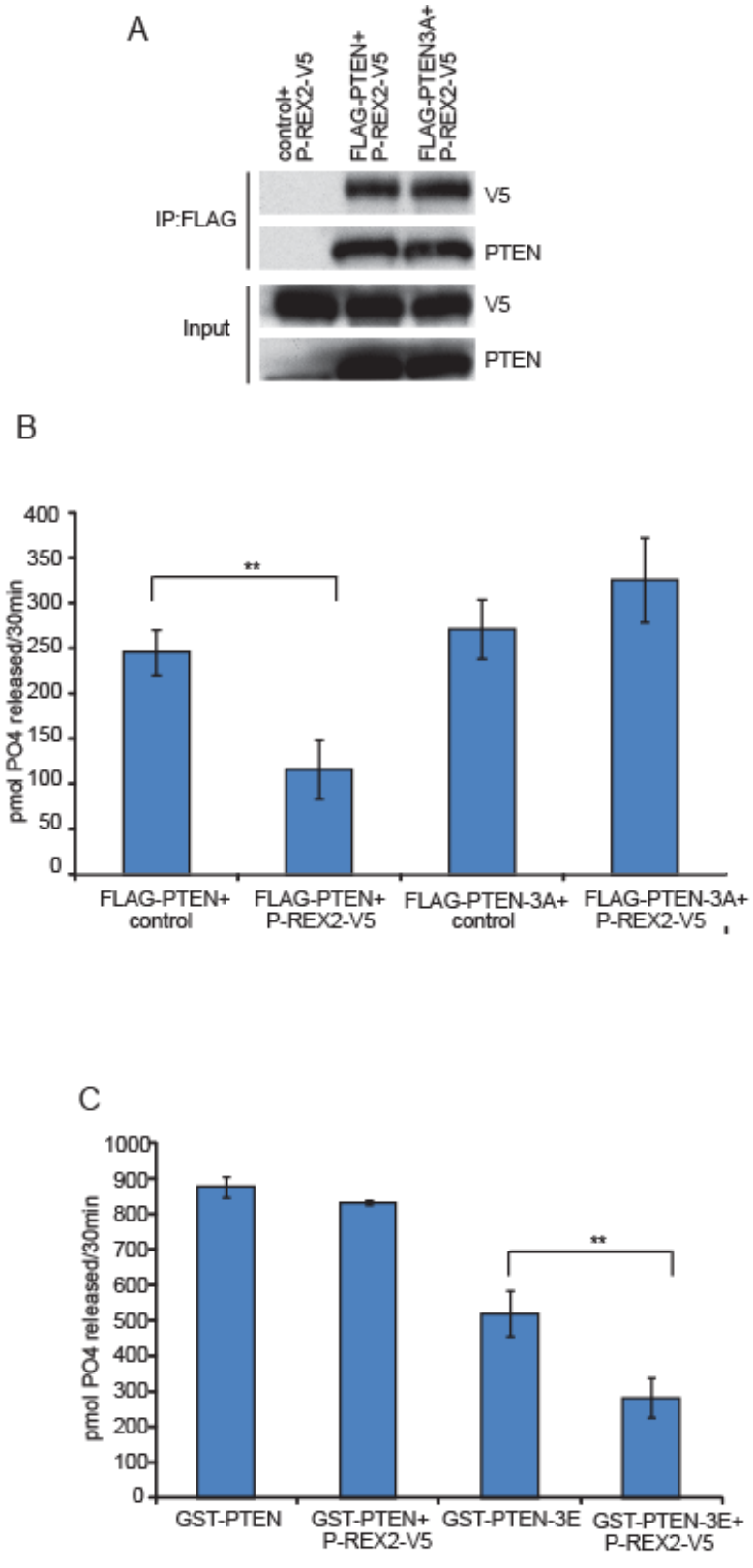
A
control+ P-REX2-V5
FLAG-PTEN+ P-REX2-V5
FLAG-PTEN3A+ P-REX2-V5
IP:FLAG
V5
PTEN
Input
V5
PTEN
B
pmol PO4 released/30min
400
350
300
250
200
150
100
50
0
**
FLAG-PTEN+ control
FLAG-PTEN+ P-REX2-V5
FLAG-PTEN-3A+ control
FLAG-PTEN-3A+ P-REX2-V5
C
pmol PO4 released/30min
1000
900
800
700
600
500
400
300
200
100
0
**
GST-PTEN
GST-PTEN+ P-REX2-V5
GST-PTEN-3E
GST-PTEN-3E+ P-REX2-V5

FIGURE 4.2

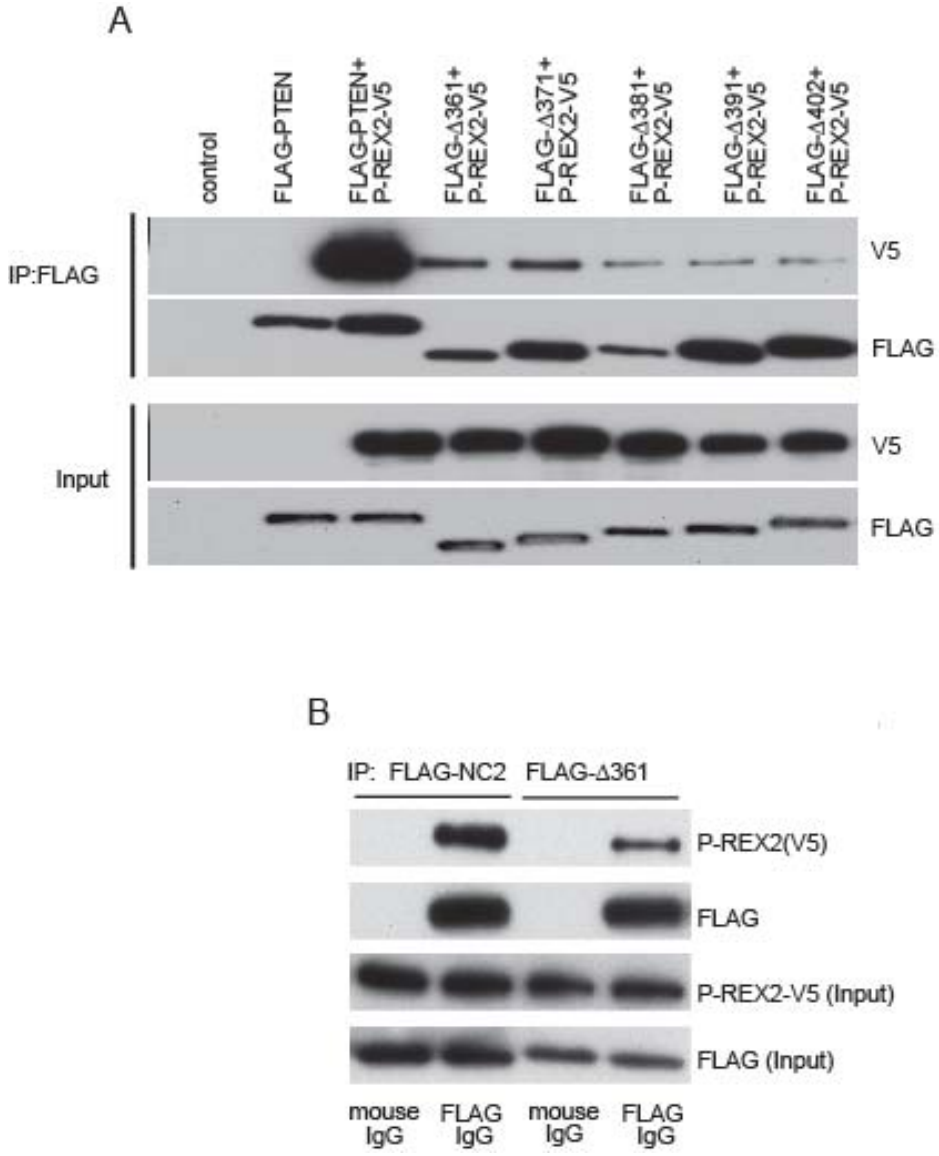
A
control
FLAG-PTEN
FLAG-PTEN+ P-REX2-V5
FLAG-Δ361+ P-REX2-V5
FLAG-Δ371+ P-REX2-V5
FLAG-Δ381+ P-REX2-V5
FLAG-Δ391+ P-REX2-V5
FLAG-Δ402+ P-REX2-V5
IP:FLAG
V5
FLAG
Input
V5
FLAG
B
IP: FLAG-NC2
FLAG-Δ361
P-REX2(V5)
FLAG
P-REX2-V5 (Input)
FLAG (Input)
mouse IgG
FLAG IgG
mouse IgG
FLAG IgG

FIGURE 4.3

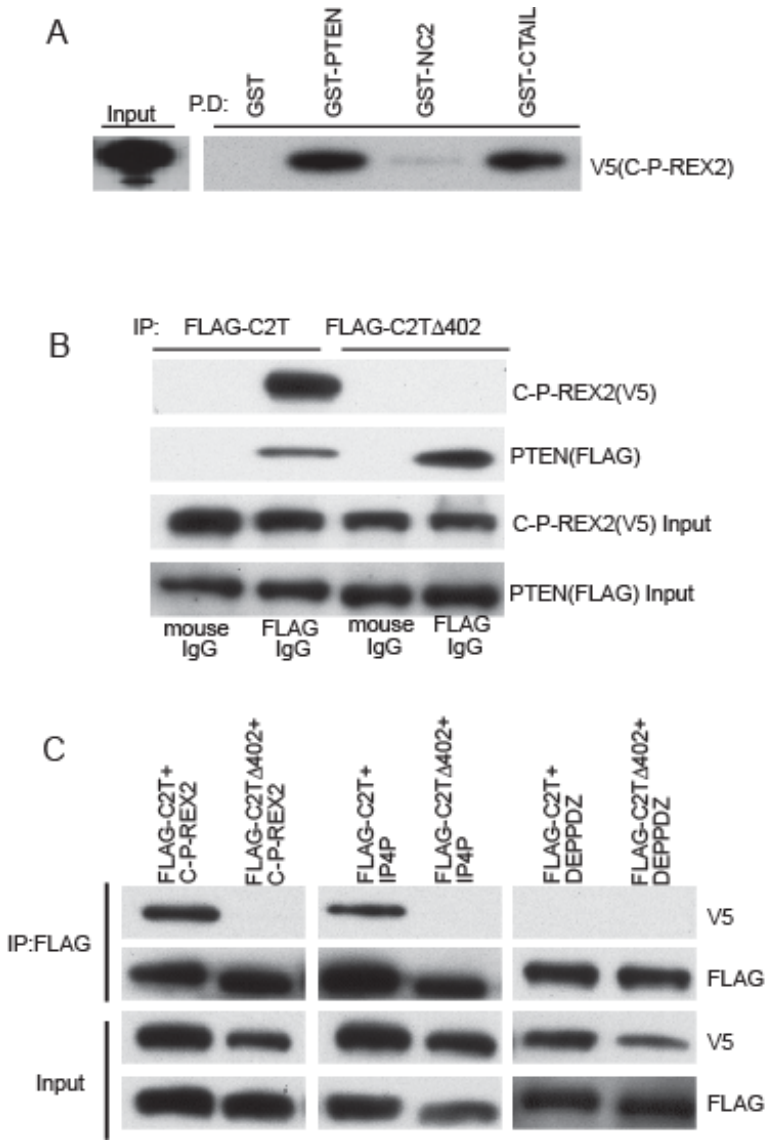
A
Input
P.D:
GST
GST-PTEN
GST-NC2
GST-CTAIL
V5(C-P-REX2)
B
IP:
FLAG-C2T
FLAG-C2TΔ402
C-P-REX2(V5)
PTEN(FLAG)
C-P-REX2(V5) Input
PTEN(FLAG) Input
mouse IgG
FLAG IgG
mouse IgG
FLAG IgG
C
FLAG-C2T+ C-P-REX2
FLAG-C2TΔ402+ C-P-REX2
FLAG-C2T+ IP4P
FLAG-C2TΔ402+ IP4P
FLAG-C2T+ DEPPDZ
FLAG-C2TΔ402+ DEPPDZ
IP:FLAG
V5
FLAG
Input
V5
FLAG

FIGURE 4.4

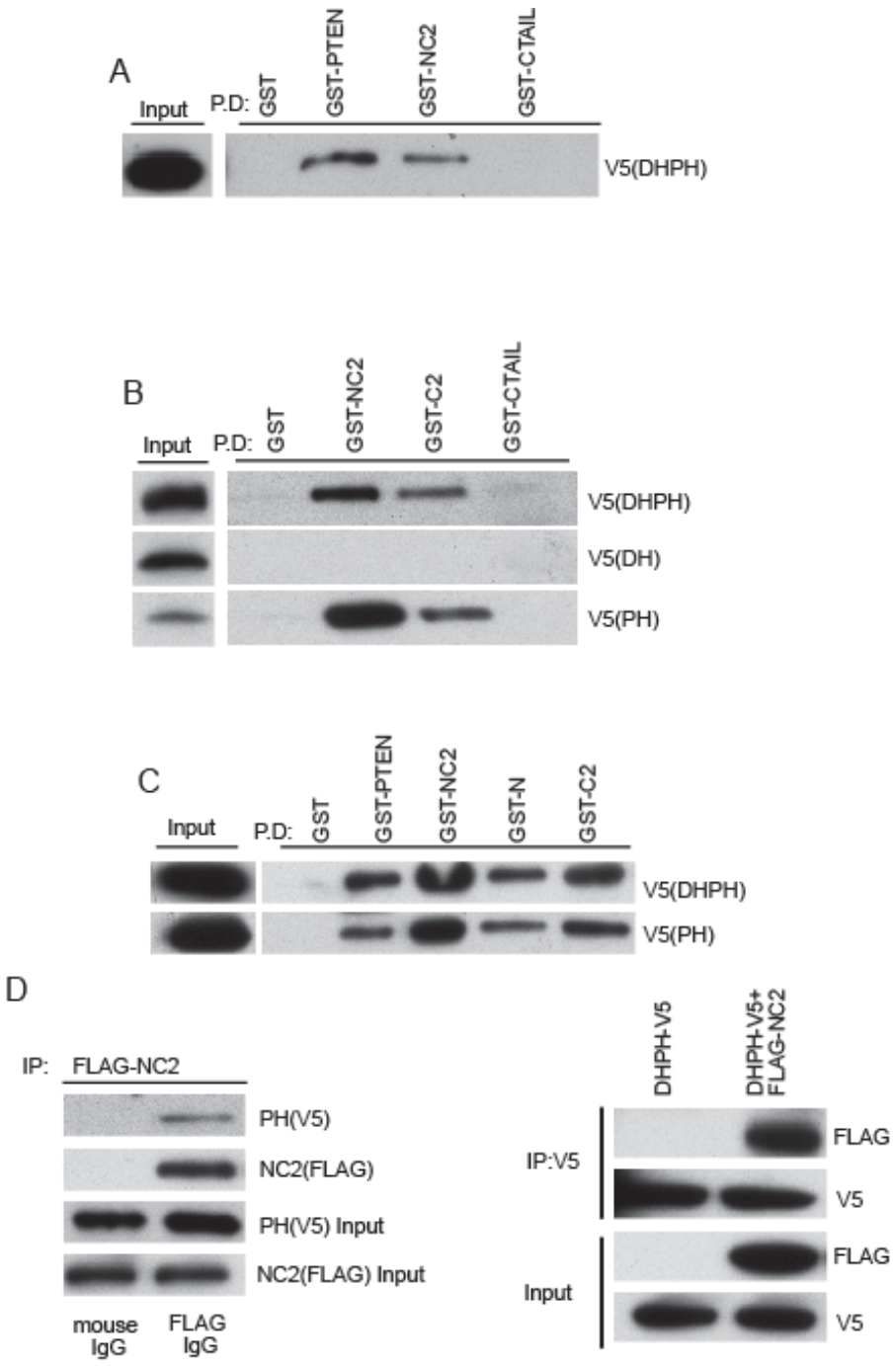
A
Input
P.D:
GST
GST-PTEN
GST-NC2
GST-CTAIL
V5(DHPH)
B
Input
P.D:
GST
GST-NC2
GST-C2
GST-CTAIL
V5(DHPH)
V5(DH)
V5(PH)
C
Input
P.D:
GST
GST-PTEN
GST-NC2
GST-N
GST-C2
V5(DHPH)
V5(PH)
D
IP:
FLAG-NC2
PH(V5)
NC2(FLAG)
PH(V5) Input
NC2(FLAG) Input
mouse IgG
FLAG IgG
DHPH-V5
DHPH-V5+ FLAG-NC2
IP:V5
FLAG
V5
Input
FLAG
V5

FIGURE 4.5

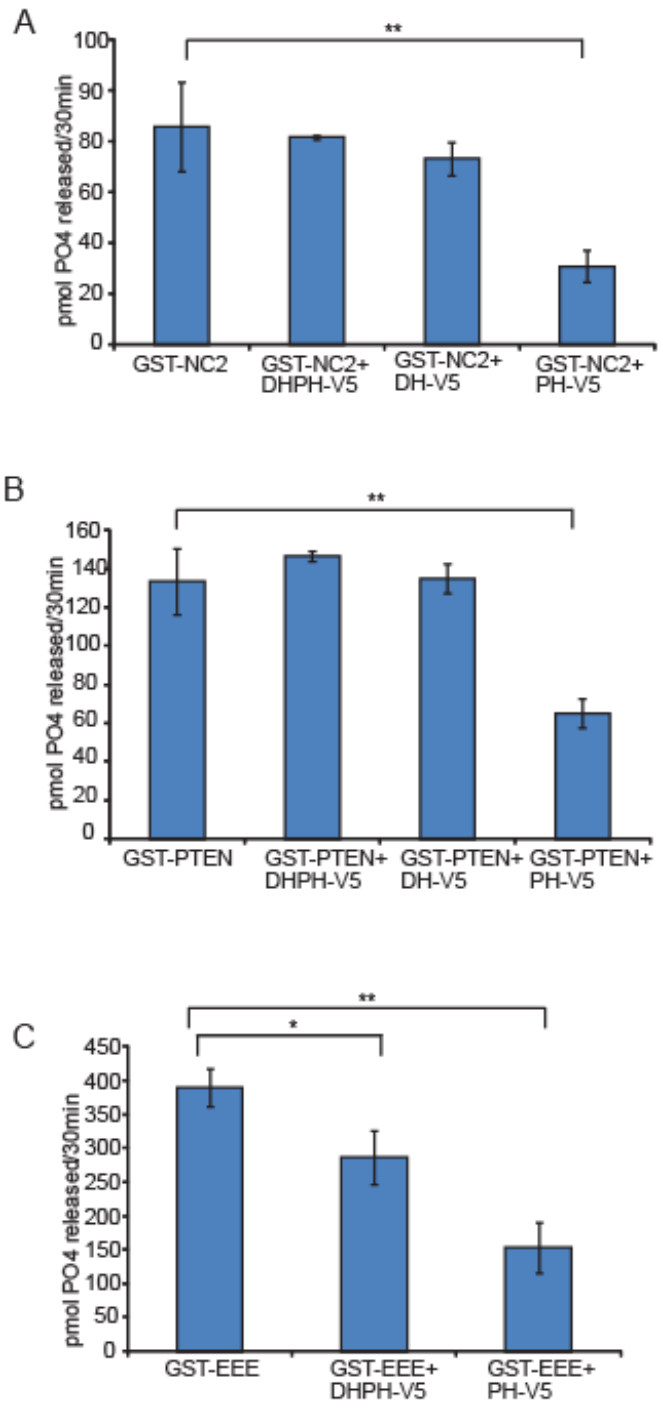
A
**
pmol PO4 released/30min
100
90
80
60
40
20
0
GST-NC2
GST-NC2+ DHPH-V5
GST-NC2+ DH-V5
GST-NC2+ PH-V5
B
**
pmol PO4 released/30min
160
140
120
100
80
60
40
20
0
GST-PTEN
GST-PTEN+ DHPH-V5
GST-PTEN+ DH-V5
GST-PTEN+ PH-V5
C
**
*
pmol PO4 released/30min
450
400
350
300
250
200
150
100
50
0
GST-EEE
GST-EEE+ DHPH-V5
GST-EEE+ PH-V5

FIGURE 4.6

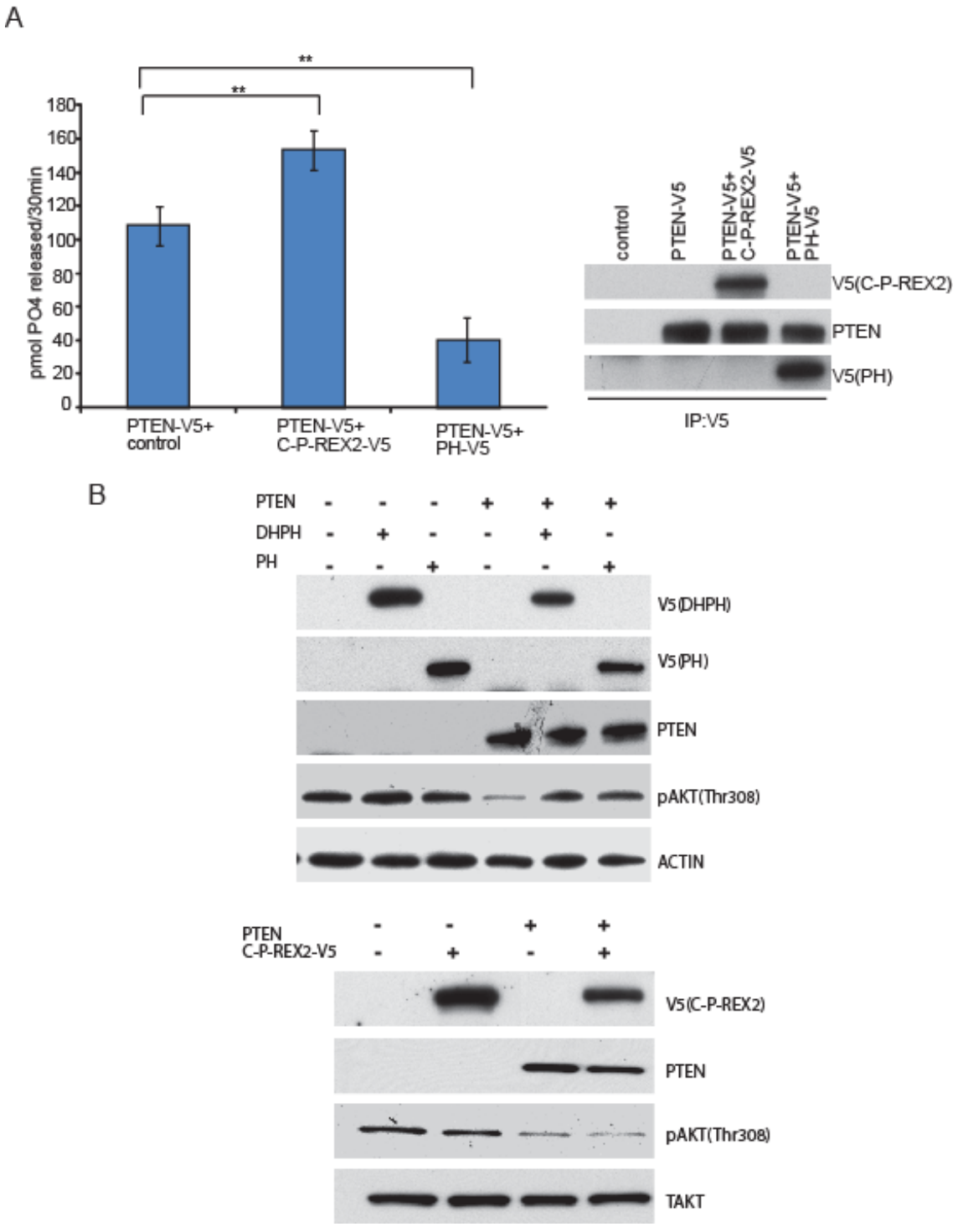
A
**
**
180
160
140
120
100
80
60
40
20
0
pmol PO4 released/30min
PTEN-V5+ control
PTEN-V5+ C-P-REX2-V5
PTEN-V5+ PH-V5
control
PTEN-V5
PTEN-V5+ C-P-REX2-V5
PTEN-V5+ PH-V5
V5(C-P-REX2)
PTEN
V5(PH)
IP:V5
B
PTEN
DHPH
PH
V5(DHPH)
V5(PH)
PTEN
pAKT(Thr308)
ACTIN
PTEN
C-P-REX2-V5
V5(C-P-REX2)
PTEN
pAKT(Thr308)
TAKT

FIGURE 4.7

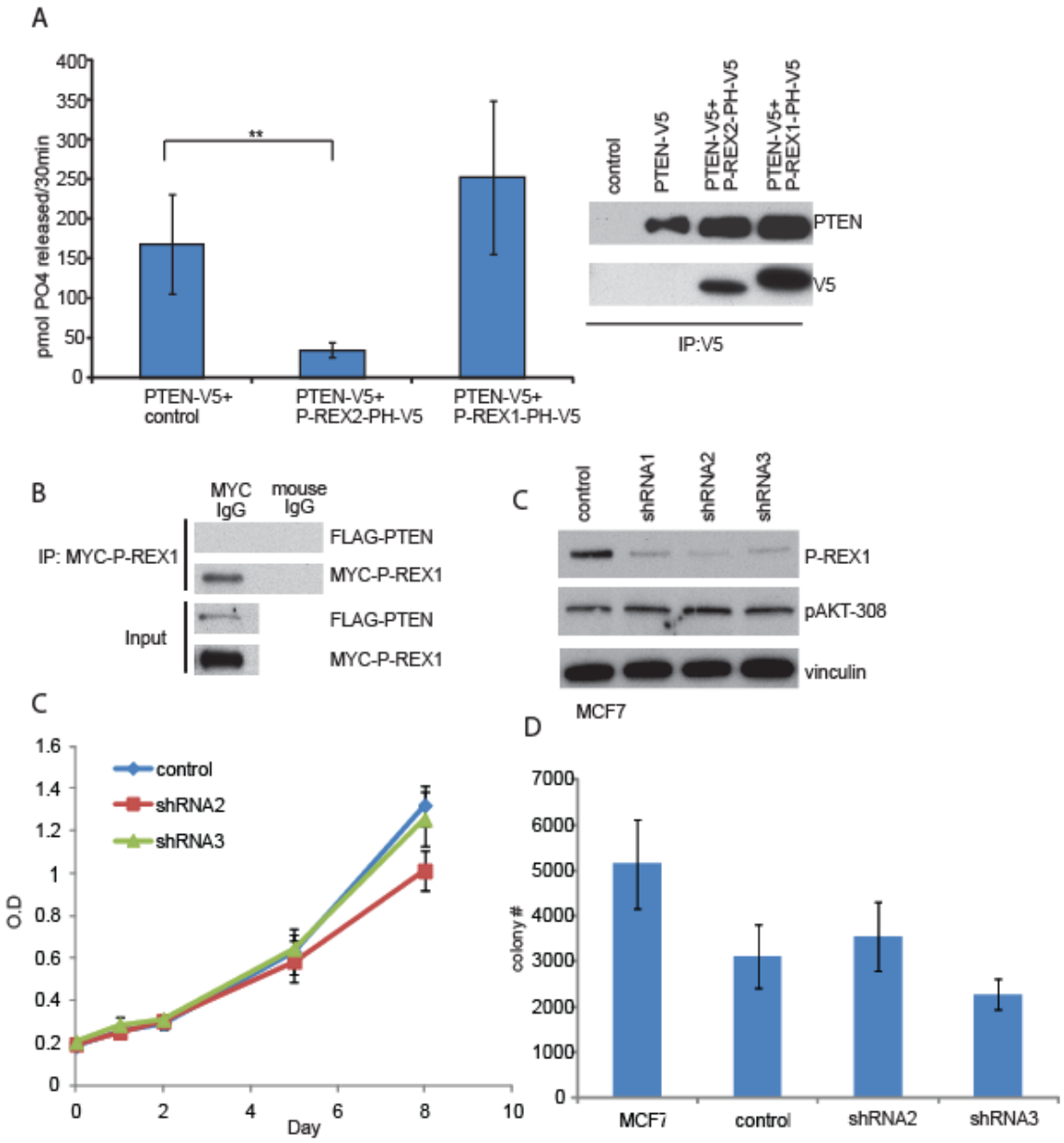
A
pmol PO4 released/30min
400
350
300
250
200
150
100
50
0
**
PTEN-V5+ control
PTEN-V5+ P-REX2-PH-V5
PTEN-V5+ P-REX1-PH-V5
control
PTEN-V5
PTEN-V5+ P-REX2-PH-V5
PTEN-V5+ P-REX1-PH-V5
PTEN
V5
IP:V5
B
MYC IgG
mouse IgG
IP: MYC-P-REX1
FLAG-PTEN
MYC-P-REX1
Input
FLAG-PTEN
MYC-P-REX1
C
control
shRNA1
shRNA2
shRNA3
P-REX1
pAKT-308
vinculin
MCF7
C
O.D
1.6
1.4
1.2
1
0.8
0.6
0.4
0.2
0
control
shRNA2
shRNA3
0
2
4
6
8
10
Day
D
colony #
7000
6000
5000
4000
3000
2000
1000
0
MCF7
control
shRNA2
shRNA3

FIGURE 4.8

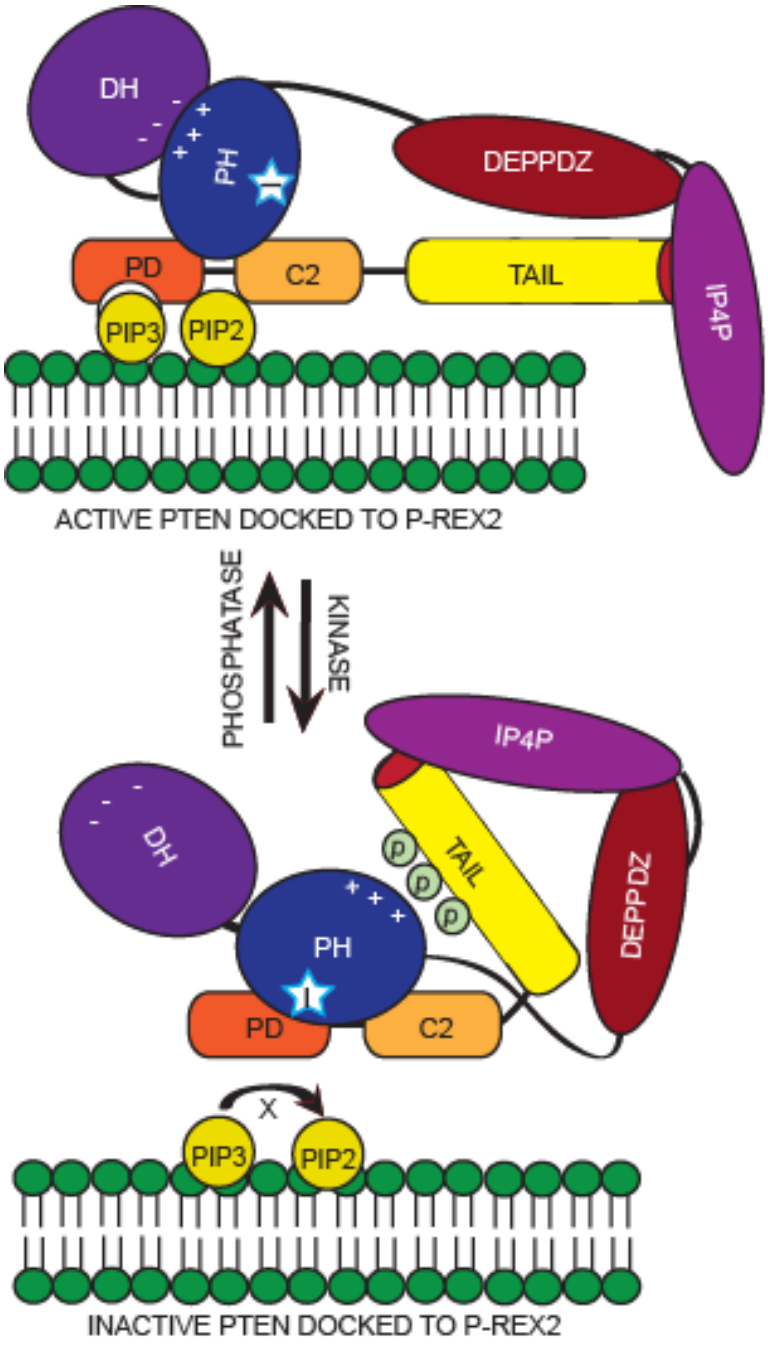
DH
PH
DEPPDZ
PD
C2
TAIL
IP4P
PIP3
PIP2
ACTIVE PTEN DOCKED TO P-REX2
PHOSPHATASE
KINASE
IP4P
DH
TAIL
DEPPDZ
PH
PD
C2
X
PIP3
PIP2
INACTIVE PTEN DOCKED TO P-REX2

FIGURE 4.9

CHAPTER V

Summary and Future Perspectives

PTEN is a *bona fide* tumor suppressor that inhibits PI3K stimulated growth, proliferation, survival, and metabolism by dephosphorylating PI(3,4,5)P3 to generate PI(4,5)P2. Our lab has identified a novel PTEN interacting protein, the Rac-GEF P-REX2, which inhibits PTEN in a non-competitive manner. In this thesis, we examine the role of P-REX2 mediated PTEN inhibition in PI3K signaling regulation, tumorigenesis, insulin signaling, and glucose metabolism and reveal a dynamic mechanism of PTEN inhibition by P-REX2.

In Chapter II, we explore the role of P-REX2 expression on cellular transformation. By overexpressing P-REX2 and the PTEN inhibitory DHPH domain in normal mammary epithelial cells, we show that P-REX2 increases PI3K signaling, promotes cell proliferation, and disrupts acini formation. Furthermore, P-REX2 cooperates with other known oncogenes including p110α E545K, c-MYC, and Her2 to transform normal cells and form tumors in mice. We also discovered several transforming cancer mutants of P-REX2. These results suggest that P-REX2 has oncogenic properties and may promote tumorigenesis.

We also show in Chapter II that P-REX2 Rac GEF activity is dispensable for PTEN inhibition. However, our studies do not address the potential role that P-REX2 Rac GEF activity may play in cellular transformation, and it will be important to address this in the future. Studies have shown that Rac regulates migration, growth, and apoptosis through various mechanisms, including activation of the transcription factor NFκB. (Sulciner et al., 1996). Activated Rac can also transform cells and initiate tumor formation in mice

(Khosravi-Far et al., 1996). Overexpression of P-REX2 and the DHPH domain may result in increased Rac activation in addition to increased PTEN inhibition and PI3K signaling, and we therefore cannot conclude that transformation is exclusively a result of increased PTEN inhibition. Several experiments can be performed to understand the contribution of Rac activation to cellular transformation. Overexpression the GEF dead P-REX2 N212A mutant instead of wild-type P-REX2 would allow us to observe the effects of P-REX2 expression on signaling and proliferation without affecting Rac activation. Furthermore, Rac deficient cells could also be utilized to determine it Rac activation is dispensable for P-REX2 mediated cellular transformation. In the same manner, it is unclear whether PTEN is required for P-REX2 transformation. We have shown previously that loss of P-REX2 in PTEN mutant cell lines does not affect proliferation; however there are many PTEN negative tumor samples that have elevated P-REX2 expression. Therefore, expressing P-REX2 in PTEN deficient cell lines and analyzing changes in proliferation and 3-D morphogenesis may provide insight into the function of P-REX2 in cellular transformation.

We have identified several transforming cancer mutations in *PREX2*, but we have not yet identified the mechanism in which these mutations activate P-REX2. Interestingly, the location of mutations described here and by Berger et. al, are dispersed throughout the coding region and are not clustered into “hot spots”, as many oncogenic mutations are, suggesting that there may be multiple ways that these mutations can affect P-REX2 function. For instance, these mutants may be more effective PTEN inhibitors. Changes in key residues may increase P-REX2 binding to PTEN, or may eliminate regulation by

the PTEN C-terminal tail, which is critical for P-REX2 inhibition as discussed in Chapter IV. Therefore, comparative binding assays and PTEN phosphatase assays will be performed in the future to determine if P-REX2 mutants are better PTEN inhibitors. Cancer mutants may also activate Rac, therefore increasing Rac activated migration, growth and apoptosis. It will be interesting to determine if any cancer mutants activate Rac in the absence of PIP3 or Gβγ, exchange GDP more efficiently, or increase Rac activated migration. Furthermore, mutations or deletions in *PREX2* may affect intramolecular interactions that may inhibit or active P-REX2 enzymatic activity. In Chapter IV, we discuss how an intramolecular interaction between the DH domain and PH domain may inhibit PH domain inhibition of PTEN. Mutations in the DH domain may disrupt this interaction, allowing for constitutive inhibition of PTEN. Also, it has been reported that the phosphatase domain of P-REX1 interacts with the DEP and PDZ domains, regulating Gβγ activation (Urano et al., 2008). Therefore, mutations in *PREX2* may also affect intramolecular interactions that regulate Rac activation.

In Chapter III, we more thoroughly analyze the role of P-REX2 in signaling regulation by examining changes in PI3K signaling in *Prex2* knockout mice. Analysis of signaling activation in *Prex2*$^{-/-}$ fibroblasts showed that loss of P-rex2 led to decreased PI3K signaling activation specifically in response to insulin. This correlated with an increase in PTEN activity following insulin stimulation in *Prex2*$^{-/-}$ fibroblasts, suggesting that decreased PI3K signaling occurs in part due to increased PTEN activity. We also discovered that P-REX2 interacts with phosphorylated insulin receptor and transports PTEN to the membrane following insulin stimulation, suggesting that P-rex2 may

specifically regulate insulin signaling by forming a complex with PTEN and activated insulin receptor. Furthemore, *Prex2*$^{-/-}$ mice exhibited decreased glucose uptake and reduced insulin tolerance. We also observed decreased insulin stimulated PI3K signaling in liver and fat tissue. PTEN activity was increased in *Prex2*$^{-/-}$ liver samples, and this correlated with an increase in insulin stimulated PIP3 levels.

Determining the mechanism of insulin stimulated PTEN regulation is an exciting topic for future study. We have shown the P-REX2 interacts with activated insulin receptor and brings PTEN to the membrane, but the implications of this interaction are unknown. It is possible that insulin stimulates PTEN C-terminal tail phosphorylation, and therefore P-REX2 inhibition, as discussed in Chapter IV. Therefore, it will be important to measure levels of PTEN phosphorylation following insulin stimulation. It will also be interesting to determine if P-REX2 inhibition of PTEN is regulated by different growth factors in other cell types. As discussed in Chapter III, leptin is an important regulator of PI3K signaling in hypothalamic neurons and stimulates PTEN phosphorylation (Ning et al., 2006). Therefore, leptin, as opposed to insulin, may be the primary regulator of P-REX2 mediated PTEN in hypothalamic neurons.

We have shown that P-REX2 inhibition of PTEN has important implications for PI3K signaling *in vivo*. It is therefore possible that deletion of P-REX2 may adversely affect tumor formation in mice with decreased PTEN expression. Mice heterozygous for *Pten* develop tumors in a variety of tissues and organs systems including the uterus, prostate, thyroid, endometrium, liver, adrenal medulla, and breast, among others (Di Cristofano et

al., 1998; Podsypanina et al., 1999; Suzuki et al., 1998; Trotman et al., 2003). It is possible that deleting *Prex2* in Pten heterozygous mice may restore the activity of the Pten present and decrease tumor formation. Generating *Prex2*$^{-/-}$/*PTEN*$^{+/-}$ mice and comparing the onset of tumor formation in these mice to *PTEN*$^{+/-}$ mice will allow us to answer this question.

Although we have demonstrated a role for P-rex2 in regulating glucose homeostasis and insulin sensitivity, we have not studied the long term effects of P-rex2 loss in mice. It will be interesting to document new phenotypes that may present themselves as *Prex2*$^{-/-}$ mice age. Increased weight and elevated fasting plasma glucose levels are often observed in insulin resistant mice at later time points, and this will be documented in the future. Furthermore, tissue specific P-REX2 knockout mice could be generated in order to determine which tissues are most affected by P-REX2 regulation of insulin signaling and glucose metabolism. It would also be informative to determine if *PREX2* expression is increased or if mutations exist in patients with Type II diabetes, as this may serve as a predictive marker for the disease.

We have shown that P-REX2 is necessary for regulating insulin signaling and glucose homeostatsis *in vivo* by regulating insulin stimulated PTEN inhibition. Therefore, uncovering the mechanism of PTEN inhibition by P-REX2 is necessary for understanding how this interaction is regulated. In Chapter IV, we discovered that P-REX2 binds to two different regions of PTEN. The inositol 4-polyphosphatase domain binds with high affinity to the PDZ binding domain of PTEN, whereas the DHPH domain

tandem, via the PH domain, interacts with the catalytic unit of PTEN comprised of the phosphatase and C2 domain. Furthermore, these interactions allow for dynamic regulation of PTEN activity. While the PH domain of P-REX2 can constitutively inhibit PTEN activity, inhibition by full length P-REX2 is inhibited by the DH domain. Phosphorylation of the C-terminal of PTEN unleashes the PH domain from DH domain inhibition, allowing for PH domain-mediated inhibition of PTEN. We also found that P-REX1, a close homolog of P-REX2, does not bind to PTEN and its PH domain does not inhibit PTEN phosphatase activity, suggesting that GEF related phosphatase inhibition may be highly specific.

Discovering that P-REX2 inhibition of PTEN occurs in a dynamic manner is exciting and provides many interesting areas of future study. We have shown that phosphorylation of the C-terminal tail controls P-REX2 inhibition, therefore it is necessary to understand how phosphorylation of the tail is regulated. CK2 is responsible for a majority of PTEN phosphorylation on Ser370, Ser380, Ser385, Thr382, while GSK3 have been shown to phosphorylate PTEN at Ser362 and Thr-366 (Al-Khouri et al., 2005; Torres and Pulido, 2001). Activation of kinases and regulation of phosphatases that target these sites is critical for regulating PTEN tail phosphorylation and PTEN inhibition. For instance, it has been reported that leptin stimulates PTEN phosphorylation in a CK2 dependent manner (Ning et al., 2006), as discussed in Chapter III. It is possible that leptin activates CK2 kinase activity, resulting in PTEN phosphorylation and inhibition by P-REX2. We have also shown that the C-terminal phosphatase domain of P-REX2 binds to the PTEN tail. Although no substrates of this phosphatase domain have yet been identified, we can

hypothesize that this domain could dephosphorylate the PTEN tail, this serving as an autoinhibitory domain by shutting off its own PTEN inhibition. The interaction between the phosphatase domain of P-REX2 and the PTEN PDZ-BD was surprising to us, as we expected binding to occur through the DEP-PDZ tandem. It is possible that the phosphatase domain forms intramolecular interactions with the PDZ domain, as observed with P-REX1 (Urano et al., 2008), which can mediate the interaction of the phosphatase domain with the PDZ-BD.

Furthermore, it would not be surprising if post-translational modifications of P-REX2 were involved in PTEN regulation in addition to PTEN phosphorylation. Studies have shown that P-REX1 can be directly phosphorylated by cyclic AMP-dependent protein kinase (PKA) resulting in inhibition of P-REX1 Rac-GEF activity. Furthermore, it has been reported that both P-REX1 and P-REX2 interact with the protein phosphatase PP1α, and in the case of P-REX1, leads to dephosphorylation of at least three residues including Ser-834, Ser-1001 and Ser-1165, and activation of Rac-GEF activity (Barber et al., 2012; Mayeenuddin and Garrison, 2006). These studies support the theory that the phosphorylation status of P-REX2 may be critical to protein function, and thusly may regulate its ability to inhibit PTEN. There may also be other effectors required for P-REX2 mediated inhibition of PTEN. P-REX2 binds to both PIP3 and Gβγ, which activates its Rac GEF activity. These two substrates are therefore attractive candidates for PTEN-P-REX2 effectors, and their effects on P-REX2 mediated PTEN inhibition will be determined.

We have also identified a new role for PH domains in phosphatase inhibition. In the case of P-REX2, the PH domain requires PTEN tail phosphorylation to unleash it from the DH domain. We hypothesize that this may be the result of an ionic interaction with the phospho-tail, but this hypothesis is not yet proven. Generating a co-crystal of the PTEN-DHPH and PTEN-PH would provide insight into how the DH domain regulates PH domain mediated PTEN inhibition. Furthermore, identification of the minimal region of the PH domain required for PTEN inhibition would allow us align this sequence to GEFs with known crystal structures, including Grp1 and Dbs and gain information on the 3-D structures important for inhibition. This information would also be useful for identifying other GEFs that may be potential PTEN inhibitors.

We have shown in Chapter II that expression of wild-type P-REX2 and P-REX2 cancer mutants increases PI3K signaling and proliferation, and transforms cells in cooperation with various oncogenes, making it a possible target for cancer therapeutics. By identifying the PH domain as the PTEN inhibitory domain, we can develop small molecule inhibitors that disrupt the PH-PTEN interaction and therefore block P-REX2 mediated PTEN inhibition. This may be a useful anti-cancer therapy for patients with PTEN positive tumors with high P-REX2 expression. Furthermore, using this small molecular inhibitor in combination therapy may be an effective treatment for tumors that are also mutant for *PIK3CA* or *ERBB2*, as discussed in Chapter II.

REFERENCES

Adey NB, et al. (2000) Threonine phosphorylation of the MMAC1/PTEN PDZ binding domain both inhibits and stimulates PDZ binding. Cancer Res 60(1):35-37.

Aghazadeh B, Lowry WE, Huang XY, & Rosen MK (2000) Structural basis for relief of autoinhibition of the Dbl homology domain of proto-oncogene Vav by tyrosine phosphorylation. Cell 102(5):625-633.

Alessi DR, et al. (1996) Mechanism of activation of protein kinase B by insulin and IGF-1. Embo J 15(23):6541-6551.

Alessi DR, et al. (1997) 3-Phosphoinositide-dependent protein kinase-1 (PDK1): structural and functional homology with the Drosophila DSTPK61 kinase. Curr Biol 7(10):776-789.

Ali IU, Schriml LM, & Dean M (1999) Mutational spectra of PTEN/MMAC1 gene: a tumor suppressor with lipid phosphatase activity. J Natl Cancer Inst 91(22):1922-1932.

Al-Khouri AM, Ma Y, Togo SH, Williams S, & Mustelin T (2005) Cooperative phosphorylation of the tumor suppressor phosphatase and tensin homologue (PTEN) by casein kinases and glycogen synthase kinase 3beta. J Biol Chem 280(42):35195-35202.

Alt JR, Cleveland JL, Hannink M, & Diehl JA (2000) Phosphorylation-dependent regulation of cyclin D1 nuclear export and cyclin D1-dependent cellular transformation. Genes Dev 14(24):3102-3114.

Anderson KE, Coadwell J, Stephens LR, & Hawkins PT (1998) Translocation of PDK-1 to the plasma membrane is important in allowing PDK-1 to activate protein kinase B. Curr Biol 8(12):684-691.

Arcaro A, et al. (2000) Class II phosphoinositide 3-kinases are downstream targets of activated polypeptide growth factor receptors. Mol Cell Biol 20(11):3817-3830.

Arden KC (2007) FoxOs in tumor suppression and stem cell maintenance. Cell 128(2):235-237.

Arteaga CL (2006) EGF receptor mutations in lung cancer: from humans to mice and maybe back to humans. Cancer Cell 9(6):421-423.

Attree O, et al. (1992) The Lowe's oculocerebrorenal syndrome gene encodes a protein highly homologous to inositol polyphosphate-5-phosphatase. Nature 358(6383):239-242.

Azzedine H, et al. (2003) Mutations in MTMR13, a new pseudophosphatase homologue of MTMR2 and Sbf1, in two families with an autosomal recessive demyelinating form of Charcot-Marie-Tooth disease associated with early-onset glaucoma. Am J Hum Genet 72(5):1141-1153.

Backer JM, et al. (1992) Phosphatidylinositol 3'-kinase is activated by association with IRS-1 during insulin stimulation. Embo J 11(9):3469-3479.

Backman SA, et al. (2004) Early onset of neoplasia in the prostate and skin of mice with tissue-specific deletion of Pten. Proc Natl Acad Sci U S A 101(6):1725-1730.

Balasenthil S, et al. (2004) p21-activated kinase-1 signaling mediates cyclin D1 expression in mammary epithelial and cancer cells. J Biol Chem 279(2):1422-1428.

Barber MA, et al. (2012) The guanine-nucleotide-exchange factor P-Rex1 is activated by protein phosphatase 1alpha. Biochem J 443(1):173-183.

Barylko B, et al. (1998) Synergistic activation of dynamin GTPase by Grb2 and phosphoinositides. J Biol Chem 273(6):3791-3797.

Begley MJ & Dixon JE (2005) The structure and regulation of myotubularin phosphatases. Curr Opin Struct Biol 15(6):614-620.

Begley MJ, et al. (2003) Crystal structure of a phosphoinositide phosphatase, MTMR2: insights into myotubular myopathy and Charcot-Marie-Tooth syndrome. Mol Cell 12(6):1391-1402.

Bellacosa A, et al. (1995) Molecular alterations of the AKT2 oncogene in ovarian and breast carcinomas. Int J Cancer 64(4):280-285.

Bellacosa A, Testa JR, Staal SP, & Tsichlis PN (1991) A retroviral oncogene, akt, encoding a serine-threonine kinase containing an SH2-like region. Science 254(5029):274-277.

Berger MF, et al. (2012) Melanoma genome sequencing reveals frequent PREX2 mutations. Nature 485(7399):502-506.

Biggs WH, 3rd, Meisenhelder J, Hunter T, Cavenee WK, & Arden KC (1999) Protein kinase B/Akt-mediated phosphorylation promotes nuclear exclusion of the winged helix transcription factor FKHR1. Proc Natl Acad Sci U S A 96(13):7421-7426.

Blondeau F, et al. (2000) Myotubularin, a phosphatase deficient in myotubular myopathy, acts on phosphatidylinositol 3-kinase and phosphatidylinositol 3-phosphate pathway. Hum Mol Genet 9(15):2223-2229.

Boettner B & Van Aelst L (2002) The role of Rho GTPases in disease development. Gene 286(2):155-174.

Bokoch GM (2003) Biology of the p21-activated kinases. Annu Rev Biochem 72:743-781.

Bose S, Wang SI, Terry MB, Hibshoosh H, & Parsons R (1998) Allelic loss of chromosome 10q23 is associated with tumor progression in breast carcinomas. Oncogene 17(1):123-127.

Bravo J, et al. (2001) The crystal structure of the PX domain from p40(phox) bound to phosphatidylinositol 3-phosphate. Mol Cell 8(4):829-839.

Brenner W, et al. (2002) Loss of tumor suppressor protein PTEN during renal carcinogenesis. Int J Cancer 99(1):53-57.

Brodbeck D, Cron P, & Hemmings BA (1999) A human protein kinase Bgamma with regulatory phosphorylation sites in the activation loop and in the C-terminal hydrophobic domain. J Biol Chem 274(14):9133-9136.

Brognard J, Sierecki E, Gao T, & Newton AC (2007) PHLPP and a second isoform, PHLPP2, differentially attenuate the amplitude of Akt signaling by regulating distinct Akt isoforms. Mol Cell 25(6):917-931.

Brown RA, Domin J, Arcaro A, Waterfield MD, & Shepherd PR (1999) Insulin activates the alpha isoform of class II phosphoinositide 3-kinase. J Biol Chem 274(21):14529-14532.

Brunet A, et al. (1999) Akt promotes cell survival by phosphorylating and inhibiting a Forkhead transcription factor. Cell 96(6):857-868.

Bruning JC, et al. (1998) A muscle-specific insulin receptor knockout exhibits features of the metabolic syndrome of NIDDM without altering glucose tolerance. Mol Cell 2(5):559-569.

Burnett PE, Barrow RK, Cohen NA, Snyder SH, & Sabatini DM (1998) RAFT1 phosphorylation of the translational regulators p70 S6 kinase and 4E-BP1. Proc Natl Acad Sci U S A 95(4):1432-1437.

Butler M, et al. (2002) Specific inhibition of PTEN expression reverses hyperglycemia in diabetic mice. Diabetes 51(4):1028-1034.

Campbell IG, et al. (2004) Mutation of the PIK3CA gene in ovarian and breast cancer. Cancer Res 64(21):7678-7681.

Carlson HE, et al. (1986) Cowden disease: gene marker studies and measurements of epidermal growth factor. Am J Hum Genet 38(6):908-917.

Carpten JD, et al. (2007) A transforming mutation in the pleckstrin homology domain of AKT1 in cancer. Nature 448(7152):439-444.

Cheever ML, et al. (2001) Phox domain interaction with PtdIns(3)P targets the Vam7 t-SNARE to vacuole membranes. Nat Cell Biol 3(7):613-618.

Chen J, Parsons S, & Brautigan DL (1994) Tyrosine phosphorylation of protein phosphatase 2A in response to growth stimulation and v-src transformation of fibroblasts. J Biol Chem 269(11):7957-7962.

Chen ML, et al. (2006) The deficiency of Akt1 is sufficient to suppress tumor development in Pten+/- mice. Genes Dev 20(12):1569-1574.

Chen WC, Lin MS, & Bai X (2005) Induction of apoptosis in colorectal cancer cells by peroxisome proliferators-activated receptor gamma activation up-regulating PTEN and inhibiting PI3K activity. Chin Med J (Engl) 118(17):1477-1481.

Chen WS, et al. (2001) Growth retardation and increased apoptosis in mice with homozygous disruption of the Akt1 gene. Genes Dev 15(17):2203-2208.

Cheney IW, et al. (1998) Suppression of tumorigenicity of glioblastoma cells by adenovirus-mediated MMAC1/PTEN gene transfer. Cancer Res 58(11):2331-2334.

Cheng JQ, et al. (1992) AKT2, a putative oncogene encoding a member of a subfamily of protein-serine/threonine kinases, is amplified in human ovarian carcinomas. Proc Natl Acad Sci U S A 89(19):9267-9271.

Cheng JQ, et al. (1996) Amplification of AKT2 in human pancreatic cells and inhibition of AKT2 expression and tumorigenicity by antisense RNA. Proc Natl Acad Sci U S A 93(8):3636-3641.

Chimini G & Chavrier P (2000) Function of Rho family proteins in actin dynamics during phagocytosis and engulfment. Nat Cell Biol 2(10):E191-196.

Cho H, et al. (2001) Insulin resistance and a diabetes mellitus-like syndrome in mice lacking the protein kinase Akt2 (PKB beta). Science 292(5522):1728-1731.

Cho SH, et al. (2004) Redox regulation of PTEN and protein tyrosine phosphatases in H(2)O(2) mediated cell signaling. FEBS Lett 560(1-3):7-13.

Choe G, et al. (2003) Analysis of the phosphatidylinositol 3'-kinase signaling pathway in glioblastoma patients in vivo. Cancer Res 63(11):2742-2746.

Coffer PJ & Woodgett JR (1991) Molecular cloning and characterisation of a novel putative protein-serine kinase related to the cAMP-dependent and protein kinase C families. Eur J Biochem 201(2):475-481.

Cong LN, et al. (1997) Physiological role of Akt in insulin-stimulated translocation of GLUT4 in transfected rat adipose cells. Mol Endocrinol 11(13):1881-1890.

Corvera S (2001) Phosphatidylinositol 3-kinase and the control of endosome dynamics: new players defined by structural motifs. Traffic 2(12):859-866.

Courtney KD, Corcoran RB, & Engelman JA (2010) The PI3K pathway as drug target in human cancer. J Clin Oncol 28(6):1075-1083.

Cremona O & De Camilli P (2001) Phosphoinositides in membrane traffic at the synapse. J Cell Sci 114(Pt 6):1041-1052.

Cross DA, Alessi DR, Cohen P, Andjelkovich M, & Hemmings BA (1995) Inhibition of glycogen synthase kinase-3 by insulin mediated by protein kinase B. Nature 378(6559):785-789.

Dadke S, Kusari A, & Kusari J (2001) Phosphorylation and activation of protein tyrosine phosphatase (PTP) 1B by insulin receptor. Mol Cell Biochem 221(1-2):147-154.

Damen JE, et al. (1996) The 145-kDa protein induced to associate with Shc by multiple cytokines is an inositol tetraphosphate and phosphatidylinositol 3,4,5-triphosphate 5-phosphatase. Proc Natl Acad Sci U S A 93(4):1689-1693.

Das B, et al. (2000) Control of intramolecular interactions between the pleckstrin homology and Dbl homology domains of Vav and Sos1 regulates Rac binding. J Biol Chem 275(20):15074-15081.

Das S, Dixon JE, & Cho W (2003) Membrane-binding and activation mechanism of PTEN. Proc Natl Acad Sci U S A 100(13):7491-7496.

Datta SR, et al. (1997) Akt phosphorylation of BAD couples survival signals to the cell-intrinsic death machinery. Cell 91(2):231-241.

Datta SR, et al. (2000) 14-3-3 proteins and survival kinases cooperate to inactivate BAD by BH3 domain phosphorylation. Mol Cell 6(1):41-51.

Davies MA, et al. (1998) Adenoviral transgene expression of MMAC/PTEN in human glioma cells inhibits Akt activation and induces anoikis. Cancer Res 58(23):5285-5290.

Debnath J, Muthuswamy SK, & Brugge JS (2003) Morphogenesis and oncogenesis of MCF-10A mammary epithelial acini grown in three-dimensional basement membrane cultures. Methods 30(3):256-268.

del Peso L, Gonzalez-Garcia M, Page C, Herrera R, & Nunez G (1997) Interleukin-3-induced phosphorylation of BAD through the protein kinase Akt. Science 278(5338):687-689.

Deleu S, Choi K, Reece JM, & Shears SB (2006) Pathogenicity of Salmonella: SopE-mediated membrane ruffling is independent of inositol phosphate signals. FEBS Lett 580(7):1709-1715.

Depowski PL, Rosenthal SI, & Ross JS (2001) Loss of expression of the PTEN gene protein product is associated with poor outcome in breast cancer. Mod Pathol 14(7):672-676.

Dhand R, et al. (1994) PI 3-kinase: structural and functional analysis of intersubunit interactions. Embo J 13(3):511-521.

Di Cristofano A, Pesce B, Cordon-Cardo C, & Pandolfi PP (1998) Pten is essential for embryonic development and tumour suppression. Nat Genet 19(4):348-355.

Diehl JA, Cheng M, Roussel MF, & Sherr CJ (1998) Glycogen synthase kinase-3beta regulates cyclin D1 proteolysis and subcellular localization. Genes Dev 12(22):3499-3511.

Diekmann D, Abo A, Johnston C, Segal AW, & Hall A (1994) Interaction of Rac with p67phox and regulation of phagocytic NADPH oxidase activity. Science 265(5171):531-533.

Djordjevic S & Driscoll PC (2002) Structural insight into substrate specificity and regulatory mechanisms of phosphoinositide 3-kinases. Trends Biochem Sci 27(8):426-432.

Dohadwala M, et al. (1994) Phosphorylation and inactivation of protein phosphatase 1 by cyclin-dependent kinases. Proc Natl Acad Sci U S A 91(14):6408-6412.

Domin J, et al. (1997) Cloning of a human phosphoinositide 3-kinase with a C2 domain that displays reduced sensitivity to the inhibitor wortmannin. Biochem J 326 (Pt 1):139-147.

Donald S, et al. (2004) P-Rex2, a new guanine-nucleotide exchange factor for Rac. FEBS Lett 572(1-3):172-176.

Donald S, et al. (2008) P-Rex2 regulates Purkinje cell dendrite morphology and motor coordination. Proc Natl Acad Sci U S A 105(11):4483-4488.

Downward J (1998) Lipid-regulated kinases: some common themes at last. Science 279(5351):673-674.

Dummler B, Ohshiro K, Kumar R, & Field J (2009) Pak protein kinases and their role in cancer. Cancer Metastasis Rev 28(1-2):51-63.

Dummler B, et al. (2006) Life with a single isoform of Akt: mice lacking Akt2 and Akt3 are viable but display impaired glucose homeostasis and growth deficiencies. Mol Cell Biol 26(21):8042-8051.

Easton RM, et al. (2005) Role for Akt3/protein kinase Bgamma in attainment of normal brain size. Mol Cell Biol 25(5):1869-1878.

Eden S, Rohatgi R, Podtelejnikov AV, Mann M, & Kirschner MW (2002) Mechanism of regulation of WAVE1-induced actin nucleation by Rac1 and Nck. Nature 418(6899):790-793.

Edwards DC, Sanders LC, Bokoch GM, & Gill GN (1999) Activation of LIM-kinase by Pak1 couples Rac/Cdc42 GTPase signalling to actin cytoskeletal dynamics. Nat Cell Biol 1(5):253-259.

Endo S, Zhou X, Connor J, Wang B, & Shenolikar S (1996) Multiple structural elements define the specificity of recombinant human inhibitor-1 as a protein phosphatase-1 inhibitor. Biochemistry 35(16):5220-5228.

Eng C, et al. (2001) PTEN mutations and proteus syndrome. Lancet 358(9298):2079-2080.

Erdmann KS, et al. (2007) A role of the Lowe syndrome protein OCRL in early steps of the endocytic pathway. Dev Cell 13(3):377-390.

Escriva M, et al. (2008) Repression of PTEN phosphatase by Snail1 transcriptional factor during gamma radiation-induced apoptosis. Mol Cell Biol 28(5):1528-1540.

Eto M, Senba S, Morita F, & Yazawa M (1997) Molecular cloning of a novel phosphorylation-dependent inhibitory protein of protein phosphatase-1 (CPI17) in smooth muscle: its specific localization in smooth muscle. FEBS Lett 410(2-3):356-360.

Eva A, Vecchio G, Rao CD, Tronick SR, & Aaronson SA (1988) The predicted DBL oncogene product defines a distinct class of transforming proteins. Proc Natl Acad Sci U S A 85(7):2061-2065.

Evers EE, et al. (2000) Rho family proteins in cell adhesion and cell migration. Eur J Cancer 36(10):1269-1274.

Ferraro B, Bepler G, Sharma S, Cantor A, & Haura EB (2005) EGR1 predicts PTEN and survival in patients with non-small-cell lung cancer. J Clin Oncol 23(9):1921-1926.

Fine B, et al. (2009) Activation of the PI3K pathway in cancer through inhibition of PTEN by exchange factor P-REX2a. Science 325(5945):1261-1265.

Ford MG, et al. (2001) Simultaneous binding of PtdIns(4,5)P2 and clathrin by AP180 in the nucleation of clathrin lattices on membranes. Science 291(5506):1051-1055.

Foulkes JG, Strada SJ, Henderson PJ, & Cohen P (1983) A kinetic analysis of the effects of inhibitor-1 and inhibitor-2 on the activity of protein phosphatase-1. Eur J Biochem 132(2):309-313.

Franke TF, Kaplan DR, Cantley LC, & Toker A (1997) Direct regulation of the Akt proto-oncogene product by phosphatidylinositol-3,4-bisphosphate. Science 275(5300):665-668.

Frech M, et al. (1997) High affinity binding of inositol phosphates and phosphoinositides to the pleckstrin homology domain of RAC/protein kinase B and their influence on kinase activity. J Biol Chem 272(13):8474-8481.

Fukuda M, Kojima T, Kabayama H, & Mikoshiba K (1996) Mutation of the pleckstrin homology domain of Bruton's tyrosine kinase in immunodeficiency impaired inositol 1,3,4,5-tetrakisphosphate binding capacity. J Biol Chem 271(48):30303-30306.

Furnari FB, Lin H, Huang HS, & Cavenee WK (1997) Growth suppression of glioma cells by PTEN requires a functional phosphatase catalytic domain. Proc Natl Acad Sci U S A 94(23):12479-12484.

Gaidarov I & Keen JH (1999) Phosphoinositide-AP-2 interactions required for targeting to plasma membrane clathrin-coated pits. J Cell Biol 146(4):755-764.

Gao T, Furnari F, & Newton AC (2005) PHLPP: a phosphatase that directly dephosphorylates Akt, promotes apoptosis, and suppresses tumor growth. Mol Cell 18(1):13-24.

Garcia JM, et al. (2004) Promoter methylation of the PTEN gene is a common molecular change in breast cancer. Genes Chromosomes Cancer 41(2):117-124.

Garofalo RS, et al. (2003) Severe diabetes, age-dependent loss of adipose tissue, and mild growth deficiency in mice lacking Akt2/PKB beta. J Clin Invest 112(2):197-208.

Gil A, et al. (2006) Nuclear localization of PTEN by a Ran-dependent mechanism enhances apoptosis: Involvement of an N-terminal nuclear localization domain and multiple nuclear exclusion motifs. Mol Biol Cell 17(9):4002-4013.

Gillooly DJ, et al. (2000) Localization of phosphatidylinositol 3-phosphate in yeast and mammalian cells. Embo J 19(17):4577-4588.

Ginn-Pease ME & Eng C (2003) Increased nuclear phosphatase and tensin homologue deleted on chromosome 10 is associated with G0-G1 in MCF-7 cells. Cancer Res 63(2):282-286.

Gorlin RJ, Cohen MM, Jr., Condon LM, & Burke BA (1992) Bannayan-Riley-Ruvalcaba syndrome. Am J Med Genet 44(3):307-314.

Guertin DA, et al. (2006) Ablation in mice of the mTORC components raptor, rictor, or mLST8 reveals that mTORC2 is required for signaling to Akt-FOXO and PKCalpha, but not S6K1. Dev Cell 11(6):859-871.

Guldberg P, et al. (1997) Disruption of the MMAC1/PTEN gene by deletion or mutation is a frequent event in malignant melanoma. Cancer Res 57(17):3660-3663.

Guo F & Zheng Y (2004) Rho family GTPases cooperate with p53 deletion to promote primary mouse embryonic fibroblast cell invasion. Oncogene 23(33):5577-5585.

Hara K, et al. (2002) Raptor, a binding partner of target of rapamycin (TOR), mediates TOR action. Cell 110(2):177-189.

Hart MJ, Eva A, Evans T, Aaronson SA, & Cerione RA (1991) Catalysis of guanine nucleotide exchange on the CDC42Hs protein by the dbl oncogene product. Nature 354(6351):311-314.

Herman GE, Finegold M, Zhao W, de Gouyon B, & Metzenberg A (1999) Medical complications in long-term survivors with X-linked myotubular myopathy. J Pediatr 134(2):206-214.

Herman PK & Emr SD (1990) Characterization of VPS34, a gene required for vacuolar protein sorting and vacuole segregation in Saccharomyces cerevisiae. Mol Cell Biol 10(12):6742-6754.

Hernandez-Negrete I, et al. (2007) P-Rex1 links mammalian target of rapamycin signaling to Rac activation and cell migration. J Biol Chem 282(32):23708-23715.

Hiles ID, et al. (1992) Phosphatidylinositol 3-kinase: structure and expression of the 110 kd catalytic subunit. Cell 70(3):419-429.

Hill K, et al. (2005) Regulation of P-Rex1 by phosphatidylinositol (3,4,5)-trisphosphate and Gbetagamma subunits. J Biol Chem 280(6):4166-4173.

Ho CM, et al. (2009) PTEN promoter methylation and LOH of 10q22-23 locus in PTEN expression of ovarian clear cell adenocarcinomas. Gynecol Oncol 112(2):307-313.

Holman GD & Kasuga M (1997) From receptor to transporter: insulin signalling to glucose transport. Diabetologia 40(9):991-1003.

Holz RW & Axelrod D (2002) Localization of phosphatidylinositol 4,5-P(2) important in exocytosis and a quantitative analysis of chromaffin granule motion adjacent to the plasma membrane. Ann N Y Acad Sci 971:232-243.

Hoopes RR, Jr., et al. (2005) Dent Disease with mutations in OCRL1. Am J Hum Genet 76(2):260-267.

Horie Y, et al. (2004) Hepatocyte-specific Pten deficiency results in steatohepatitis and hepatocellular carcinomas. J Clin Invest 113(12):1774-1783.

Hu P, Mondino A, Skolnik EY, & Schlessinger J (1993) Cloning of a novel, ubiquitously expressed human phosphatidylinositol 3-kinase and identification of its binding site on p85. Mol Cell Biol 13(12):7677-7688.

Hwang SL, et al. (2005) Rac2 expression and mutation in human brain tumors. Acta Neurochir (Wien) 147(5):551-554; discussion 554.

Hyvola N, et al. (2006) Membrane targeting and activation of the Lowe syndrome protein OCRL1 by rab GTPases. Embo J 25(16):3750-3761.

Ikenoue T, Inoki K, Zhao B, & Guan KL (2008) PTEN acetylation modulates its interaction with PDZ domain. Cancer Res 68(17):6908-6912.

Ingley E & Hemmings BA (1994) Pleckstrin homology (PH) domains in signal transduction. J Cell Biochem 56(4):436-443.

Inoki K, Li Y, Xu T, & Guan KL (2003) Rheb GTPase is a direct target of TSC2 GAP activity and regulates mTOR signaling. Genes Dev 17(15):1829-1834.

Inoki K, Li Y, Zhu T, Wu J, & Guan KL (2002) TSC2 is phosphorylated and inhibited by Akt and suppresses mTOR signalling. Nat Cell Biol 4(9):648-657.

Ishihara H, et al. (2003) Association of the polymorphisms in the 5'-untranslated region of PTEN gene with type 2 diabetes in a Japanese population. FEBS Lett 554(3):450-454.

Ishikura S, Koshkina A, & Klip A (2008) Small G proteins in insulin action: Rab and Rho families at the crossroads of signal transduction and GLUT4 vesicle traffic. Acta Physiol (Oxf) 192(1):61-74.

Itoh T, et al. (2001) Role of the ENTH domain in phosphatidylinositol-4,5-bisphosphate binding and endocytosis. Science 291(5506):1047-1051.

Janssens V & Goris J (2001) Protein phosphatase 2A: a highly regulated family of serine/threonine phosphatases implicated in cell growth and signalling. Biochem J 353(Pt 3):417-439.

Jaworski J, Spangler S, Seeburg DP, Hoogenraad CC, & Sheng M (2005) Control of dendritic arborization by the phosphoinositide-3'-kinase-Akt-mammalian target of rapamycin pathway. J Neurosci 25(49):11300-11312.

JeBailey L, et al. (2004) Skeletal muscle cells and adipocytes differ in their reliance on TC10 and Rac for insulin-induced actin remodeling. Mol Endocrinol 18(2):359-372.

JeBailey L, et al. (2007) Ceramide- and oxidant-induced insulin resistance involve loss of insulin-dependent Rac-activation and actin remodeling in muscle cells. Diabetes 56(2):394-403.

Jiang ZY, et al. (2003) Insulin signaling through Akt/protein kinase B analyzed by small interfering RNA-mediated gene silencing. Proc Natl Acad Sci U S A 100(13):7569-7574.

Jones DH, et al. (2000) Type I phosphatidylinositol 4-phosphate 5-kinase directly interacts with ADP-ribosylation factor 1 and is responsible for phosphatidylinositol 4,5-bisphosphate synthesis in the golgi compartment. J Biol Chem 275(18):13962-13966.

Jones PF, Jakubowicz T, & Hemmings BA (1991) Molecular cloning of a second form of rac protein kinase. Cell Regul 2(12):1001-1009.

Jordan P, Brazao R, Boavida MG, Gespach C, & Chastre E (1999) Cloning of a novel human Rac1b splice variant with increased expression in colorectal tumors. Oncogene 18(48):6835-6839.

Joseph RE & Norris FA (2005) Substrate specificity and recognition is conferred by the pleckstrin homology domain of the Dbl family guanine nucleotide exchange factor P-Rex2. J Biol Chem 280(30):27508-27512.

Kanai F, et al. (2001) The PX domains of p47phox and p40phox bind to lipid products of PI(3)K. Nat Cell Biol 3(7):675-678.

Kandasamy K & Srivastava RK (2002) Role of the phosphatidylinositol 3'-kinase/PTEN/Akt kinase pathway in tumor necrosis factor-related apoptosis-inducing ligand-induced apoptosis in non-small cell lung cancer cells. Cancer Res 62(17):4929-4937.

Katome T, et al. (2003) Use of RNA interference-mediated gene silencing and adenoviral overexpression to elucidate the roles of AKT/protein kinase B isoforms in insulin actions. J Biol Chem 278(30):28312-28323.

Kavanaugh WM, et al. (1996) Multiple forms of an inositol polyphosphate 5-phosphatase form signaling complexes with Shc and Grb2. Curr Biol 6(4):438-445.

Kavran JM, et al. (1998) Specificity and promiscuity in phosphoinositide binding by pleckstrin homology domains. J Biol Chem 273(46):30497-30508.

Khayat ZA, Tong P, Yaworsky K, Bloch RJ, & Klip A (2000) Insulin-induced actin filament remodeling colocalizes actin with phosphatidylinositol 3-kinase and GLUT4 in L6 myotubes. J Cell Sci 113 Pt 2:279-290.

Khosravi-Far R, et al. (1996) Oncogenic Ras activation of Raf/mitogen-activated protein kinase-independent pathways is sufficient to cause tumorigenic transformation. Mol Cell Biol 16(7):3923-3933.

Kim DH, et al. (2002) mTOR interacts with raptor to form a nutrient-sensitive complex that signals to the cell growth machinery. Cell 110(2):163-175.

Kim EK, et al. (2011) Selective activation of Akt1 by mammalian target of rapamycin complex 2 regulates cancer cell migration, invasion, and metastasis. Oncogene 30(26):2954-2963.

Kim KY, Cho HS, Jung WH, Kim SS, & Cheon HG (2007) Phosphatase and tensin homolog deleted on chromosome 10 suppression is an important process in peroxisome proliferator-activated receptor-gamma signaling in adipocytes and myotubes. Mol Pharmacol 71(6):1554-1562.

Kim RH & Mak TW (2006) Tumours and tremors: how PTEN regulation underlies both. Br J Cancer 94(5):620-624.

Kim SA, Vacratsis PO, Firestein R, Cleary ML, & Dixon JE (2003) Regulation of myotubularin-related (MTMR)2 phosphatidylinositol phosphatase by MTMR5, a catalytically inactive phosphatase. Proc Natl Acad Sci U S A 100(8):4492-4497.

Kido Y, Burks DJ, Withers D, Bruning JC, Kahn CR, White MF, Accili D (2000) Tissue-specific insulin resistance in mice with mutations in the insulin receptor, IRS-1, and IRS-2. J Clin Invest. 105(2):199-205.

Klippel A, Kavanaugh WM, Pot D, & Williams LT (1997) A specific product of phosphatidylinositol 3-kinase directly activates the protein kinase Akt through its pleckstrin homology domain. Mol Cell Biol 17(1):338-344.

Koga H, et al. (1999) Tetratricopeptide repeat (TPR) motifs of p67(phox) participate in interaction with the small GTPase Rac and activation of the phagocyte NADPH oxidase. J Biol Chem 274(35):25051-25060.

Kohn AD, Summers SA, Birnbaum MJ, & Roth RA (1996) Expression of a constitutively active Akt Ser/Thr kinase in 3T3-L1 adipocytes stimulates glucose uptake and glucose transporter 4 translocation. J Biol Chem 271(49):31372-31378.

Kong D, et al. (1997) PTEN1 is frequently mutated in primary endometrial carcinomas. Nat Genet 17(2):143-144.

Kotelevets L, et al. (2005) Implication of the MAGI-1b/PTEN signalosome in stabilization of adherens junctions and suppression of invasiveness. FASEB J 19(1):115-117.

Kruszynska YT & Olefsky JM (1996) Cellular and molecular mechanisms of non-insulin dependent diabetes mellitus. J Investig Med 44(8):413-428.

Kulik G & Weber MJ (1998) Akt-dependent and -independent survival signaling pathways utilized by insulin-like growth factor I. Mol Cell Biol 18(11):6711-6718.

Kumar CC, et al. (2001) Expression, purification, characterization and homology modeling of active Akt/PKB, a key enzyme involved in cell survival signaling. Biochim Biophys Acta 1526(3):257-268.

Kumar V, Zhang MX, Swank MW, Kunz J, & Wu GY (2005) Regulation of dendritic morphogenesis by Ras-PI3K-Akt-mTOR and Ras-MAPK signaling pathways. J Neurosci 25(49):11288-11299.

Kuo YC, et al. (2008) Regulation of phosphorylation of Thr-308 of Akt, cell proliferation, and survival by the B55alpha regulatory subunit targeting of the protein phosphatase 2A holoenzyme to Akt. J Biol Chem 283(4):1882-1892.

Kurlawalla-Martinez C, et al. (2005) Insulin hypersensitivity and resistance to streptozotocin-induced diabetes in mice lacking PTEN in adipose tissue. Mol Cell Biol 25(6):2498-2510.

Kurose K, et al. (2001) Frequent loss of PTEN expression is linked to elevated phosphorylated Akt levels, but not associated with p27 and cyclin D1 expression, in primary epithelial ovarian carcinomas. Am J Pathol 158(6):2097-2106.

Kushner JA, et al. (2005) Phosphatase and tensin homolog regulation of islet growth and glucose homeostasis. J Biol Chem 280(47):39388-39393.

Kutateladze T & Overduin M (2001) Structural mechanism of endosome docking by the FYVE domain. Science 291(5509):1793-1796.

Kwon YG, Lee SY, Choi Y, Greengard P, & Nairn AC (1997) Cell cycle-dependent phosphorylation of mammalian protein phosphatase 1 by cdc2 kinase. Proc Natl Acad Sci U S A 94(6):2168-2173.

Lane J, Martin TA, Mansel RE, & Jiang WG (2008) The expression and prognostic value of the guanine nucleotide exchange factors (GEFs) Trio, Vav1 and TIAM-1 in human breast cancer. Int Semin Surg Oncol 5:23.

Lee JO, et al. (1999) Crystal structure of the PTEN tumor suppressor: implications for its phosphoinositide phosphatase activity and membrane association. Cell 99(3):323-334.

Lee JY, et al. (2009) Id-1 activates Akt-mediated Wnt signaling and p27(Kip1) phosphorylation through PTEN inhibition. Oncogene 28(6):824-831.

Lee K, et al. (2008) Vav3 oncogene activates estrogen receptor and its overexpression may be involved in human breast cancer. BMC Cancer 8:158.

Lee SR, et al. (2002) Reversible inactivation of the tumor suppressor PTEN by H2O2. J Biol Chem 277(23):20336-20342.

Lee YR, et al. (2007) Peroxisome proliferator-activated receptor gamma and retinoic acid receptor synergistically up-regulate the tumor suppressor PTEN in human promyeloid leukemia cells. Int J Hematol 85(3):231-237.

Lemmon MA (2003) Phosphoinositide recognition domains. Traffic 4(4):201-213.

Lemmon MA & Ferguson KM (2000) Signal-dependent membrane targeting by pleckstrin homology (PH) domains. Biochem J 350 Pt 1:1-18.

Li DM & Sun H (1998) PTEN/MMAC1/TEP1 suppresses the tumorigenicity and induces G1 cell cycle arrest in human glioblastoma cells. Proc Natl Acad Sci U S A 95(26):15406-15411.

Li G, et al. (2002) Conditional loss of PTEN leads to precocious development and neoplasia in the mammary gland. Development 129(17):4159-4170.

Li J, et al. (1998) The PTEN/MMAC1 tumor suppressor induces cell death that is rescued by the AKT/protein kinase B oncogene. Cancer Res 58(24):5667-5672.

Li J, et al. (1997) PTEN, a putative protein tyrosine phosphatase gene mutated in human brain, breast, and prostate cancer. Science 275(5308):1943-1947.

Li L, Liu F, & Ross AH (2003) PTEN regulation of neural development and CNS stem cells. J Cell Biochem 88(1):24-28.

Li L, et al. (2002) PTEN in neural precursor cells: regulation of migration, apoptosis, and proliferation. Mol Cell Neurosci 20(1):21-29.

Li Z, Paik JH, Wang Z, Hla T, & Wu D (2005) Role of guanine nucleotide exchange factor P-Rex-2b in sphingosine 1-phosphate-induced Rac1 activation and cell migration in endothelial cells. Prostaglandins Other Lipid Mediat 76(1-4):95-104.

Liao Y & Hung MC (2010) Physiological regulation of Akt activity and stability. Am J Transl Res 2(1):19-42.

Liaw D, et al. (1997) Germline mutations of the PTEN gene in Cowden disease, an inherited breast and thyroid cancer syndrome. Nat Genet 16(1):64-67.

Lindsay CR, et al. (2011) P-Rex1 is required for efficient melanoblast migration and melanoma metastasis. Nat Commun 2:555.

Lioubin MN, et al. (1996) p150Ship, a signal transduction molecule with inositol polyphosphate-5-phosphatase activity. Genes Dev 10(9):1084-1095.

Liu F, et al. (2005) PTEN enters the nucleus by diffusion. J Cell Biochem 96(2):221-234.

Liu JL, et al. (2005) Nuclear PTEN-mediated growth suppression is independent of Akt down-regulation. Mol Cell Biol 25(14):6211-6224.

Loewith R, et al. (2002) Two TOR complexes, only one of which is rapamycin sensitive, have distinct roles in cell growth control. Mol Cell 10(3):457-468.

Lu J, et al. (2009) Stem cell factor SALL4 represses the transcriptions of PTEN and SALL1 through an epigenetic repressor complex. PLoS One 4(5):e5577.

Lu W, Gong D, Bar-Sagi D, & Cole PA (2001) Site-specific incorporation of a phosphotyrosine mimetic reveals a role for tyrosine phosphorylation of SHP-2 in cell signaling. Mol Cell 8(4):759-769.

Maddika S, et al. (2011) WWP2 is an E3 ubiquitin ligase for PTEN. Nat Cell Biol 13(6):728-733.

Maehama T & Dixon JE (1998) The tumor suppressor, PTEN/MMAC1, dephosphorylates the lipid second messenger, phosphatidylinositol 3,4,5-trisphosphate. J Biol Chem 273(22):13375-13378.

Manning BD, Tee AR, Logsdon MN, Blenis J, & Cantley LC (2002) Identification of the tuberous sclerosis complex-2 tumor suppressor gene product tuberin as a target of the phosphoinositide 3-kinase/akt pathway. Mol Cell 10(1):151-162.

Manser E, Leung T, Salihuddin H, Zhao ZS, & Lim L (1994) A brain serine/threonine protein kinase activated by Cdc42 and Rac1. Nature 367(6458):40-46.

Marion E, et al. (2002) The gene INPPL1, encoding the lipid phosphatase SHIP2, is a candidate for type 2 diabetes in rat and man. Diabetes 51(7):2012-2017.

Marsh DJ, et al. (1998) Germline PTEN mutations in Cowden syndrome-like families. J Med Genet 35(11):881-885.

Marsh DJ, et al. (1999) PTEN mutation spectrum and genotype-phenotype correlations in Bannayan-Riley-Ruvalcaba syndrome suggest a single entity with Cowden syndrome. Hum Mol Genet 8(8):1461-1472.

Mayeenuddin LH & Garrison JC (2006) Phosphorylation of P-Rex1 by the cyclic AMP-dependent protein kinase inhibits the phosphatidylinositiol (3,4,5)-trisphosphate and Gbetagamma-mediated regulation of its activity. J Biol Chem 281(4):1921-1928.

Mayo LD & Donner DB (2001) A phosphatidylinositol 3-kinase/Akt pathway promotes translocation of Mdm2 from the cytoplasm to the nucleus. Proc Natl Acad Sci U S A 98(20):11598-11603.

McManus EJ, et al. (2004) The in vivo role of PtdIns(3,4,5)P3 binding to PDK1 PH domain defined by knockin mutation. Embo J 23(10):2071-2082.

Miki H, Yamaguchi H, Suetsugu S, & Takenawa T (2000) IRSp53 is an essential intermediate between Rac and WAVE in the regulation of membrane ruffling. Nature 408(6813):732-735.

Mirshamsi S, Laidlaw HA, Ning K, Anderson E, Burgess LA, Gray A, Sutherland C, Ashford ML (2004) Leptin and insulin stimulation of signalling pathways in arcuate nucleus neurones: PI3K dependent actin reorganization and KATP channel activation. BMC Neuroscience (5):54:1-18.

Misra S, Miller GJ, & Hurley JH (2001) Recognizing phosphatidylinositol 3-phosphate. Cell 107(5):559-562.

Miwa W, et al. (1996) Isolation of DNA sequences amplified at chromosome 19q13.1-q13.2 including the AKT2 locus in human pancreatic cancer. Biochem Biophys Res Commun 225(3):968-974.

Moasser MM (2007) The oncogene HER2: its signaling and transforming functions and its role in human cancer pathogenesis. Oncogene 26(45):6469-6487.

Montero JC, Seoane S, Ocana A, & Pandiella A (2011) P-Rex1 participates in Neuregulin-ErbB signal transduction and its expression correlates with patient outcome in breast cancer. Oncogene 30(9):1059-1071.

Moorehead RA, et al. (2003) Insulin-like growth factor-II regulates PTEN expression in the mammary gland. J Biol Chem 278(50):50422-50427.

Moorhead GB, De Wever V, Templeton G, & Kerk D (2009) Evolution of protein phosphatases in plants and animals. Biochem J 417(2):401-409.

Mutter GL, et al. (2001) Molecular identification of latent precancers in histologically normal endometrium. Cancer Res 61(11):4311-4314.

Myers MP, et al. (1997) P-TEN, the tumor suppressor from human chromosome 10q23, is a dual-specificity phosphatase. Proc Natl Acad Sci U S A 94(17):9052-9057.

Nakao K, et al. (2004) High-resolution analysis of DNA copy number alterations in colorectal cancer by array-based comparative genomic hybridization. Carcinogenesis 25(8):1345-1357.

Nakashima N, Sharma PM, Imamura T, Bookstein R, & Olefsky JM (2000) The tumor suppressor PTEN negatively regulates insulin signaling in 3T3-L1 adipocytes. J Biol Chem 275(17):12889-12895.

Nassar N, Hoffman GR, Manor D, Clardy JC, & Cerione RA (1998) Structures of Cdc42 bound to the active and catalytically compromised forms of Cdc42GAP. Nat Struct Biol 5(12):1047-1052.

Ning K, Miller LC, Laidlaw HA, Burgess LA, Perera NM, Downes CP, Leslie NR, Ashford ML (2006) A novel leptin signalling pathway via PTEN inhibition in hypothalamic cell lines and pancreatic beta-cells. EMBO J. 25(11):2377-2387.

Ning K, Miller LC, Laidlaw HA, Watterson KR, Gallagher J, Sutherland C, Ashford ML (2009) Leptin-dependent phosphorylation of PTEN mediates actin restructuring and activation of ATP-sensitive K+ channels. J Biol Chem. 284(14):9331-9340.

Niswender KD, Baskin DG, & Schwartz MW (2004) Insulin and its evolving partnership with leptin in the hypothalamic control of energy homeostasis. Trends Endocrinol Metab 15(8):362-369.

Niswender KD, Morrison CD, Clegg DJ, Olson R, Baskin DG, Myers MG Jr, Seeley RJ, Schwartz MW (2003) Insulin activation of phosphatidylinositol 3-kinase in the hypothalamic arcuate nucleus: a key mediator of insulin-induced anorexia. Diabetes. 52(2):227-231.

Niswender KD, Morton GJ, Stearns WH, Rhodes CJ, Myers MG Jr, Schwartz MW (2001) Intracellular signalling. Key enzyme in leptin-induced anorexia. Nature. 413(6858):794-795.

Oda K, et al. (2008) PIK3CA cooperates with other phosphatidylinositol 3'-kinase pathway mutations to effect oncogenic transformation. Cancer Res 68(19):8127-8136.

Oda K, Stokoe D, Taketani Y, & McCormick F (2005) High frequency of coexistent mutations of PIK3CA and PTEN genes in endometrial carcinoma. Cancer Res 65(23):10669-10673.

Odriozola L, Singh G, Hoang T, & Chan AM (2007) Regulation of PTEN activity by its carboxyl-terminal autoinhibitory domain. J Biol Chem 282(32):23306-23315.

Ogg S & Ruvkun G (1998) The C. elegans PTEN homolog, DAF-18, acts in the insulin receptor-like metabolic signaling pathway. Mol Cell 2(6):887-893.

Okumura K, et al. (2006) PCAF modulates PTEN activity. J Biol Chem 281(36):26562-26568.

Okumura K, Zhao M, DePinho RA, Furnari FB, & Cavenee WK (2005) PTEN: a novel anti-oncogenic function independent of phosphatase activity. Cell Cycle 4(4):540-542.

Olofsson B (1999) Rho guanine dissociation inhibitors: pivotal molecules in cellular signalling. Cell Signal 11(8):545-554.

Olsen JV, et al. (2006) Global, in vivo, and site-specific phosphorylation dynamics in signaling networks. Cell 127(3):635-648.

Ono H, et al. (2001) Regulation of phosphoinositide metabolism, Akt phosphorylation, and glucose transport by PTEN (phosphatase and tensin homolog deleted on chromosome 10) in 3T3-L1 adipocytes. Mol Endocrinol 15(8):1411-1422.

O'Rahilly S (2007) Human obesity and insulin resistance: lessons from experiments of nature. Novartis Found Symp 286:13-20; discussion 20-13, 162-163, 196-203.

Ostman A, Frijhoff J, Sandin A, & Bohmer FD (2011) Regulation of protein tyrosine phosphatases by reversible oxidation. J Biochem 150(4):345-356.

Pan Y, Weinman EJ, & Dai JL (2008) Na+/H+ exchanger regulatory factor 1 inhibits platelet-derived growth factor signaling in breast cancer cells. Breast Cancer Res 10(1):R5.

Panaretou C, Domin J, Cockcroft S, & Waterfield MD (1997) Characterization of p150, an adaptor protein for the human phosphatidylinositol (PtdIns) 3-kinase. Substrate presentation by phosphatidylinositol transfer protein to the p150.Ptdins 3-kinase complex. J Biol Chem 272(4):2477-2485.

Parsons DW, et al. (2005) Colorectal cancer: mutations in a signalling pathway. Nature 436(7052):792.

Patel L, et al. (2001) Tumor suppressor and anti-inflammatory actions of PPARgamma agonists are mediated via upregulation of PTEN. Curr Biol 11(10):764-768.

Peng XD, et al. (2003) Dwarfism, impaired skin development, skeletal muscle atrophy, delayed bone development, and impeded adipogenesis in mice lacking Akt1 and Akt2. Genes Dev 17(11):1352-1365.

Perez-Tenorio G, et al. (2007) PIK3CA mutations and PTEN loss correlate with similar prognostic factors and are not mutually exclusive in breast cancer. Clin Cancer Res 13(12):3577-3584.

Perren A, et al. (2000) Mutation and expression analyses reveal differential subcellular compartmentalization of PTEN in endocrine pancreatic tumors compared to normal islet cells. Am J Pathol 157(4):1097-1103.

Peterson RT & Schreiber SL (1999) Kinase phosphorylation: Keeping it all in the family. Curr Biol 9(14):R521-524.

Podsypanina K, et al. (1999) Mutation of Pten/Mmac1 in mice causes neoplasia in multiple organ systems. Proc Natl Acad Sci U S A 96(4):1563-1568.

Qin J, et al. (2009) Upregulation of PIP3-dependent Rac exchanger 1 (P-Rex1) promotes prostate cancer metastasis. Oncogene 28(16):1853-1863.

Raftopoulou M, Etienne-Manneville S, Self A, Nicholls S, & Hall A (2004) Regulation of cell migration by the C2 domain of the tumor suppressor PTEN. Science 303(5661):1179-1181.

Rahdar M, et al. (2009) A phosphorylation-dependent intramolecular interaction regulates the membrane association and activity of the tumor suppressor PTEN. Proc Natl Acad Sci U S A 106(2):480-485.

Rameh LE & Cantley LC (1999) The role of phosphoinositide 3-kinase lipid products in cell function. J Biol Chem 274(13):8347-8350.

Rasheed BK, et al. (1997) PTEN gene mutations are seen in high-grade but not in low-grade gliomas. Cancer Res 57(19):4187-4190.

Raught B, et al. (2004) Phosphorylation of eucaryotic translation initiation factor 4B Ser422 is modulated by S6 kinases. Embo J 23(8):1761-1769.

Reardon W, Zhou XP, & Eng C (2001) A novel germline mutation of the PTEN gene in a patient with macrocephaly, ventricular dilatation, and features of VATER association. J Med Genet 38(12):820-823.

Risinger JI, Hayes AK, Berchuck A, & Barrett JC (1997) PTEN/MMAC1 mutations in endometrial cancers. Cancer Res 57(21):4736-4738.

Rittinger K, et al. (1997) Crystal structure of a small G protein in complex with the GTPase-activating protein rhoGAP. Nature 388(6643):693-697.

Robertson GP, et al. (1998) In vitro loss of heterozygosity targets the PTEN/MMAC1 gene in melanoma. Proc Natl Acad Sci U S A 95(16):9418-9423.

Robinson FL & Dixon JE (2005) The phosphoinositide-3-phosphatase MTMR2 associates with MTMR13, a membrane-associated pseudophosphatase also mutated in type 4B Charcot-Marie-Tooth disease. J Biol Chem 280(36):31699-31707.

Rodriguez-Viciana P, et al. (1994) Phosphatidylinositol-3-OH kinase as a direct target of Ras. Nature 370(6490):527-532.

Rohatgi R, et al. (1999) The interaction between N-WASP and the Arp2/3 complex links Cdc42-dependent signals to actin assembly. Cell 97(2):221-231.

Rordorf-Nikolic T, Van Horn DJ, Chen D, White MF, & Backer JM (1995) Regulation of phosphatidylinositol 3'-kinase by tyrosyl phosphoproteins. Full activation requires occupancy of both SH2 domains in the 85-kDa regulatory subunit. J Biol Chem 270(8):3662-3666.

Rosenfeldt H, Vazquez-Prado J, & Gutkind JS (2004) P-REX2, a novel PI-3-kinase sensitive Rac exchange factor. FEBS Lett 572(1-3):167-171.

Ross AH & Gericke A (2009) Phosphorylation keeps PTEN phosphatase closed for business. Proc Natl Acad Sci U S A 106(5):1297-1298.

Rossman KL, Der CJ, & Sondek J (2005) GEF means go: turning on RHO GTPases with guanine nucleotide-exchange factors. Nat Rev Mol Cell Biol 6(2):167-180.

Ruggeri BA, Huang L, Wood M, Cheng JQ, & Testa JR (1998) Amplification and overexpression of the AKT2 oncogene in a subset of human pancreatic ductal adenocarcinomas. Mol Carcinog 21(2):81-86.

Salim K, et al. (1996) Distinct specificity in the recognition of phosphoinositides by the pleckstrin homology domains of dynamin and Bruton's tyrosine kinase. Embo J 15(22):6241-6250.

Salvesen HB, et al. (2001) PTEN methylation is associated with advanced stage and microsatellite instability in endometrial carcinoma. Int J Cancer 91(1):22-26.

Samuels Y, et al. (2004) High frequency of mutations of the PIK3CA gene in human cancers. Science 304(5670):554.

Sander EE, et al. (1998) Matrix-dependent Tiam1/Rac signaling in epithelial cells promotes either cell-cell adhesion or cell migration and is regulated by phosphatidylinositol 3-kinase. J Cell Biol 143(5):1385-1398.

Sano H, et al. (2003) Insulin-stimulated phosphorylation of a Rab GTPase-activating protein regulates GLUT4 translocation. J Biol Chem 278(17):14599-14602.

Sarbassov DD, et al. (2004) Rictor, a novel binding partner of mTOR, defines a rapamycin-insensitive and raptor-independent pathway that regulates the cytoskeleton. Curr Biol 14(14):1296-1302.

Sarbassov DD, Guertin DA, Ali SM, & Sabatini DM (2005) Phosphorylation and regulation of Akt/PKB by the rictor-mTOR complex. Science 307(5712):1098-1101.

Sauter G, Maeda T, Waldman FM, Davis RL, & Feuerstein BG (1996) Patterns of epidermal growth factor receptor amplification in malignant gliomas. Am J Pathol 148(4):1047-1053.

Schmidt A & Hall A (2002) The Rho exchange factor Net1 is regulated by nuclear sequestration. J Biol Chem 277(17):14581-14588.

Schnelzer A, et al. (2000) Rac1 in human breast cancer: overexpression, mutation analysis, and characterization of a new isoform, Rac1b. Oncogene 19(26):3013-3020.

Schu PV, et al. (1993) Phosphatidylinositol 3-kinase encoded by yeast VPS34 gene essential for protein sorting. Science 260(5104):88-91.

Schurmann A, et al. (2000) p21-activated kinase 1 phosphorylates the death agonist bad and protects cells from apoptosis. Mol Cell Biol 20(2):453-461.

Schwartz MW & Porte D, Jr. (2005) Diabetes, obesity, and the brain. Science 307(5708):375-379.

Senderek J, et al. (2003) Mutations in a gene encoding a novel SH3/TPR domain protein cause autosomal recessive Charcot-Marie-Tooth type 4C neuropathy. Am J Hum Genet 73(5):1106-1119.

Serrano M, Lin AW, McCurrach ME, Beach D, & Lowe SW (1997) Oncogenic ras provokes premature cell senescence associated with accumulation of p53 and p16INK4a. Cell 88(5):593-602.

Shen WH, et al. (2007) Essential role for nuclear PTEN in maintaining chromosomal integrity. Cell 128(1):157-170.

Shepherd PR, Withers DJ, & Siddle K (1998) Phosphoinositide 3-kinase: the key switch mechanism in insulin signalling. Biochem J 333 (Pt 3):471-490.

Silva A, et al. (2008) PTEN posttranslational inactivation and hyperactivation of the PI3K/Akt pathway sustain primary T cell leukemia viability. J Clin Invest 118(11):3762-3774.

Singh B, Ittmann MM, & Krolewski JJ (1998) Sporadic breast cancers exhibit loss of heterozygosity on chromosome segment 10q23 close to the Cowden disease locus. Genes Chromosomes Cancer 21(2):166-171.

Song X, et al. (2001) Phox homology domains specifically bind phosphatidylinositol phosphates. Biochemistry 40(30):8940-8944.

Songyang Z, et al. (1993) SH2 domains recognize specific phosphopeptide sequences. Cell 72(5):767-778.

Soria JC, et al. (2002) Lack of PTEN expression in non-small cell lung cancer could be related to promoter methylation. Clin Cancer Res 8(5):1178-1184.

Sosa MS, et al. (2010) Identification of the Rac-GEF P-Rex1 as an essential mediator of ErbB signaling in breast cancer. Mol Cell 40(6):877-892.

Stal O, et al. (2003) Akt kinases in breast cancer and the results of adjuvant therapy. Breast Cancer Res 5(2):R37-44.

Stambolic V, et al. (2001) Regulation of PTEN transcription by p53. Mol Cell 8(2):317-325.

Stambolic V, et al. (1998) Negative regulation of PKB/Akt-dependent cell survival by the tumor suppressor PTEN. Cell 95(1):29-39.

Steck PA, et al. (1997) Identification of a candidate tumour suppressor gene, MMAC1, at chromosome 10q23.3 that is mutated in multiple advanced cancers. Nat Genet 15(4):356-362.

Stephens L, et al. (1998) Protein kinase B kinases that mediate phosphatidylinositol 3,4,5-trisphosphate-dependent activation of protein kinase B. Science 279(5351):710-714.

Stephens LR, et al. (1997) The G beta gamma sensitivity of a PI3K is dependent upon a tightly associated adaptor, p101. Cell 89(1):105-114.

Stephens LR, Jackson TR, & Hawkins PT (1993) Agonist-stimulated synthesis of phosphatidylinositol(3,4,5)-trisphosphate: a new intracellular signalling system? Biochim Biophys Acta 1179(1):27-75.

Stocker H, et al. (2002) Living with lethal PIP3 levels: viability of flies lacking PTEN restored by a PH domain mutation in Akt/PKB. Science 295(5562):2088-2091.

Stoyanov B, et al. (1995) Cloning and characterization of a G protein-activated human phosphoinositide-3 kinase. Science 269(5224):690-693.

Suetsugu S, et al. (2006) Optimization of WAVE2 complex-induced actin polymerization by membrane-bound IRSp53, PIP(3), and Rac. J Cell Biol 173(4):571-585.

Sulciner DJ, et al. (1996) rac1 regulates a cytokine-stimulated, redox-dependent pathway necessary for NF-kappaB activation. Mol Cell Biol 16(12):7115-7121.

Suzuki A, et al. (1998) High cancer susceptibility and embryonic lethality associated with mutation of the PTEN tumor suppressor gene in mice. Curr Biol 8(21):1169-1178.

Takahashi Y, Morales FC, Kreimann EL, & Georgescu MM (2006) PTEN tumor suppressor associates with NHERF proteins to attenuate PDGF receptor signaling. Embo J 25(4):910-920.

Tamura M, et al. (1999) PTEN interactions with focal adhesion kinase and suppression of the extracellular matrix-dependent phosphatidylinositol 3-kinase/Akt cell survival pathway. J Biol Chem 274(29):20693-20703.

Tamura M, et al. (1998) Inhibition of cell migration, spreading, and focal adhesions by tumor suppressor PTEN. Science 280(5369):1614-1617.

Tanaka H, Fujita N, & Tsuruo T (2005) 3-Phosphoinositide-dependent protein kinase-1-mediated IkappaB kinase beta (IkkB) phosphorylation activates NF-kappaB signaling. J Biol Chem 280(49):40965-40973.

Tang X, Powelka AM, Soriano NA, Czech MP, & Guilherme A (2005) PTEN, but not SHIP2, suppresses insulin signaling through the phosphatidylinositol 3-kinase/Akt pathway in 3T3-L1 adipocytes. J Biol Chem 280(23):22523-22529.

Tao J, Malbon CC, & Wang HY (2001) Insulin stimulates tyrosine phosphorylation and inactivation of protein-tyrosine phosphatase 1B in vivo. J Biol Chem 276(31):29520-29525.

Tashiro H, et al. (1997) Mutations in PTEN are frequent in endometrial carcinoma but rare in other common gynecological malignancies. Cancer Res 57(18):3935-3940.

Tatsumoto T, Xie X, Blumenthal R, Okamoto I, & Miki T (1999) Human ECT2 is an exchange factor for Rho GTPases, phosphorylated in G2/M phases, and involved in cytokinesis. J Cell Biol 147(5):921-928.

Taylor GS, Maehama T, & Dixon JE (2000) Myotubularin, a protein tyrosine phosphatase mutated in myotubular myopathy, dephosphorylates the lipid second messenger, phosphatidylinositol 3-phosphate. Proc Natl Acad Sci U S A 97(16):8910-8915.

Terakawa N, Kanamori Y, & Yoshida S (2003) Loss of PTEN expression followed by Akt phosphorylation is a poor prognostic factor for patients with endometrial cancer. Endocr Relat Cancer 10(2):203-208.

Toker A & Cantley LC (1997) Signalling through the lipid products of phosphoinositide-3-OH kinase. Nature 387(6634):673-676.

Tolkacheva T, et al. (2001) Regulation of PTEN binding to MAGI-2 by two putative phosphorylation sites at threonine 382 and 383. Cancer Res 61(13):4985-4989.

Torres J & Pulido R (2001) The tumor suppressor PTEN is phosphorylated by the protein kinase CK2 at its C terminus. Implications for PTEN stability to proteasome-mediated degradation. J Biol Chem 276(2):993-998.

Trotman LC, et al. (2003) Pten dose dictates cancer progression in the prostate. PLoS Biol 1(3):E59.

Trotman LC, et al. (2007) Ubiquitination regulates PTEN nuclear import and tumor suppression. Cell 128(1):141-156.

Tsao H, Zhang X, Benoit E, & Haluska FG (1998) Identification of PTEN/MMAC1 alterations in uncultured melanomas and melanoma cell lines. Oncogene 16(26):3397-3402.

Ueda S, Kataoka T, & Satoh T (2008) Activation of the small GTPase Rac1 by a specific guanine-nucleotide-exchange factor suffices to induce glucose uptake into skeletal-muscle cells. Biol Cell 100(11):645-657.

Urano D, Nakata A, Mizuno N, Tago K, & Itoh H (2008) Domain-domain interaction of P-Rex1 is essential for the activation and inhibition by G protein betagamma subunits and PKA. Cell Signal 20(8):1545-1554.

Valiente M, et al. (2005) Binding of PTEN to specific PDZ domains contributes to PTEN protein stability and phosphorylation by microtubule-associated serine/threonine kinases. J Biol Chem 280(32):28936-28943.

Van Themsche C, Leblanc V, Parent S, & Asselin E (2009) X-linked inhibitor of apoptosis protein (XIAP) regulates PTEN ubiquitination, content, and compartmentalization. J Biol Chem 284(31):20462-20466.

Vanhaesebroeck B & Waterfield MD (1999) Signaling by distinct classes of phosphoinositide 3-kinases. Exp Cell Res 253(1):239-254.

Vanhaesebroeck B, et al. (1997) P110delta, a novel phosphoinositide 3-kinase in leukocytes. Proc Natl Acad Sci U S A 94(9):4330-4335.

Vazquez F & Devreotes P (2006) Regulation of PTEN function as a PIP3 gatekeeper through membrane interaction. Cell Cycle 5(14):1523-1527.

Vazquez F, Ramaswamy S, Nakamura N, & Sellers WR (2000) Phosphorylation of the PTEN tail regulates protein stability and function. Mol Cell Biol 20(14):5010-5018.

Venkateswarlu K, Gunn-Moore F, Oatey PB, Tavare JM, & Cullen PJ (1998) Nerve growth factor- and epidermal growth factor-stimulated translocation of the ADP-ribosylation factor-exchange factor GRP1 to the plasma membrane of PC12 cells requires activation of phosphatidylinositol 3-kinase and the GRP1 pleckstrin homology domain. Biochem J 335 (Pt 1):139-146.

Virolle T, et al. (2001) The Egr-1 transcription factor directly activates PTEN during irradiation-induced signalling. Nat Cell Biol 3(12):1124-1128.

Volinia S, et al. (1995) A human phosphatidylinositol 3-kinase complex related to the yeast Vps34p-Vps15p protein sorting system. Embo J 14(14):3339-3348.

Voronov SV, et al. (2008) Synaptojanin 1-linked phosphoinositide dyshomeostasis and cognitive deficits in mouse models of Down's syndrome. Proc Natl Acad Sci U S A 105(27):9415-9420.

Walker EH, Perisic O, Ried C, Stephens L, & Williams RL (1999) Structural insights into phosphoinositide 3-kinase catalysis and signalling. Nature 402(6759):313-320.

Wang Q, et al. (1999) Protein kinase B/Akt participates in GLUT4 translocation by insulin in L6 myoblasts. Mol Cell Biol 19(6):4008-4018.

Wang S, et al. (2003) Prostate-specific deletion of the murine Pten tumor suppressor gene leads to metastatic prostate cancer. Cancer Cell 4(3):209-221.

Wang SI, et al. (1997) Somatic mutations of PTEN in glioblastoma multiforme. Cancer Res 57(19):4183-4186.

Wang X, et al. (2001) Regulation of elongation factor 2 kinase by p90(RSK1) and p70 S6 kinase. Embo J 20(16):4370-4379.

Wang X, et al. (2007) NEDD4-1 is a proto-oncogenic ubiquitin ligase for PTEN. Cell 128(1):129-139.

Watt SA, Kular G, Fleming IN, Downes CP, & Lucocq JM (2002) Subcellular localization of phosphatidylinositol 4,5-bisphosphate using the pleckstrin homology domain of phospholipase C delta1. Biochem J 363(Pt 3):657-666.

Welch HC, et al. (2002) P-Rex1, a PtdIns(3,4,5)P3- and Gbetagamma-regulated guanine-nucleotide exchange factor for Rac. Cell 108(6):809-821.

Welsh GI, et al. (2005) Role of protein kinase B in insulin-regulated glucose uptake. Biochem Soc Trans 33(Pt 2):346-349.

Weng LP, Brown JL, Baker KM, Ostrowski MC, & Eng C (2002) PTEN blocks insulin-mediated ETS-2 phosphorylation through MAP kinase, independently of the phosphoinositide 3-kinase pathway. Hum Mol Genet 11(15):1687-1696.

Weng LP, Brown JL, & Eng C (2001) PTEN coordinates G(1) arrest by down-regulating cyclin D1 via its protein phosphatase activity and up-regulating p27 via its lipid phosphatase activity in a breast cancer model. Hum Mol Genet 10(6):599-604.

Weng LP, et al. (2001) Transient ectopic expression of PTEN in thyroid cancer cell lines induces cell cycle arrest and cell type-dependent cell death. Hum Mol Genet 10(3):251-258.

Weng LP, et al. (1999) PTEN suppresses breast cancer cell growth by phosphatase activity-dependent G1 arrest followed by cell death. Cancer Res 59(22):5808-5814.

White MF (1998) The IRS-signalling system: a network of docking proteins that mediate insulin action. Mol Cell Biochem 182(1-2):3-11.

White MF & Kahn CR (1994) The insulin signaling system. J Biol Chem 269(1):1-4.

Whiteman DC, et al. (2002) Nuclear PTEN expression and clinicopathologic features in a population-based series of primary cutaneous melanoma. Int J Cancer 99(1):63-67.

Wijesekara N, et al. (2005) Muscle-specific Pten deletion protects against insulin resistance and diabetes. Mol Cell Biol 25(3):1135-1145.

Wolfe BA, McDonald WH, Yates JR, 3rd, & Gould KL (2006) Phospho-regulation of the Cdc14/Clp1 phosphatase delays late mitotic events in S. pombe. Dev Cell 11(3):423-430.

Wong GW, Knowles GC, Mak TW, Ferrando AA, & Zuniga-Pflucker JC (2012) HES1 opposes a PTEN-dependent check on survival, differentiation, and proliferation of TCRbeta-selected mouse thymocytes. Blood 120(7):1439-1448.

Wu JQ, et al. (2009) PP1-mediated dephosphorylation of phosphoproteins at mitotic exit is controlled by inhibitor-1 and PP1 phosphorylation. Nat Cell Biol 11(5):644-651.

Wu X, et al. (2000) Evidence for regulation of the PTEN tumor suppressor by a membrane-localized multi-PDZ domain containing scaffold protein MAGI-2. Proc Natl Acad Sci U S A 97(8):4233-4238.

Wu X, Senechal K, Neshat MS, Whang YE, & Sawyers CL (1998) The PTEN/MMAC1 tumor suppressor phosphatase functions as a negative regulator of the phosphoinositide 3-kinase/Akt pathway. Proc Natl Acad Sci U S A 95(26):15587-15591.

Wu Y, et al. (2000) Interaction of the tumor suppressor PTEN/MMAC with a PDZ domain of MAGI3, a novel membrane-associated guanylate kinase. J Biol Chem 275(28):21477-21485.

Wymann MP, Zvelebil M, & Laffargue M (2003) Phosphoinositide 3-kinase signalling--which way to target? Trends Pharmacol Sci 24(7):366-376.

Xu AW, Kaelin CB, Takeda K, Akira S, Schwartz MW, Barsh GS (2005) PI3K integrates the action of insulin and leptin on hypothalamic neurons. J Clin Invest. 115(4):951-958.

Yang ZZ, et al. (2005) Dosage-dependent effects of Akt1/protein kinase Balpha (PKBalpha) and Akt3/PKBgamma on thymus, skin, and cardiovascular and nervous system development in mice. Mol Cell Biol 25(23):10407-10418.

Yang ZZ, et al. (2003) Protein kinase B alpha/Akt1 regulates placental development and fetal growth. J Biol Chem 278(34):32124-32131.

Yu J, et al. (1998) Regulation of the p85/p110 phosphatidylinositol 3'-kinase: stabilization and inhibition of the p110alpha catalytic subunit by the p85 regulatory subunit. Mol Cell Biol 18(3):1379-1387.

Yu Z, et al. (2002) PTEN associates with the vault particles in HeLa cells. J Biol Chem 277(43):40247-40252.

Yuan TL & Cantley LC (2008) PI3K pathway alterations in cancer: variations on a theme. Oncogene 27(41):5497-5510.

Zhang H, et al. (2003) Loss of Tsc1/Tsc2 activates mTOR and disrupts PI3K-Akt signaling through downregulation of PDGFR. J Clin Invest 112(8):1223-1233.

Zhang J, et al. (1998) A type II phosphoinositide 3-kinase is stimulated via activated integrin in platelets. A source of phosphatidylinositol 3-phosphate. J Biol Chem 273(23):14081-14084.

Zhang Y, et al. (2003) Rheb is a direct target of the tuberous sclerosis tumour suppressor proteins. Nat Cell Biol 5(6):578-581.

Zhang Z, Shen K, Lu W, & Cole PA (2003) The role of C-terminal tyrosine phosphorylation in the regulation of SHP-1 explored via expressed protein ligation. J Biol Chem 278(7):4668-4674.

Zhao JJ, et al. (2003) Human mammary epithelial cell transformation through the activation of phosphatidylinositol 3-kinase. Cancer Cell 3(5):483-495.

Zheng J, et al. (1996) Identification of the binding site for acidic phospholipids on the pH domain of dynamin: implications for stimulation of GTPase activity. J Mol Biol 255(1):14-21.

Zhou BP, et al. (2001) Cytoplasmic localization of p21Cip1/WAF1 by Akt-induced phosphorylation in HER-2/neu-overexpressing cells. Nat Cell Biol 3(3):245-252.

Zhou BP, et al. (2001) HER-2/neu induces p53 ubiquitination via Akt-mediated MDM2 phosphorylation. Nat Cell Biol 3(11):973-982.

Zhou X, et al. (2001) Association of germline mutation in the PTEN tumour suppressor gene and Proteus and Proteus-like syndromes. Lancet 358(9277):210-211.

Zhou XP, et al. (2000) Epigenetic PTEN silencing in malignant melanomas without PTEN mutation. Am J Pathol 157(4):1123-1128.

Zhou XP, et al. (2000) Germline and germline mosaic PTEN mutations associated with a Proteus-like syndrome of hemihypertrophy, lower limb asymmetry, arteriovenous malformations and lipomatosis. Hum Mol Genet 9(5):765-768.

Zvelebil MJ, et al. (1996) Structural and functional diversity of phosphoinositide 3-kinases. Philos Trans R Soc Lond B Biol Sci 351(1336):217-223.